UC Davis

UC Davis Electronic Theses and Dissertations

Title

The fate of California's forests under climate change, novel fire regimes, and management interventions

Permalink

https://escholarship.org/uc/item/7q23r0wp

ISBN

9798193264583

Author

Saberi, Saba Juliet

Publication Date

2026-09-08

Peer reviewed|Thesis/dissertation

eScholarship.org Powered by the California Digital Library
University of California

The fate of California's forests under climate change, novel fire regimes, and management interventions

By

SABA JULIET SABERI
DISSERTATION

Submitted in partial satisfaction of the requirements for the degree of

DOCTOR OF PHILOSOPHY

in

Ecology

in the

OFFICE OF GRADUATE STUDIES

of the

UNIVERSITY OF CALIFORNIA

DAVIS

Approved:

Hugh D. Safford, Chair

Derek J.N. Young

Andrew M. Latimer

Committee in Charge

2026

Copyright © by Saba Juliet Saberi

ABSTRACT

The fire regimes, or the frequency, severity, spatial pattern, and seasonality of wildland fires of forested ecosystems in western North America are changing rapidly. In the mixed conifer forests of the Sierra Nevada, shifting fire regimes can be attributed to a combination of the following: the removal of indigenous land stewardship, over a century of fire suppression, and hotter, drier, conditions due to anthropogenic climate change. The removal of fire from the system created large patches of dense, homogenous forest with high fuel loads unlike the historical forest mosaic containing a variety of gaps and openings, and these large dense patches are more likely to burn at high severity. Since many forests types in the Sierra Nevada are adapted to low severity, high frequency fire, the departure from historic fire regimes has led to shifts in forest structure and composition, which raise important questions about the future of forest ecosystems under a changing climate. In areas where fires repeatedly burn at high severity in short time frames, there is a risk of conversion to non-forested types since trees may not have time to grow to maturity and provide seed source for the next generation. In this dissertation, I investigated forest responses to shifting fire regimes as well as management interventions (namely fuel treatments) taken to mitigate high severity fire effects throughout mixed conifer forests of the Sierra Nevada.

In chapter one, I examined the effectiveness of fuel treatments installed before three 2021 fires (the Caldor, Dixie, and Tamarack fires) which span multiple forest types in the central and northern Sierra Nevada. Within each fire perimeter, a variety of fuel treatment types were implemented in different combinations and at different frequencies,

including thinning, masticating, piling, pile burning, and broadcast burning. I used a transect-based field protocol to collect data on four trees every 25 meters running from an untreated area to a treated area within each of the three fires. I then implemented generalized additive mixed models in a Bayesian framework to determine 1) which, if any, fuel treatment types reduced the probability of tree mortality, and 2) if tree injury surrogates (bole char, crown scorch, and crown torch) explain the mechanism of mortality. I found thinning and broadcast burning reduced tree mortality the most, and that conditioning on fire injury components such as bole char, crown scorch, and crown torch explained most of the treatment effect. In addition, I found that following piling with a pile burn reduced tree mortality more than just piling alone. Despite the challenge of using observational data to quantify the effects of non-random fuel treatments, the Bayesian modeling framework allowed me to account for multiple treatment types without reducing statistical power and can be easily implemented by other researchers investigating fuel treatment effectiveness across large spatial scales.

In chapter two, I expanded upon an existing Random Forest modeling framework for postfire live tree identification using bands from Sentinel-2 imagery, which was originally created to identify live trees at one year post fire. To see if the model could distinguish any post-fire delayed tree mortality (tree mortality between 2 and 5 years postfire). I assessed the model's ability to identify live trees at one, three, and five years postfire by training the model on NAIP imagery at those time steps. I used four sample fires in Sequoia National Forest and Kings Canyon National Park in the Southern Nevada to train the model on a total of 6000 photo interpreted NAIP pixels. I found the model could

reliably predict delayed mortality at one, three, and five years post-fire with high accuracy, although delayed tree mortality was not particularly prominent across the fires. I also created RdNBR maps at each time step and thresholded them into binary live/dead using a high severity threshold cutoff to demonstrate a quick managers might currently assess tree mortality and found that the RdNBR method overestimated live trees when compared to my Random Forest model. As with most spectral-based remote sensing studies, the model could not reliably between tree recovery and shrub regeneration, suggesting that incorporation of 3D structure data could help to improve this gap.

In chapter three, I sampled regeneration plots in three older fire perimeters (Freds (2004), Long (2011) and Caples (2019)) within the 2021 Caldor fire to investigate the drivers of conifer regeneration in short interval reburns. Here, short interval reburns are defined as two fires occurring within a 30 year period. Among the four sampled fires, between 64% and 88% of plots had stand replacement density (175 seedlings/ha) of seedlings regardless of age. I used generalized linear mixed models to predict seedling density as a function of reburn interval (years between fires), distance to seed source, shrub cover, severity of the first fire, and several other forest structure and topo climatic variables, separating models by pine species and shade tolerant species. Reburn interval was a strong driver of post-fire seedling density in the case of pine species but not shade tolerant species. In the case of zero year shade tolerant species, reburn interval interacted with shrub cover to influence seedling density such that increased shrub cover corresponded with slightly increased seedling density, suggesting a nurse effect. Overall, a higher shade tolerant species density compared to pine species density post-fire was reflective of the biological legacy of

shade tolerant species dominance, and two fires were quick succession are not enough to overturn that legacy. The results of this study suggest that incorporation of reburn history into existing post-fire regeneration planning tools provides important context that can further aid managers seeking to identify areas with high reforestation need.

ACKNOWLEDGEMENTS

I want to thank my advisor Hugh Safford for taking me on as a student. He connected me to countless fire ecology researchers and practitioners, supported my research ideas and gave me a tremendous amount of autonomy while still providing feedback and mentorship throughout my time at UC Davis. His light-hearted nature, ability to bridge research and management, and deep first-hand knowledge of the natural history of California inspires me to emulate him during my own career. Thank you to Andrew Latimer, whose expertise and encouragement made me realize that I enjoy statistics far more than I thought I did. Thank you to Derek Young who kept me connected to the remote sensing world as well as for his support in shaping the field methods for my third chapter. Andrew and Derek's attention to detail and thoughtful feedback was essential to helping me build my confidence as a scientist. I would also like to thank Malcom North for his support during the earlier part of my degree program, and to Amanda Crump for introducing me to translational science, extension work, and for serving as an examiner for my qualifying exam at the last minute.

Thank you to the people I overlapped with at the Safford Lab: Ashley Grupenhoff, Emily Brodie, Tara Ursell, Sara Winsemius, Marie Fleming, and Becky Wayman: although our time together was not particularly long, your support and willingness to give me your time helped me navigate the maze that is graduate school. To my lab mate Tessa Putz, I am so grateful to have gone through this journey with you! From course work to writing grant proposals to bouncing research thoughts off each other, your constant presence and support has meant everything. I would also like to thank my cohort-mates and the student graduate group: our family dinners, happy hours at Sophia's, and camping trips created a sense of home and community that I will cherish forever.

This research would not have been possible without help from countless people. Thank you to Becky Estes for providing the material and intellectual support for two field seasons throughout the Eldorado National forest. Thank you to Kristen Shive and Alison Paulson and their respective field technicians for sharing their data for Chapter 1. To my field technicians across both seasons: Terra Wilson, Dasha Pechurina, Iris Bookholz, Emily Chen, Shaghig Terzian, Sophia Lodigiani, Carolyn Welch, and Jujú Eulensen-Wallace – this dissertation would not have been possible without you. Our adventures tromping through burned forests searching for seedlings and finding beautiful wildflowers was my favorite part of this degree.

Thank you to my parents, Arefeh and Reza, for taking me to Sequoia National Park when I was six years old: that trip sparked a lifelong love of nature that I feel lucky to share with you. Thank you also for always encouraging me to pursue my goals. To my dogs Douglas-Fur and General Sherman, thank you for providing steadfast company throughout

this process. Finally, to my husband Beau, I truly could not have done this without you. Thank you for listening to my practice talks, proofreading abstracts, giving feedback on multiple iterations of figures, going backpacking with me and the dogs when I wanted to clear my head, for cooking dinner and taking me out for a sweet treat…the list could go on forever. Behind every person accomplishing a years-long project is an incredible partner that keeps them grounded and keeps life running smoothly in the background. I'm so lucky for that person to be you.

This research was made possible from multiple funding sources, including the University of California Eugene Cota Robles Fellowship, the Joint Fire Science Program Graduate Innovation Award (GRIN), as well cooperative agreements with the USDA Forest Service and the US Geological Survey. I am particularly grateful to have had federal funding during a period where funding for climate change research and science in general is threatened.

The studies in this dissertation were conducted on the tribal lands of the Washoe, Nisenan, Mountain Maidu and Konkow Maidu people. These people have called these lands home and used fire to manage them since time immemorial. The forced removal of Indigenous people disrupted millennia of land stewardship and ruptured deep connections to the land. The legacy of settler colonialism continues to pose significant barriers to Indigenous peoples' ability to conduct cultural burning and ceremony to this day.

TABLE OF CONTENTS

CHAPTER 1. A CAUSAL MODEL FRAMEWORK FOR EVALUATING FUEL TREATMENT EFFECTIVENESS AFTER THREE 2021 WILDFIRES 1
ABSTRACT 2
INTRODUCTION 3
METHODS 10
RESULTS 18
DISCUSSION 24
LIMITATIONS 27
CONCLUSION 30
REFERENCES 32
SUPPLEMENTARY INFORMATION (S1) 39
CHAPTER 2. QUANTIFYING POST-FIRE LIVE TREE PRESENCE AND SPATIAL VARIATION USING SENTINEL-2 TIME SERIES 55
ABSTRACT 56
INTRODUCTION 57
METHODS 61
RESULTS 71
DISCUSSION 78
LIMITATIONS 82
CONCLUSION 85
ACKNOWLEDGEMENTS 86
REFERENCES 87
SUPPLEMENTARY INFORMATION (S2) 95
CHAPTER 3. DRIVERS OF CONIFER REGENERATION IN SUCCESSIVELY BURNED AREAS IN THE CENTRAL SIERRA NEVADA 103
ABSTRACT 104
INTRODUCTION 105
METHODS 111
RESULTS 118
DISCUSSION 132
LIMITATIONS 141
CONCLUSION 143
REFERENCES 145

CHAPTER 1. A CAUSAL MODEL FRAMEWORK FOR EVALUATING FUEL TREATMENT EFFECTIVENESS AFTER THREE 2021 WILDFIRES

Saba J. Saberi, Hugh D. Safford, Kristen L. Shive, Alison K. Paulson

ABSTRACT

In recent decades, there has been an increase in the forested area burned by high severity wildfire in the western US, due to a combination of increased fuels driven by fire suppression and erasure of indigenous land stewardship and the warming climate. These dense forests are particularly at risk of burning at high severity in hot, dry conditions from anthropogenic climate change. Fuel treatments, or activities that reduce surface, ladder, and/or canopy fuels and in turn create fire-resilient forest stands, are one way to mitigate the effects of wildfire by modifying fire behavior. As more land management agencies across state and federal lands invest in fuel treatment implementation and monitoring to increase forest resilience and protect communities in the wildland urban interface, there is increasing need to quantify the impacts of fuel treatments. In this study, we used transect-based field data from three large 2021 California wildfires (Caldor, Dixie, and Tamarack fires) to quantify the effects of highly varied and complex fuel treatment histories on tree mortality. Using a Bayesian framework, we deconstructed the pathway from fuel treatment to tree mortality reduction by considering how fuel treatments affect tree injury levels (bole char, crown scorch, and crown torch), and how injury levels affect tree mortality. We found that thinning and broadcast burns, especially when applied together, corresponded highly to reduced tree mortality. In addition, we found that fuel treatments' reduction of crown scorch is the primary mechanism by which tree mortality is reduced. We also found mastication and fuel piling without follow-up pile reduction to be associated with higher fire effects such as bole char height. While we could not make broad inferences due to the partially confounded nature of the fuel treatment types and the forest types that they were applied in, the Bayesian analysis framework allowed us to quantify uncertainty and produce a novel method of fuel treatment effectiveness analysis that could be applied on a much larger spatial and temporal scale, especially as harmonized fuel treatment databases become available.

INTRODUCTION

In California and more broadly the North American West, the overall area impacted by high-severity wildfires and the sizes of forest patches burned at high severity have both increased in recent decades (Stevens et al. 2017, Steel et al. 2018, Parks and Abatzoglou 2020). Increased occurrence of high severity burning is in part due to increasingly homogenous, dense forests resulting from a century of fire suppression and erasure of Indigenous land stewardship by settler colonialism and is further exacerbated by anthropogenic climate change (Whitman et al. 2015, Westerling 2016, Siedl et al. 2017, Williams et al. 2019, Vinyeta 2022). Increased threats to structures as more people live in the wildland-urban interface or WUI have led to federal agency response to increase efforts in fuel treatments to reduce forest fuels. (Stephens et al. 2012a). Fuel treatment refers to any activity that creates fire-resilient forest stands and includes reducing surface, ladder, and/or canopy fuels (Agee and Skinner 2005). Silvicultural methods used in forest treatments can be used on their own or together, and include mechanical commercial and noncommercial thinning, hand thinning, mastication, slashing and piling, regeneration harvest, herbicide applications, and prescribed fire (Jain et al. 2012). Reducing wildland fire hazard can act as forest restoration in that the initial resilience of the treated stand is reinforced by further fuel reduction (Prichard et al. 2021). Fuel treatments are based on principles of fire resistance: reducing surface fuels reduces potential flame length and leads to less torching (when flame lengths pass a critical threshold and fire moves from the surface into tree crowns) while decreasing crown density reduces the potential for crown fire by making tree-to-tree burning less probable (Agee and Skinner 2005). Additionally, a goal of fuel treatments can be to keep big trees of fire-resistant species (e.g., those with thick bark such as Ponderosa pine (*Pinus ponderosa)* or Douglas-fir (*Pseudotsuga menziesii* var. *menziesii*)) to restore historic forest structure, decrease mortality, and safeguard the forest's major seed producers (Agee and Skinner 2005).

Research into the effectiveness of fuel treatments in reducing fire severity and tree mortality is robust and spans multiple forest types throughout North America. For example, the national Fire and Fire Surrogate (FFS) study measured the effectiveness and ecological outcomes of commonly used treatments at 12 sites across the western and eastern USA (McIver et al. 2008). Treatments were designed to create stands so that 80% of dominant and co-dominant trees would survive wildfires under 80th-percentile weather conditions (Stephens and Moghaddas 2005). Many papers resulted from this study, with some key findings being that at the stand level, mechanical treatments that were followed with prescribed fire were the most effective at reducing surface fire and crown fire behavior (Schmidt et al 2008). Across most of these experimental sites, the need for repeat treatments for actual restorative effects was demonstrated (Waldrop et al. 2008), while many treatments did have the initial impact of reducing fuel loads (Youngblood et al. 2008). Later investigations into the longer-term effects of fuel treatments showed that the initial treatment effects are reduced over time and that initial treatments can sometimes increase fine woody fuels because of activity inputs from thinning and mastication. Additionally, at seven years, the net effect of mechanical treatment only was similar to a fire treatment (Stephens et al. 2012b). Fuel treatment longevity can be increased by staggering treatments when repeat treatments are too costly (Stephens et al. 2012b). No single study of fuel treatments 'proves' that fuel treatments work, but the body of existing literature provides strong evidence that thinning and prescribed burning are highly effective (Pollet and Omi 2002, Stephens et al. 2009, 2012a, 2013; Safford et al. 2012, Kalies and Yocom-Kent 2016, Prichard et al. 2017, Prichard et al. 2021, Shive et al. 2024). Notably, in the yellow pine and mixed conifer forests which dominate the Sierra Nevada, management activities that reduce stand density, fuel loads, and increase the prevalence of fire and drought tolerant species equate to ecological restoration as well (Safford and Stevens 2017, Safford et al. 2021).

Investigations of fuel treatment effectiveness have some limitations due to logistical and liability constraints. For example, investigations are more likely to be observational than experimental given that it is difficult to experimentally produce crown fire under extreme weather conditions (due to threat to life and property). Furthermore, landscape-level assessments of treatments are challenging due to the interspersed nature of fuel treatments. Most studies are only able to report on site-level effects because they are not designed to assess treatment efficacy at broad spatial scales (McKinney et al. 2022). In addition, inferences from smaller studies are not necessarily scalable to the regional level, although methods have recently been developed to scale up site-specific treatment nomenclature to a regional one (Fallon et al. 2025), as more of the fire science community's efforts focus on broad-scale effects of fuel treatments.

Another challenge in fuel treatment effectiveness research is the validity of the treatment records. For federal lands, The Forest Service Activity Tracking System (also referred to as FACTS) is a federal database used to track planned, accomplished, and completed land management actions, such as timber harvest, hazard tree removal, pre-commercial thinning, herbicide application, and broadcast burns (USDA Forest Service 2026). One of the main reliability challenges with using the FACTS database is in part because it is a relational dataset that is not shared in full with the public (Call et al. 2025), and there are often spatial and temporal gaps in observations, as well as instances of duplicate records (Knight et al. 2022). In addition, there may be records of planned activities that have not been updated as completed, leaving the FACTS user unsure of the treatment's final status and inclined perhaps to omit records that may in fact be completed. Researchers are responding to recent investments by state and federal land management in fuel treatment implementation and evidence-driven assessments by organizing unified state (California Wildfire and Forest Resilience Task Force 2026, Knight et al. 2022) and

national fuel treatment databases (TWIG, or the Treatment and Wildfire Interagency Geodatabase, Call et al. 2025).

Some knowledge gaps remain in the study of fuel treatment effectiveness. While there is some evidence suggesting the effectiveness of restorative fuel treatment even under extreme fire weather (Safford et al. 2012, Povak et al. 2020, Prichard et al. 2020) continued tracking and investigation into their efficacy is still warranted as novel fire behavior is difficult to predict. Existing fire behavior models are unable to predict mass fires, which occur when large continuous areas burn with high intensity for long periods of time and result from a coupling of combustion with atmospheric circulation (Stephens et al. 2022). Mass fires are becoming more frequent due to huge fuel loads exacerbated by drought and insect-driven mortality (Stephens et al. 2022). Understanding the impacts that fuel treatments can have on fire behavior, particularly whether they can still modify fire behavior in the case of mass fires, remains poorly understood. Beyond the need to characterize forest responses to novel fire conditions, this research is important to conduct as there is work claiming that thinned forests have more percent basal area mortality than un-thinned forests postfire (measured less than one year postfire; Baker and Hanson 2022). Work by Hanson et al. claiming that unmanaged (i.e., untreated) forests burn at lower severity has been questioned by others in the scientific community (Stephenson et al. 2024, Potter and Osuwu 2026) on grounds of flawed methodology and divergent results from other work by multiple research groups. Such reports can sow seeds of doubt and create perceived uncertainty in the science that hinders decision-making, as seen in a recent opinion of the US Court of Appeals for the Ninth Circuit, which concluded that, in reference to a forest restoration project, “The project’s proposed methodology of variable density thinning is both highly controversial and highly uncertain.” (*BARK* et al. *v. U.S. Forest Service* 2019). Thus, there remains a need to continue to characterize the effects of fuel treatments in forest restoration and fire behavior modification to mitigate perceived

uncertainty, especially when results can directly inform policy and management. In addition, despite the increase in pace and scale of fuel treatment implementation, there remains a lack of empirical evidence on landscape-level fuel treatment effectiveness, driven in part by the lack of explicit distinction between site-level and landscape-level studies (McKinney et al. 2022). Explicit characterization of the spatial scale of fuel treatment effectiveness in future studies can remedy this issue. Some management-driven research questions that remain unanswered include: Do certain types of fuel treatments lead to increased fire effects (as opposed to decreased)? How much does the time since previous treatment matter in reducing fire effects from a subsequent wildfire? What is the optimal size of a fuel treatment designed to reduce tree mortality? The ability to answer these questions can help to optimize the size, location, and spatial orientation of treatments to increase their efficacy in future fires.

Remaining uncertainty in fuel treatment effectiveness is driven primarily by research methods. For example, questions remain about the effect that fuel treatments can have in potentially mitigating future wildfires. Less than ten percent of treated areas have interacted with wildfires during their effective lifespans (Barnett et al. 2016), and the challenge remains in accounting for the multiple factors impacting treatment outcomes with observational methods and limited data. Given the small spatial extent on which individual treatments are implemented, uncertainty around effect estimates can be large, and inference can be limited. In the case of non-random treatment application across a landscape, statistical consideration through a Bayesian causal approach may be appropriate. With a Bayesian causal approach, Bayesian statistics are used to update probabilistic models and combined with causal frameworks (such as DAGS or directed acyclic graphs, which can decompose pathways leading to a desired outcome) to estimate the effect of a treatment (Arif and MacNiel 2022). Despite the notion that casual inference is limited to only experimental research, causal inference can still be used in observational

studies, and explicit consideration of confounding factors or variables can clarify the relationship between variables in a system (Arif and MacNeil 2022).To date, no study has used a Bayesian causal framework to quantify uncertainty around fuel treatment effects in forested landscapes. One study used a Bayesian approach to conduct a meta-analysis of short-term effects of fuel treatments on fuel loading (Grupenhoff et al. 2025), and another used a Bayesian approach to quantify selection biases in post-fire restoration of sagebrush ecosystems of the western US (Simler Williamson and Geronimo 2022).Our study aims to use Bayesian causal inference to better understand fuel treatment effectiveness in three of California's recent high profile fires that occurred under extreme fire weather conditions that are becoming increasingly more common.

Research Questions and Hypotheses

This project addresses the following research questions as applied to three large 2021 wildfires (the Caldor fire, the Dixie fire, and the tamarack Fire): Q1) What effect do different treatments have on the probability of tree mortality, and to what extent does the age of the last treatment prior to fire matter? Q2) Are the effects of treatments on tree mortality explained by metrics/components of tree injury? Q3) When multiple treatments (of different types) are applied, are there interactions among the treatments? Note that in this case, tree mortality refers to immediate post-fire mortality as measured one or in some cases two years postfire.

H1) We hypothesize that fuel treatments will reduce tree mortality in all three fires, but that the magnitude of effects will vary depending on treatment type, frequency, and the pre-existing vegetation type. We anticipate that broadly, areas that have had any fuel treatment will have less tree mortality than untreated control areas. We expect that successful *fuel reduction* treatments will be more effective at reducing tree mortality than *fuel rearrangement* treatments. Fuel reduction

treatments refer to treatments where thinned trees and fuels are removed from the site, whereas with fuel rearrangements, thinned trees and fuels are left in piles on the landscape (Pollet and Omi 2002, Prichard et al. 2021). We also expect that more recently treated areas will be affiliated with less tree mortality, as older treated areas will have had more time to reaccumulate fuels. H2) We hypothesize that the effects of treatments on tree mortality will be largely explained by tree injury, quantified via bole char, crown scorch, and crown torch (Figure 1.1). Trees are primarily killed by fire because of cambium necrosis due to heat transfer to the crown, root, and stem tissue, although partial injuries to parts of the tree can also cause mortality (Hood et al. 2018). In line with this logic, post-fire tree mortality has historically been modeled as a function of fire injury (e.g. crown scorch and torch, bole char; Woolley et al. 2012). As a result, we expect any reduction in tree mortality due to treatments to be explained by tree injury components. H3) We expect that areas that experienced combined mechanical treatment and prescribed fire treatment will have less tree mortality than areas that had one treatment type alone, in line with other empirical findings (Webster and Halpern 2010, Kalies and Yocom Kent 2016). Additionally, we expect areas that have fuel piling to only reduce mortality if they are followed up with pile burning, which has been documented in the Lake Tahoe Basin Management Unit (Safford et al. 2009, Safford and Saberi 2026).

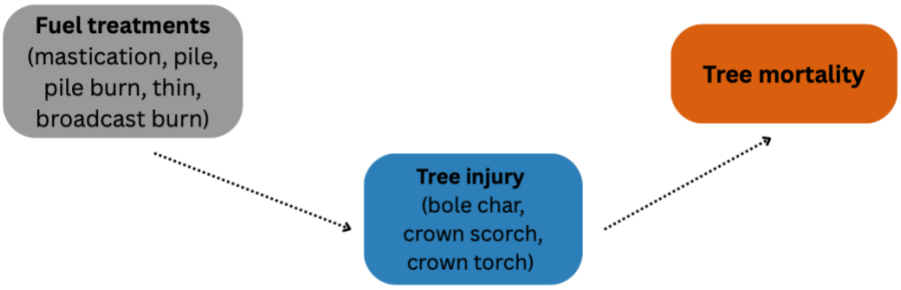


Figure 1.1. Directed acyclic graph (DAG) showing the causal pathway from fuel treatments to reduced tree mortality (solid black line), which is mediated by tree injury components (dashed black lines). (In causal inference, the term 'mediator' refers to the variable that lies on the causal pathway between an exposure variable and the outcome).

METHODS

Study area

The fires studied in this project are all from the highly publicized 2021 fire season (Figure 2). The Dixie fire was the largest single-source fire in state history, and the Caldor fire was also one of the top twenty largest fires in state history (Cal Fire 2024). The Dixie fire burned 389,837 ha across five counties and in Lassen and Plumas National Forests. The Caldor fire burned 89,773 hectares in the Eldorado National Forest and part of the Lake Tahoe Basin Management Unit, destroying over 1000 structures (Cal Fire 2021). The Dixie Fire was the first known fire to cross the Sierra Nevada crest, and the Caldor Fire did the same the following day. Lastly, the Tamarack fire burned 27,776 ha in the Humboldt-Toiyabe National Forest and began initially in the remote wilderness. Its location in the backcountry and other higher-priority fires led to the initial decision to let the fire burn, which caused public outrage when the town of Markleeville was threatened (Chabria and Wigglesworth 2021). In addition to the high-profile nature of these fires, they produced large area of high burn severity, with 11% in the Tamarack, 31% in the Caldor, and 24% in the Dixie as determined by thresholds set by the interagency Monitoring Trends in Burn Severity Program (USGS, USDOI, USFS 2026).

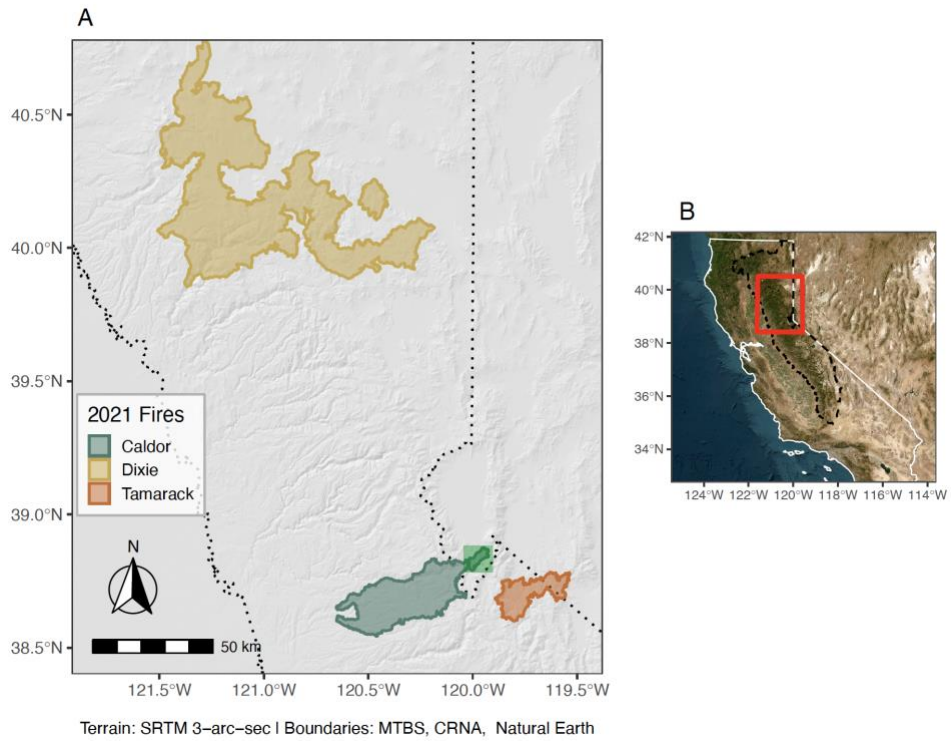


Figure 1.2. A) Map showing fires included in the study in yellow, green, and orange outlines, and the Sierra Nevada Bioregion in dotted black lines. The green box overlaying the eastern island of the Caldor fire shows where transects were placed (Lake Tahoe Basin Management Unit only). B) Reference map: Red box shows extent of study area, black dotted line shows the Sierra Nevada Bioregion, and white line shows California state boundary.

The three fires are all situated in eastern California, with the Dixie fire occurring in the southern Cascade Mountains and the northern Sierra Nevada on both the eastern and western slopes, and the portion of the Caldor used for this analysis and the Tamarack Fire occurring east of the Sierra Nevada crest. The climate is broadly characterized as Mediterranean with cool, wet winters and warm dry summers. The western side of the Sierra Nevada receives more precipitation than the east side, which lies in a rain shadow and is influenced by the climate of the Great Basin with colder winters and more summer rainfall (Dettinger et al. 2018). All three fires occurred in forest types that historically experienced frequent fire at a mean interval of 11-16 years with typically low to moderate fire severity effects (Safford and Stevens 2017). The three fires were all primarily within yellow pine and mixed conifer forest types and included ponderosa pine (*Pinus*

ponderosa Lawson & C. Lawson), sugar pine (*Pinus lambertiana* Douglas), Jeffrey pine (*Pinus jeffreyi* Grev. & Balf.), white fir (*Abies concolor* (Gordon & Glend.) Hildebr.), incense-cedar (*Calocedrus decurrens* (Torr.) Florin), and Pacific Douglas-fir (*Pseudotsuga menziesii* (Mirb.) Franco var. men-ziesii), with a variable component of black oak (*Quercus kelloggii* Newb.) and canyon live oak (*Quercus chrysolepis*). Sampling sites at higher elevations contained red fir (*Abies magnifica* A. Murray bis), and lodgepole pine (*Pinus contorta* Louden ssp. murrayana (Grev. & Balf.) Critchf.). The historical fire return interval in red fir was approximately 33-40 years (median-mean; Van de Water and Safford 2011). The Tamarack fire occurred within the transition zone between the yellow pine mixed conifer forests of the Sierra Nevada and the pinyon-juniper forests of the Great Basin, so the untreated areas often included a higher component of single-leaf pinyon pine (*Pinus monophylla)* and juniper (*Juniperus osteosperma).* Understories were dominated by shrubs in the *Ceanothus* and *Arctostaphylos* genera.

Data for this project were collected primarily during the summer months of 2022 across all three fires, although some field work to scout locations and collect missing slope data was conducted in the preceding and subsequent summers (2021 and 2023, respectively). Within the footprint of each fire, the US Forest Service (USFS) Forest Activity Tracking System (FACTS) database was queried and units where treatments occurred between 2001 and 2020 were selected. Because the planning for this study began prior to the development of cleaned databases such as TWIG, we circumvented the uncertainty associated with FACTS by using spatial information provided by managers on the ground on each of the national forests. In the Lake Tahoe Management Basin, for example, managers shared shapefiles on treatment units that did not appear in FACTS at all.

For each fire, we aimed to install 20 transects within the fire footprint. Final transect numbers varied (17 in Caldor, 16 in Tamarack, 23 in Dixie) to due to incorrect transect installation.

In the Caldor Fire, site locations were restricted to the Lake Tahoe Basin Management Unit portion of the fire only due to the project funders' (League to Save Lake Tahoe, The Tahoe Fund, and the Southern Nevada Public Land Management Act [SNPLMA]) interest in understanding the effect of fuel treatments in highly threatened landscapes in and adjacent to the WUI. Within units where treatment occurred, transects were centered at random points along the boundaries between units treated for fuels and adjacent untreated areas. Transect locations were chosen to represent a gradient of forest types, topography, and treatment types, where possible. Field protocol followed that of Safford et al. 2012 (see paper for detailed figures on transect design). Each 225-meter transect included ten sampling points spaced 25 meters apart: five points in treated forest and five in untreated forest. Since our sampling areas generally experienced fire burning upslope from treated areas into untreated areas, our transect sampling usually began in treated forest and moved uphill into untreated forest.

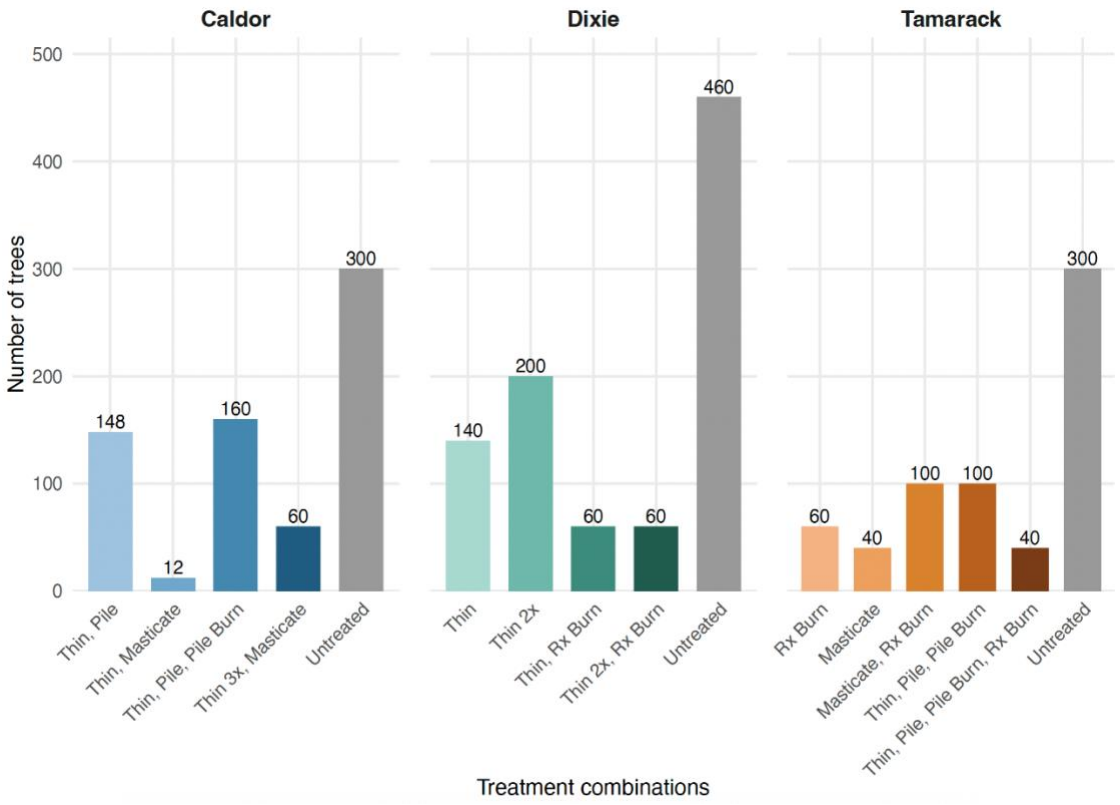


Figure1.3. Combinations of treatment types for each fire, with number of trees sampled listed above the bar. Rx burn = broadcast burn. Thin 2x = thinned two times, Thin 3x = thinned three times.

At each sampling point, tree-based measurements on four trees in each of the four compass quadrants were carried out (the nearest tree > 10 cm dbh). Measurements included tree species identification, live or dead status, tree height, diameter at breast height (dbh), height to live crown (an estimate of pre-fire status), bole-char, scorch, and torch heights, as well as scorch and torch percent. In addition to tree-based measurements, structure and vegetation composition measurements were also taken. At each point, the stand basal area (for live and dead trees) was estimated using a basal area gauge using a basal area factor of 20. The factor was reduced if fewer than five trees were counted. The density of live and dead trees in an 8-meter radius was estimated using a laser range finder, and slope and aspect were measured using a clinometer and compass.

Overstory and shrub cover along the entire transect was measured using a line-intercept method (Safford et al. 2012).

Data Analysis

Prior to data analysis, data standardizing, reduction, and scaling were conducted. Data for the three fires were collected by three different crews using identical methods but slightly different nomenclature for the different treatment types. To standardize the treatment dataset, we created a data frame with the columns “Thin”, “Masticate”, “Pile”, “Pile Burn”, and “Broadcast Burn”, where each column could have a value of 0, 1, 2, or 3, representing the number of times that treatment was received. Every treatment predictor had either a value of 0 or 1, with the exception of “Thin,” which had values of 2 and 3 (Table S1.1). Additional data columns included ‘years since last treatment’, which represented the years prior to each 2021 fire that the last treatment occurred, and ‘distance from boundary’, which represented the distance into the treatment area from the treatment boundary edge (meters). These treatment-related data columns were then attributed to each unique fire, transect, and sampling point combination for each of the 57 transects across the three fires. At the tree level, variables selected for modeling included: tree status (live or dead), species, dbh, bole char height, percent scorch, and percent scorch. This reduced list of variables resulted from calculating correlation coefficients between all tree-level variables and removing any variables with $r > 0.5$ (tree height, height to live crown, scorch height, and torch height). Dbh was centered and scaled, as was the distance from treatment boundary variable.

To determine the effect that the different treatments had on tree mortality, we fit Bayesian generalized additive mixed-effects models (GAMMs) using the ‘brms’ package in R (Bürkner et al. 2017). To specifically evaluate whether the effects of treatments operated through fire injury mechanisms, we used a multi-step approach. First, we estimated the effect of treatment on tree

mortality by considering the five treatment predictors as fixed effects and no fire injury covariates (bole char height, percent scorch volume, and percent torch volume). Other predictor variables included years since last treatment and distance from the boundary edge, as we wanted to know if these variables influenced mortality as well. The response variable was modeled at the tree level, with mortality modeled with a Bernoulli distribution and a logit link since mortality represents a single binary outcome (dead or alive). Fixed effects included the five treatment types (thin, masticate, pile, pile burn, and broadcast burn), years since last treatment, and distance from treatment edge. Additionally, a non-linear fixed effect of tree dbh was modeled using a penalized thin-plate regression spline (allowing a flexible estimation of the relationship between dbh and mortality instead of assuming linearity). Random effects included a random intercept and random slope for dbh varying by species, and nested random intercepts for fires, transects within each fire, and sampling points within each transect to account for the hierarchical sampling design. Note that at each sampling point four trees were sampled. Before fitting each model, we conducted a prior predictive check to ensure that chosen priors were plausible. Weakly informative normal priors on fixed effects, and exponential priors on random effects and standard deviations were evaluated by sampling exclusively from the prior (Tables S1.2 – S.1.4).

Next, we modeled the mediator pathways: fire injury components as a function of treatments and mortality as a function of fire injury components (Figure 1). First we modeled bole char height, percent crown scorch, and percent crown torch as separate outcomes, each as a function of the five treatment predictors. The same fixed and random effects were used, although for bole char a Gaussian family was used, and percent crown scorch and torch were converted to ordinal categorical outcomes (low = 0-49%, moderate = 50-99%, complete = 100%). Percent crown scorch and torch were modeled ordinally due to the uneven distribution of the data, and because initial attempts at modeling the variables continuously (using zero- and one-inflated beta

regressions) resulted in the models failing to converge. Crown scorch and torch were modeled using cumulative logistic regression, which models the probability of an observation falling into or below each ordered category. Each of the ordinal models had the same fixed and random effects structure, and priors were informed by the approximate baseline proportions of trees in each ordinal category, specified as weakly informative normal priors on the logit scale and exponential priors on variance components (Tables S1.5- S1.8).

We also fit four models for the fire injury ~ mortality pathway. First, we fit one tree mortality model including all three tree injury components, then created another three models where mortality was a function of each individual injury component (bole char, percent crown scorch and torch). Effects for each treatment–fire injury component–mortality pathway were quantified by producing a posterior distribution for each predictor. Early investigations showed the tree mortality model including all three tree injury components to outperform all three of the individual mortality ~ tree injury models, so we report on the combined model only (Table S1.8)

Each of the models (1) mortality ~ treatments model, 2-4) the three individual tree injury components ~ treatments models, and 5) the mortality ~ the three tree injury components combined model) were fit using 4 Markov chains, each run for 4,000 iterations. Due to the complex nature of the random-effects structure, the target average proposal acceptance rate (adapt delta) was increased to 0.99 to reduce divergent transitions. We also conducted posterior predictive checks using 'pp_check' to visually verify if the models accurately described the data. Lastly, we compared model performance using leave one out or 'LOO' cross-validation to see which Bayesian model had better out-of-sample predictive accuracy by looking at the ELPD difference, which is the difference in expected log predictive density (Vehtari et al. 2017). Computing the ratio between ELPD difference the standard error difference is like a Z-score like heuristic and can help determine whether one model's predictive performance is distinguishable from another's (Vehtari et al. 2017).

For only the mortality ~ treatments model, we tested if there were any interactions between the five different treatment types. We ran one model with all possible pairwise interactions and examined the posterior distributions to see which, if any, pairwise treatment combinations had interactions.

RESULTS

Overall, areas with thinning and broadcast burns had reduced tree mortality, and tree mortality was largely explained by the fire injury components. For our first research question (what is the effect of various treatments on tree mortality?) we found that thinning and broadcast burns were most effective at reducing tree mortality. Thinning reduced the odds of tree mortality by 54% (b = -0.78, 95% CI = [-1.29, -0.28]), while broadcast burns reduced the odds of tree mortality by 59% (b=-0.89, 95% CI = [-1.68, -0.1]. The 95% percent credible intervals of the posterior distributions for these two treatment types did not cross one (which, on a log odds ratio scale, corresponds to a probability of 0) (Figure 1.4, Table S1.9). The remaining treatment types (piling, pile burning, and mastication) had wider credible intervals and thus more uncertainty around effect on tree mortality. For pile burns, although the credible interval did cross one and could not be interpreted as corresponding to reduced tree mortality, most of the posterior distribution did lie between 0 and 1, meaning that there was still some effect of reduced mortality (Figure 1.4). Both piling and mastication had very wide 95% credible intervals, and the tails of their posterior distribution corresponded to an increase in tree mortality. Every year (>0) that passed since the last treatment prior to the 2021 fire was affiliated with a roughly 2% increase in tree mortality (b= 0.02, 95% CI= [0.24, -0.45]), and additional 25 m distance (the distance between each sampling point along a transect) was affiliated with a 4% decrease in the odds of tree mortality. However, since both 95% credible intervals for the posterior distributions of years since last treatment and distance to

treatment boundary edge were more centered around 1, they could not be interpreted as having a credible effect on tree mortality.

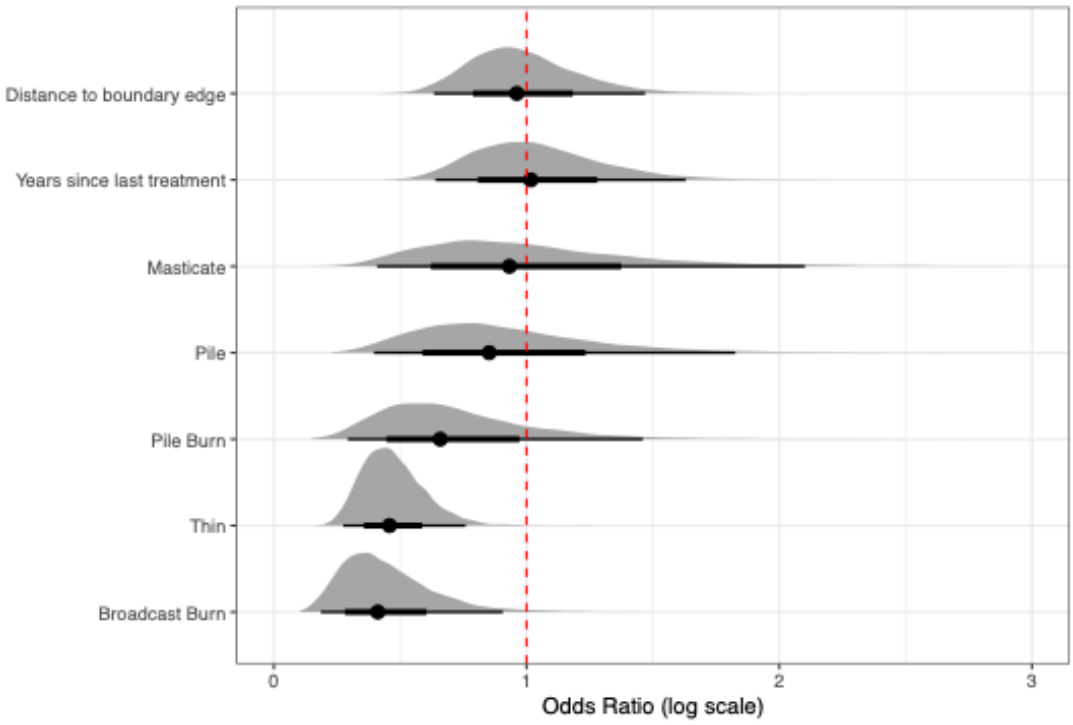


Figure 1.4. Posterior distributions for the tree mortality model as a function of treatments. Distributions show credible intervals for each of the five treatments, distance to treatment boundary edge, and years since last treatment on an odds ratio scale. The inner band reflects the 66% credible interval, and the outer band reflects the 95% credible interval. If the posterior distribution crosses 1, then that variable does not reduce tree mortality.

After running the pairwise treatment interaction model, we did not find any evidence of treatment interactions when looking at all fires pooled together. An important note is that although the 95% credible interval for the interaction between piling fuels and pile burning crossed zero (b = -0.32, 95% CI = [-1.14, 0.53]) such that there was high uncertainty about an interaction effect, the additive effect of the two treatments showed a 90% posterior probability that piling fuels would further reduce mortality if it was followed up by pile burning. When plotting the predicted probability of mortality, piling alone had a similar mortality probability (80 %) to no treatment (82%),

but piling followed with pile burns showed decreased mortality probability to 69% (Figure 1.5, Table S.10). We then separated the dataset by fire and found a treatment interaction in the Dixie fire between thins and broadcast burns. We found that broadcast burns, when following thins, decreased tree mortality more than just thins alone (Figure 1.6, Table S1.11). However, the 95% credible interval does cross zero (-0.94 to 0.13,) mostly in the in the tail of the distribution so there is not strong statistical evidence for the interaction.

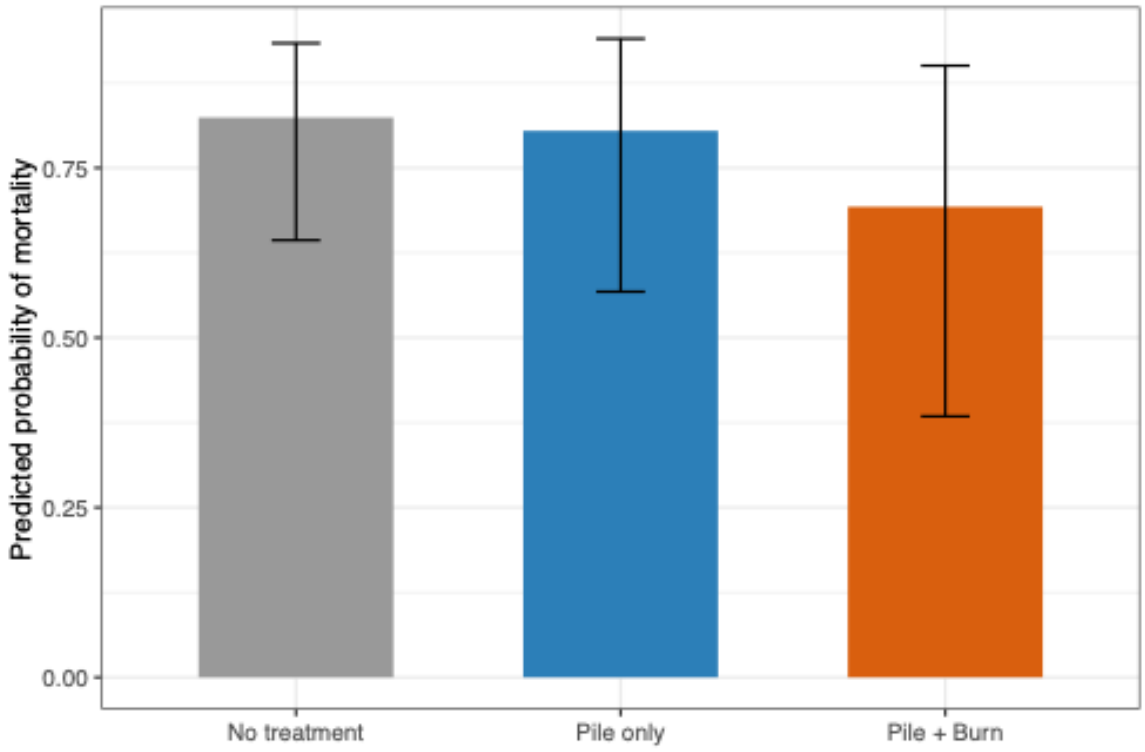


Figure 1.5: Predicted probability of tree mortality in the case of no treatment, fuel piling only, and fuel piling and pile burning. Error bars show the 95% credible interval.

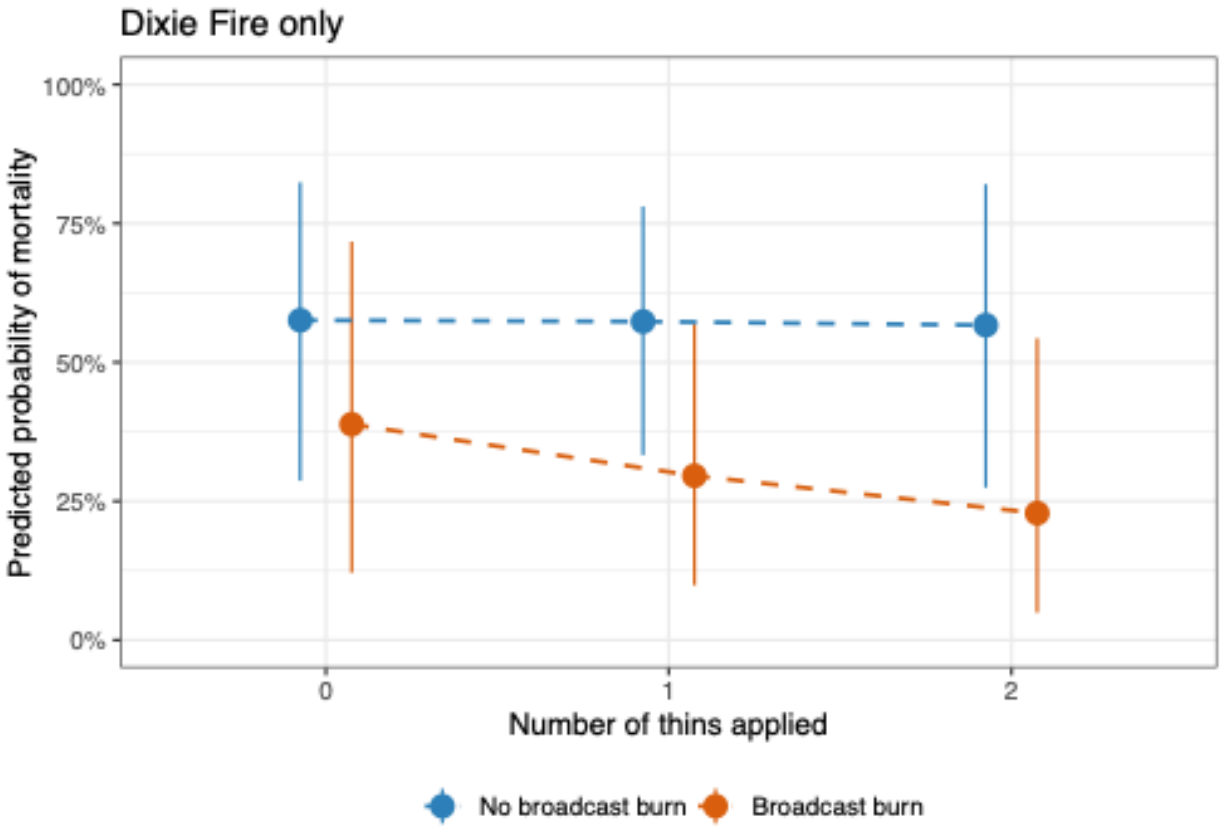


Figure 1.6: The effect of thinning on predicted probability of tree mortality, given no broadcast burn (blue) vs broadcast burn (orange) in the Dixie fire only. Error bars show 95% credible interval.

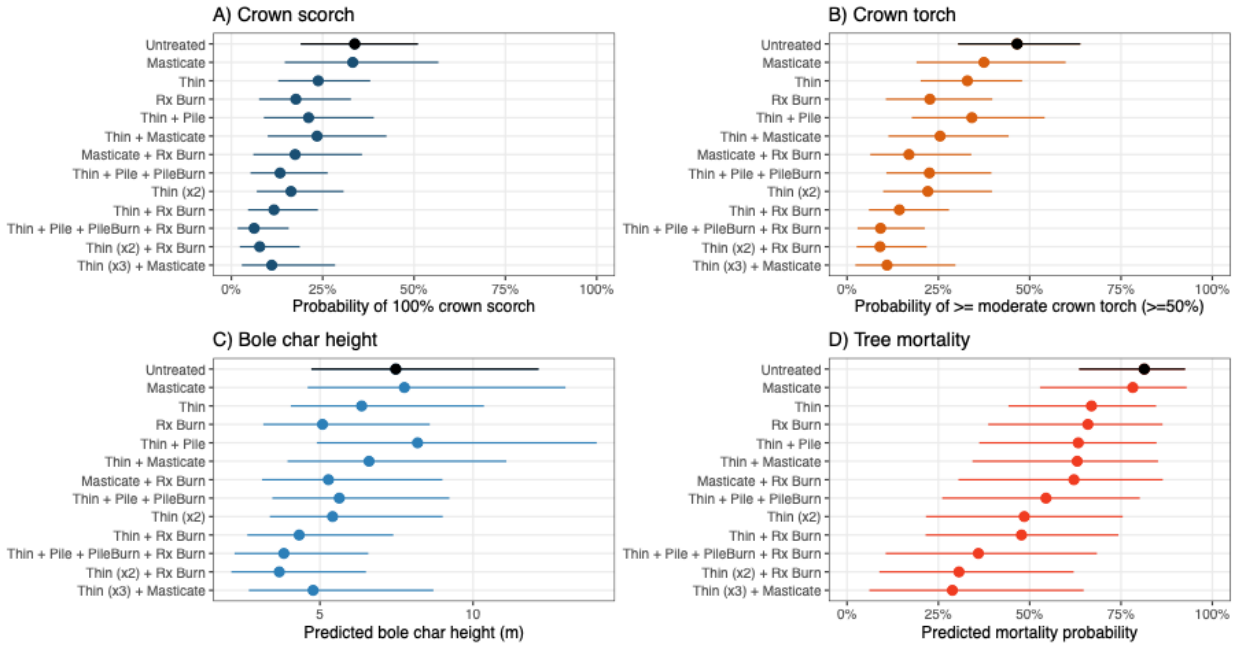


Figure 1.7. Comparison of predicted values of tree injury components (A-C) and tree mortality (D), all as a function of observed treatment types. A) shows estimates of probability of 100% crown scorch (%), B) shows probability of at least moderate crown scorch (%), C) shows predicted bole char height (m) and D) shows tree probability of tree mortality (%). Panels A-C are derived from the three individual tree injury components ~ treatment models, and panel D is derived from the tree mortality ~ treatment model. The error bars show the 95% credible interval.

Next, we examined the effect of treatment type on tree injury components by predicting tree injury component values (Figure 1.7 A-C, Tables S1.12- S1.14) and plotting estimates. For ease of visual comparison, we also plotted tree mortality values (Figure 1.7 D) as a function of treatment types (from the tree mortality ~ treatments model displayed in Figure 1.4). In general, multiple treatments, especially those that included multiple thins followed by some type of burn, corresponded to lower values of tree injury components than single-entry treatment types. In the case of bole char height, thinning and piling fuels led to higher char heights than the untreated control (Figure 1.7 C, Table S1.12). The lowest predicted probability of complete crown scorch corresponded to the "Thin + pile + pile burn + Rx burn" treatment, followed by two thins + Rx burn (Figure 1.7 A, Table S1.13). The multiple thins followed up by either broad cast burn or mastication corresponded to the lowest values for all the tree injury components (Figure 1.7 A-C).

When comparing predicted tree mortality probability to the predicted tree injury component probabilities, we found some similarities and important distinctions. For example, multiple thins followed by broadcast burn or mastication also corresponded to the lowest mortality probability (Figure 1.7 D, Table S1.9). Mastication led to higher average bole chart height than no treatment at all, and only slightly reduced crown scorch, crown torch, and tree mortality compared to no treatment (Figure 1.7 A-D). The confidence intervals for probability of 100% crown scorch were the tightest, followed by crown torch, then bole char height, and the widest for tree mortality, suggesting that the treatment types explain more of the variability in tree injury component estimates.

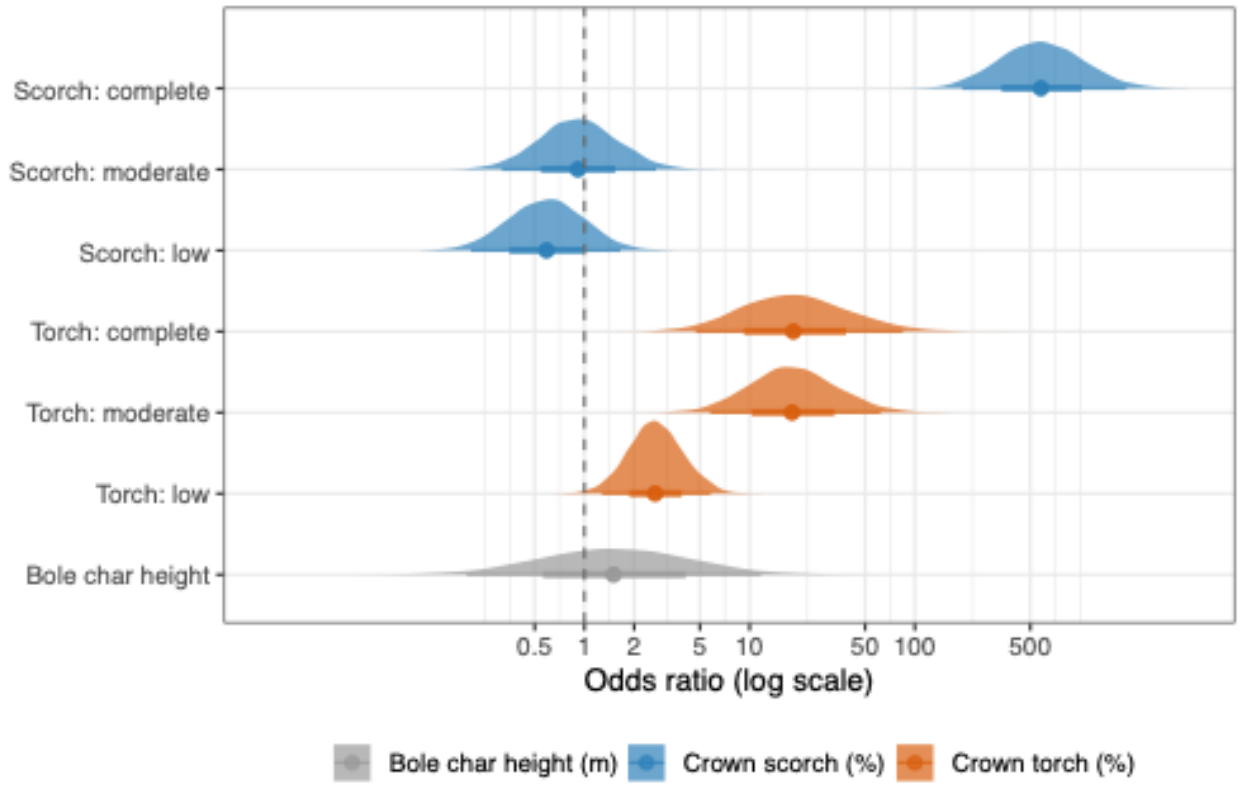


Figure 1.8. Posterior distributions fort the tree mortality model as a function of tree injury components. Scorch and torch percents were modeled on the ordinal scale, with categories of low (0-50%), moderate (51-99%), and complete (100%). Distributions show credible intervals for each of the five treatments, distance to treatment boundary edge, and years since last treatment on an odds ratio scale. The inner band reflects the 66% credible interval, and the outer band reflects the 95% credible interval. If the posterior distribution crosses 1, that is affiliated with increased tree mortality.

When comparing the mortality ~ treatments model to the mortality ~ tree injury components model, we found tree injury components to be stronger predictors of mortality than treatments. Complete scorch was by far the strongest predictor of tree mortality probability, (Figure 1.8, Table S1.15), in that complete or 100% scorch was affiliated with a roughly 500% increased chance of tree mortality relative to information about treatment type alone. Complete, moderate, and low torch were also strong predictors of tree mortality. The 95% credible intervals for the posterior distribution of moderate and low scorch as well as bole char height crossed 1, indicating high uncertainty that they explained tree mortality well. The confidence interval for bole char height was the widest. The ratio between ELPD, (expected log predictive density difference) and the standard error of difference between the mortality ~ treatments model and mortality ~ tree injury model was 12.5, meaning that tree injury explained mortality 12.5 times better than treatment type did.

DISCUSSION

In this study, we used a Bayesian causal approach to quantify the effects of fuel treatments implemented at varying times prior to three 2021 fires in California: the Dixie, Caldor, and Tamarack fires. Across all three fires, thinning and broadcast burning were effective at reducing tree mortality, and combination treatments (multiple thins followed by burning) were most effective. In general, we did not detect treatment interactions except in the case of the Dixie fire. In the Dixie fire, broadcast burning reduced tree mortality when preceded by thinning treatments. The further reduction in tree mortality because of thinning with follow up broadcast burns in the Dixie fire specifically has been documented in another study (Shive et al. 2024), which also noted that mechanical thinning treatments with no follow up fire treatments did not differ from the untreated areas. Additionally, fuels rearrangement treatments, such as thinning and piling fuels but not

burning those piles, corresponded to higher tree injury component measurements like bole char, and were also associated with higher probability of tree mortality. While fuels rearrangement treatments have been documented as leading to amplified fire behavior (Safford et al. 2009, Prichard et al. 2020, Safford and Saberi 2026), this study shows that some treatments (such as mastication and piling) lead to tree mortality outcomes that are worse than doing no treatment at all, a finding that has important implications for managers deciding which treatment types to implement. Given investment by government and land management agencies in fuel treatments as a means of increasing forest resilience to wildfire, evidence that shows that fuel piles must be removed to have an impact is important to justify project funding and increasing workforce capacity.

Our multi-step modeling approach showed that treatments reduce tree mortality by way of tree injury, a mechanism which is generally accepted by researchers and practitioners but has not been explicitly tested in observational fuel treatment studies. Tree injury components, particularly crown scorch, explained most of the mortality reduction effect of treatments. The samples that had the lowest tree mortality had thinning and/or broadcast burns applied to them and had very low values of wildfire-driven crown scorch. Complete or 100% crown scorch was also an incredibly strong predictor of tree mortality, a finding which supports other research suggesting that crown scorch is the most important predictor of fire-caused tree mortality (Sieg et al. 2006, Hood et al. 2018). It is important to note that high levels of crown scorch do not by definition mean certain tree mortality, since buds and meristems have differential survival rates than needles and can still grow back after fire (Hood et al. 2018). Bole char height was not a strong predictor of tree mortality, even though it indicates the amount of heat from the fire and flame height (Hood et al. 2018). That bole char height did not predict tree mortality could be an artifact of our methods: we measured bole char as a visual average across each tree's entire height. This method may have captured brief licks

of flame that were hot enough to leave a char mark but not sustained in duration to cause mortality (Hood et al. 2018). Notably, bole char heights were particularly high for mechanical treatments such as mastication and piling, which substantiates other findings that show increased fireline intensity from residual slash (Stephens et al. 2009, Safford and Saberi 2026).

Our study also showed that information about tree injury is more helpful in predicting tree mortality than information about treatment types alone. LOO cross validation showed the tree injury components to explain tree mortality better than the treatment models and that, combined with the fact that the treatment types explained the tree injury components, suggest that complete crown scorch and crown torch are the main mechanism for tree mortality. By breaking down the pathway from fuel treatment to tree mortality (into fuel treatment → tree injury → tree mortality), finding that treatments reduce tree mortality, and that tree injury components of crown scorch and torch explain the differences in tree mortality, we infer that fuel treatments reduce tree mortality by way of reducing tree injury to the crown. While drivers of fire-induced tree death have been studied before, modeling tree mortality by explicitly linking fuel treatment types to tree injury components and quantifying uncertainty around those effects has not to our knowledge been done before. Our findings about most effective treatment types generally corroborate other studies that show thin and burn treatments reduce fire severity, and in turn, tree mortality the most (Fulé et al. 2012, Martinson and Omi 2013, Kalies and Yocom Kent 2016, Prichard et al. 2020, Brodie et al. 2024, Davis et al. 2024, Shive et al. 2024, Radcliffe et al. 2024), and additionally show that this trend remains consistent even in large, high severity fires that generally burned under extreme weather conditions. Application of our Bayesian causal framework to landscape-level studies can help to elucidate remaining questions about fuel treatment effectiveness at broader spatial scales.

Although statistical uncertainty was high, longer timespans since the last treatment corresponded to an increased probability of tree mortality, and there is much evidence in the

literature to corroborate this finding. Depending on the forest type, the longevity of fuel treatments can vary, but their ability to reduce wildfire severity (and in turn, tree mortality) declines over time (Hood et al. 2020, Davis et al. 2024, Radcliffe et al. 2024). In low-elevation dry forests dominated by ponderosa pine and Douglas-fir, fuel treatments are unlikely to remain effective for longer than historical mean fire return intervals (~20 years, Hood et al. 2020). Additionally, fine and coarse woody fuels remained unchanged between 1 and 7 years after thinning and prescribed burning in mixed conifer forests (Stephens et al. 2012a, Hood et al. 2020). In the Sierra Nevada, fuel loads can exceed pre-treatment levels after 30 years (Keifer et al. 2006). Research in the Northeastern Cascades sites of the Fire and Fire Surrogate study suggest that maintenance treatments are needed 15 years after initial treatments to reduce the potential for tree mortality in subsequent wildfires (Radcliffe et al. 2024). The longevity of fuel treatments can also be extended when they interact with wildfires. In some areas, particularly when fire effects are low to moderate, wildfires can act as a fuels reduction treatment or a maintenance treatment (Collins et al. 2016, Jeronimo et al. 2019, Chamberlain et al. 2023, Low et al. 2023). Further research into how wildfire interactions with fuel treatments impact postfire stand trajectories is needed, and our understanding of this relationship can be improved with finer-grain information on treatment dates and specific fire dates. Furthermore, standardized fuel treatment datasets such as TWIG provide the opportunity to conduct longer-term research on fuel treatment and wildfire interaction impacts.

LIMITATIONS

This study is one of the first of its kind to use a Bayesian causal approach to quantify uncertainty of fuel treatment effectiveness, as well as use a multi-step modeling approach to break down the pathways that go from fuel treatments to tree mortality. Like other fuel treatment effectiveness studies, inference is limited because there were few replicates of specific treatment

combinations. Given that the treatment combinations were sometimes fire-specific (in that there were not completely consistent treatment combinations across all three fires), we were only able to evaluate their impact within the context of the forest type. Furthermore, the treatment combinations were reflective of the forest type and appropriate management style. For example, the fact that treatment interactions were only detected in the Dixie fire is mostly an artifact of specific treatment combinations being inextricable from fire identities (Figure 1.3). The Lake Tahoe Management Basin Unit (LTMBU) is a high-profile recreation area, and there have been multiple thinning treatments with the intention of protecting the WUI that surrounds much of the lake itself. The LTBMU primarily conducts mechanical and/or hand thins and 'creepy pile burns', where fuel piles are ignited and surface fires are allowed to 'creep' from one pile to the next (K. Jacobson, US Forest Service, *pers. comm*.). As a result, the combination of thinning + broadcast burn did not occur in the LTBMU samples. Similarly, the dominance of pinyon-juniper and a generally sparser forest type in the Humboldt-Toiyabe National Forest (where the Tamarack fire occurred) meant that hand thinning was more commonly applied (Alison Paulson, *pers. comm)*. Only one transect sampled in the Tamarack fire had a thinning + fire treatment (Thin, pile, pile burn, broadcast burn), and this was likely why we could not detect a signal with high statistical confidence. While different statistical methods can be employed to try and parse apart treatment effects, descriptive context from managers on the ground can help to explain much of the nuance in results, and local institutional knowledge embedded in this study helped to increase confidence in results. The limited sample size for specific and unique treatment combinations in each fire and/or management can reflect different treatment objectives between WUI and non-WUI areas (Reinhardt et al. 2021), as well as workforce capacity and funding. Although consolidating treatment combinations into coarser categories such as thin and thin + fire can increase the statistical power in detecting treatment effects, disaggregating data can help identify challenges

and opportunities with specific treatment types that would be otherwise impossible. For example, the backlog of fuel piles is a known issue across many public lands, particularly because fuel piles can serve as concentrated ignition points and produce high ember loads when interacting with fire (Barker et al. 2025).

Another limitation of this study is that we did not have exact dates for every specific treatment entry, and, across the three-fire dataset only had information about the date of the most recent treatment (hence the variable years since last treatment). Reliable information about individual treatment dates could help us answer questions about the effect of different time intervals between treatment types, and future work could involve using more unified datasets like TWIG. Additionally, while the transect-based method for field data collection allowed for consistent methods between fires we sampled, it limited us to a linear spatial analysis, and we only collected data on 40 trees per transect. Future studies could increase the spatial scale of this investigation by placing buffers around treatment polygons and adjacent and spatially identical untreated polygons to detect the effect of fuel treatments on tree mortality reduction. Similarly, the limited spatial scale of just three fires meant that we could not meaningfully incorporate day of fire weather into our analyses. This was because for all the LTBMU are and large parts of the Tamarack fire that we sampled, nearly all our sampling points burned in a single day under identical fire weather conditions, while the parts of the Dixie were much further apart from each other and burned under differing fire weather conditions. Increasing the spatial extent of future studies to include dozens or even hundreds of fires could allow for a statistically powerful assessment of the impact of day-of fire weather.

Finally, although the credible interval for the effect of distance from treatment boundary edge on tree mortality crossed zero, trees in treated areas located further from the treatment boundary were associated with a lower probability of mortality. The limited statistical evidence of

this trend is likely in part because two transects in both the Caldor and Tamarack fires were treated on both sides (albeit with different treatment types, which is why they were retained in the dataset for analysis), so the signal attenuation of tree mortality was likely more difficult to detect. In addition, the transects were only 225 meters long, which may not be long enough to detect a reduction in tree mortality. Despite this, other studies have shown similar trends of reduced tree mortality along an untreated-treated transect (Safford et al. 2009, Safford et al. 2012, Saberi and Safford 2026). Given that the landscape effects of fuel treatments (that is, the effects of fuel treatments beyond the treatment boundary) are of high interest to both managers and researchers, future studies which either extend the length of the field transect or utilize geographic information systems and remote sensing methods to detect signal attenuation are needed.

CONCLUSION

In conclusion, this investigation is one of the first of its kind to use a Bayesian causal modeling approach to quantify fuel treatment effectiveness. We sampled three very large fires in California with varied treatment histories. While the treatment combinations were confounded with each unique fire and forest type, our approach corroborates other findings that thinning and broadcast burning, along with repeat treatments, are the most effective at reducing tree mortality. We also found that on its own, mastication was the least effective treatment type in reducing tree mortality. We used a piecewise modeling approach to breakdown the causal pathways of the treatment effect and found that tree injury components of crown scorch and torch explain why the treatments reduce tree mortality, which has never been explicitly done before. We also highlight the importance of removing fuels from the landscape, as piling fuels without burning them led to higher estimates of bole char height. While we were unable to interpret findings outside the context of this set of fires, this analysis framework can be a starting point for future investigations

conducted on larger spatial and temporal scales. Our reporting of treatment effect on the odds ratio of tree mortality may be particularly helpful to managers interested in understanding how much specific treatment types reduce the probability of tree mortality, as that is often a desired outcome in addition to other restoration goals. As more land management agencies invest in implementing fuel treatments and monitoring outcomes, this analysis framework can be used as a powerful tool for quantifying the effects of fuel treatments that interact with wildfires and their impacts on forest stands across the North American West.

REFERENCES

Agee, J.K., Skinner, C.N., 2005. Basic principles of forest fuel reduction treatments. Forest Ecology and Management, Relative Risk Assessments for Decision –Making Related To Uncharacteristic Wildfire 211, 83–96. https://doi.org/10.1016/j.foreco.2005.01.034

Arif, S., MacNeil, M.A., 2023. Applying the structural causal model framework for observational causal inference in ecology. Ecological Monographs 93, e1554. https://doi.org/10.1002/ecm.1554

Baker, B.C., Hanson, C.T., 2022. Cumulative Tree Mortality from Commercial Thinning and a Large Wildfire in the Sierra Nevada, California. Land 11, 995. https://doi.org/10.3390/land11070995

Barker, J., Voorhis, J., Crotty, S.M., 2025. Assessing costs and constraints of forest residue disposal by pile burning. Front. For. Glob. Change 7. https://doi.org/10.3389/ffgc.2024.1496190

Brodie, E.G., Knapp, E.E., Brooks, W.R., Drury, S.A., Ritchie, M.W., 2024. Forest thinning and prescribed burning treatments reduce wildfire severity and buffer the impacts of severe fire weather. Fire Ecology 20, 17. https://doi.org/10.1186/s42408-023-00241-z

Bürkner, P.-C., 2017. brms: An R Package for Bayesian Multilevel Models Using Stan. Journal of Statistical Software 80, 1–28. https://doi.org/10.18637/jss.v080.i01

California Wildfire and Forest Resilience Task Force, 2026. California Wildfire and Landscape Resilience Interagency Treatment Dashboard. State of California. Available at: wildfiretaskforce.org /treatment-dashboard. Accessed 2 August 2026.

Cal Fire. 2021. Caldor Fire, California Department of Forestry and Fire Protection. Available at: https://www.fire.ca.gov/incidents/2021/8/14/caldor-fire/. Accessed 17 August 2024.

Cal Fire. 2024. Top 20 Largest California Wildfires. Available at: https://www.fire.ca.gov/our-impact/statistics. Accessed 17 August 2024.

Call, A., Tomczyk, N., Withnall, K.A., Dappen, P.R., Heusinkveld, D., Mueller, S., Holloway, B., Shennan, K., Herring, J., Franko, A., Colavito, M.M., Kimple, A.D., Meador, A.S., Stevens-Rumann, C.S., 2025. A new geodatabase of fuel treatments across federal lands in the USA. Sci Data 12, 1485. https://doi.org/10.1038/s41597-025-05859-z

Chabria, A., and Wigglesworth A. 2021. 'California and Federal Officials Disagree on Letting Some Wildfires Burn. *Los Angeles Times*, August 1, 2021.

Chamberlain, C.P., Cova, G.R., Cansler, C.A., North, M.P., Meyer, M.D., Jeronimo, S.M.A., Kane, V.R., 2023. Consistently heterogeneous structures observed at multiple spatial scales across fire-intact reference sites. Forest Ecology and Management 550, 121478. https://doi.org/10.1016/j.foreco.2023.121478

Collins, B.M., Lydersen, J.M., Fry, D.L., Wilkin, K., Moody, T., Stephens, S.L., 2016. Variability in vegetation and surface fuels across mixed-conifer-dominated landscapes with over 40 years of natural fire. Forest Ecology and Management 381, 74–83. https://doi.org/10.1016/j.foreco.2016.09.010

Davis, K.T., Peeler, J., Fargione, J., Haugo, R.D., Metlen, K.L., Robles, M.D., Woolley, T., 2024. Tamm review: A meta-analysis of thinning, prescribed fire, and wildfire effects on subsequent wildfire severity in conifer dominated forests of the Western US. Forest Ecology and Management 561, 121885. https://doi.org/10.1016/j.foreco.2024.121885

Dettinger, M.D., Alpert, H., Battles, J.J., Kusel, J., Safford, H., Fougeres, D., Knight, C., Miller, L., Sawyer, S., 2018. Sierra Nevada summary report. California's Fourth Climate Change Assessment (No. SUM-CCCA4-2018-004). California Energy Commission/Natural Resources Agency.

Fallon, K., Abatzoglou, J.T., Hurteau, M.D., Butz, R.J., Buchanan, B., Pierce, J., McNamara, J., Cattau, M., Seydi, S.T., Sadegh, M., 2025. A novel methodology to assess fuel treatment effectiveness: application to California's forests. International Journal of Wildland Fire 34, WF24220. https://doi.org/10.1071/WF24220

Fulé, P.Z., Crouse, J.E., Roccaforte, J.P., Kalies, E.L., 2012. Do thinning and/or burning treatments in western USA ponderosa or Jeffrey pine-dominated forests help restore natural fire behavior? Forest Ecology and Management 269, 68–81. https://doi.org/10.1016/j.foreco.2011.12.025

Grupenhoff, A.R., Young, D.J.N., Barbato, M., Latimer, A.M., 2025. Evaluating short-term effects of fuel treatments on fuel loading in western US dry conifer forests: A meta-analysis. Forest Ecology and Management 590, 122808. https://doi.org/10.1016/j.foreco.2025.122808

Hood, S.M., Varner, J.M., Mantgem, P. van, Cansler, C.A., 2018. Fire and tree death: understanding and improving modeling of fire-induced tree mortality. Environ. Res. Lett. 13, 113004. https://doi.org/10.1088/1748-9326/aae934

Hood, S.M., Keyes, C.R., Bowen, K.J., Lutes, D.C., Seielstad, C., 2020. Fuel Treatment Longevity in Ponderosa Pine-Dominated Forest 24 Years After Cutting and Prescribed Burning. Front. For. Glob. Change 3. https://doi.org/10.3389/ffgc.2020.00078

Jain, T., Battaglia, M., Han, H.-S., Graham, R., Keyes, C., Fried, J., Sandquist, J., 2012. A Comprehensive Guide to Fuel Management Practices for Dry Mixed Conifer Forests in the Northwestern United States. Joint Fire Science Program Synthesis Reports.

Jeronimo, S.M.A., Kane, V.R., Churchill, D.J., Lutz, J.A., North, M.P., Asner, G.P., Franklin, J.F., 2019. Forest structure and pattern vary by climate and landform across active-fire landscapes in the montane Sierra Nevada. Forest Ecology and Management 437, 70–86. https://doi.org/10.1016/j.foreco.2019.01.033

Kalies, E.L., Yocom Kent, L.L., 2016. Tamm Review: Are fuel treatments effective at achieving ecological and social objectives? A systematic review. Forest Ecology and Management 375, 84–95. https://doi.org/10.1016/j.foreco.2016.05.021

Knight, C.A., Tompkins, R.E., Wang, J.A., York, R., Goulden, M.L., Battles, J.J., 2022. Accurate tracking of forest activity key to multi-jurisdictional management goals: A case study in California. Journal of Environmental Management 302, 114083. https://doi.org/10.1016/j.jenvman.2021.114083

Low, K.E., Battles, J.J., Tompkins, R.E., Dillingham, C.P., Stephens, S.L., Collins, B.M., 2023. Shaded fuel breaks create wildfire-resilient forest stands: lessons from a long-term study in the Sierra Nevada. Fire Ecology 19, 29. https://doi.org/10.1186/s42408-023-00187-2

Martinson, E., Omi, P., 2013. Fuel Treatments and Fire Severity: A Meta-Analysis. Joint Fire Science Program Synthesis Reports. RMRS-RP-103WWW.

McIver, J.D., Boerner, R.E.J., Hart, S.C., 2008. The national fire and fire surrogate study: Ecological consequences of alternative fuel reduction methods in seasonally dry forests. Forest Ecology and Management 255, 3075–3080. https://doi.org/10.1016/j.foreco.2008.01.035

McKinney, S.T., Abrahamson, I., Jain, T., Anderson, N., 2022. A systematic review of empirical evidence for landscape-level fuel treatment effectiveness. Fire Ecology 18, 21. https://doi.org/10.1186/s42408-022-00146-3

Pollet, J., Omi, P.N., 2002. Effect of thinning and prescribed burning on crown fire severity in ponderosa pine forests. International Journal of Wildland Fire 11, 1–10. https://doi.org/10.1071/wf01045

Potter, C., Owusu, S., 2026. Does Private Forest Land Management Result in Higher Burn Severity from Wildfires in Timberlands of the Pacific States? Open Journal of Forestry 16, 202–222. https://doi.org/10.4236/ojf.2026.163013

Povak, N.A., Kane, V.R., Collins, B.M., Lydersen, J.M., Kane, J.T., 2020. Multi-scaled drivers of severity patterns vary across land ownerships for the 2013 Rim Fire, California. Landscape Ecol 35, 293–318. https://doi.org/10.1007/s10980-019-00947-z

Prichard, S.J., Stevens-Rumann, C.S., Hessburg, P.F., 2017. Tamm Review: Shifting global fire regimes: Lessons from reburns and research needs. Forest Ecology and Management 396, 217–233. https://doi.org/10.1016/j.foreco.2017.03.035

Prichard, S.J., Povak, N.A., Kennedy, M.C., Peterson, D.W., 2020. Fuel treatment effectiveness in the context of landform, vegetation, and large, wind-driven wildfires. Ecological Applications 30, e02104. https://doi.org/10.1002/eap.2104

Prichard, S.J., Hessburg, P.F., Hagmann, R.K., Povak, N.A., Dobrowski, S.Z., Hurteau, M.D., Kane, V.R., Keane, R.E., Kobziar, L.N., Kolden, C.A., North, M., Parks, S.A., Safford, H.D., Stevens, J.T., Yocom, L.L., Churchill, D.J., Gray, R.W., Huffman, D.W., Lake, F.K., Khatri-Chhetri, P., 2021. Adapting western North American forests to climate change and wildfires: 10 common questions. Ecological Applications 31, e02433. https://doi.org/10.1002/eap.2433

Radcliffe, D.C., Bakker, J.D., Churchill, D.J., Alvarado, E.C., Peterson, D.W., Laughlin, M.M., Harvey, B.J., 2024. How are long-term stand structure, fuel profiles, and potential fire behavior affected by fuel treatment type and intensity in Interior Pacific Northwest forests? Forest Ecology and Management 553, 121594. https://doi.org/10.1016/j.foreco.2023.121594

Reinhardt, E.D., Keane, R.E., Calkin, D.E., Cohen, J.D., 2008. Objectives and considerations for wildland fuel treatment in forested ecosystems of the interior western United States. Forest Ecology and Management 256, 1997–2006. https://doi.org/10.1016/j.foreco.2008.09.016

Safford, H.D., Schmidt, D.A., Carlson, C.H., 2009. Effects of fuel treatments on fire severity in an area of wildland–urban interface, Angora Fire, Lake Tahoe Basin, California. Forest Ecology and Management 258, 773–787. https://doi.org/10.1016/j.foreco.2009.05.024

Safford, H.D., Stevens, J.T., Merriam, K., Meyer, M.D., Latimer, A.M., 2012. Fuel treatment effectiveness in California yellow pine and mixed conifer forests. Forest Ecology and Management 274, 17–28. https://doi.org/10.1016/j.foreco.2012.02.013

Safford, H.D., Stevens, J.T., 2017. Natural range of variation for yellow pine and mixed-conifer forests in the Sierra Nevada, southern Cascades, and Modoc and Inyo National Forests, California, USA. General Technical Report PSW-GTR-256. Albany, CA: U.S. Department of Agriculture, Forest Service, Pacific Southwest Research Station. https://doi.org/10.2737/PSW-GTR-256.

Safford, H.D., Butz, R.J., Bohlman, G.N., Coppoletta, M., Estes, B.L., Gross, S.E., Merriam, K.E., Meyer, M.D., Molinari, N.A., Wuenschel, A., 2021. Fire Ecology of the North American

Mediterranean-Climate Zone, in: Greenberg, C.H., Collins, B. (Eds.), Fire Ecology and Management: Past, Present, and Future of US Forested Ecosystems, Managing Forest Ecosystems. Springer International Publishing, Cham, pp. 337–392. https://doi.org/10.1007/978-3-030-73267-7_9

Safford, H.D., Saberi, S., 2026. Fuel treatment effects on fire severity during the Caldor Fire (2021), Lake Tahoe, California, USA. Forest Ecology and Management 603, 123424. https://doi.org/10.1016/j.foreco.2025.123424

Seidl, R., Thom, D., Kautz, M., Martin-Benito, D., Peltoniemi, M., Vacchiano, G., Wild, J., Ascoli, D., Petr, M., Honkaniemi, J., Lexer, M.J., Trotsiuk, V., Mairota, P., Svoboda, M., Fabrika, M., Nagel, T.A., Reyer, C.P.O., 2017. Forest disturbances under climate change. Nature Clim Change 7, 395–402. https://doi.org/10.1038/nclimate3303

Schmidt, D.A., Taylor, A.H., Skinner, C.N., 2008. The influence of fuels treatment and landscape arrangement on simulated fire behavior, Southern Cascade range, California. Forest Ecology and Management 255, 3170–3184. https://doi.org/10.1016/j.foreco.2008.01.023

Sieg, H. C., McMillin, J.D., Fowler, J.F., Allen, K.K., Negron, J.F., Wadleigh, L.L., Anhold, J.A., Gibson, K.E., 2006. Best Predictors for Postfire Mortality of Ponderosa Pine Trees in the Intermountain West. Forest Science 52, 718–728. https://doi.org/10.1093/forestscience/52.6.718

Simler-Williamson, A.B., Germino, M.J., 2022. Statistical considerations of nonrandom treatment applications reveal region-wide benefits of widespread post-fire restoration action. Nature Communications 13, 3472. https://doi.org/10.1038/s41467-022-31102-z

Shive, K.L., Coppoletta, M., Wayman, R.B., Paulson, A.K., Wilson, K.N., Abatzaglou, J.T., Saberi, S.J., Estes, B., Safford, H.D., 2024. Thinning with follow-up burning treatments have increased effectiveness at reducing severity in California's largest wildfire. Forest Ecology and Management 572, 122171. https://doi.org/10.1016/j.foreco.2024.122171

Steel, Z.L., Koontz, M.J., Safford, H.D., 2018. The changing landscape of wildfire: burn pattern trends and implications for California's yellow pine and mixed conifer forests. Landscape Ecol 33, 1159–1176. https://doi.org/10.1007/s10980-018-0665-5

Stephens, S.L., Moghaddas, J.J., 2005. Experimental fuel treatment impacts on forest structure, potential fire behavior, and predicted tree mortality in a California mixed conifer forest. Forest Ecology and Management 215, 21–36. https://doi.org/10.1016/j.foreco.2005.03.070

Stephens, S.L., Moghaddas, J.J., Edminster, C., Fiedler, C.E., Haase, S., Harrington, M., Keeley, J.E., Knapp, E.E., McIver, J.D., Metlen, K., Skinner, C.N., Youngblood, A., 2009. Fire treatment effects on vegetation structure, fuels, and potential fire severity in western U.S. forests. Ecological Applications 19, 305–320. https://doi.org/10.1890/07-1755.1

Stephens, S.L., McIver, J.D., Boerner, R.E.J., Fettig, C.J., Fontaine, J.B., Hartsough, B.R., Kennedy, P.L., Schwilk, D.W., 2012a. The Effects of Forest Fuel-Reduction Treatments in the United States. BioScience 62, 549–560. https://doi.org/10.1525/bio.2012.62.6.6

Stephens, S.L., Collins, B.M., Roller, G., 2012b. Fuel treatment longevity in a Sierra Nevada mixed conifer forest. Forest Ecology and Management 285, 204–212. https://doi.org/10.1016/j.foreco.2012.08.030

Stephens, S.L., Agee, J.K., Fulé, P.Z., North, M.P., Romme, W.H., Swetnam, T.W., Turner, M.G., 2013. Managing Forests and Fire in Changing Climates. Science 342, 41–42. https://doi.org/10.1126/science.1240294

Stephens, S.L., Bernal, A.A., Collins, B.M., Finney, M.A., Lautenberger, C., Saah, D., 2022. Mass fire behavior created by extensive tree mortality and high tree density not predicted by operational fire behavior models in the southern Sierra Nevada. Forest Ecology and Management 518, 120258. https://doi.org/10.1016/j.foreco.2022.120258

Stephenson, N.L., Soderberg, D.N., Flickinger, J.A., Caprio, A.C., Das, A.J., 2024. Effects of recent wildfires on giant sequoia groves were anomalous at millennial timescales: a response to Hanson et al. Fire Ecology 20, 89. https://doi.org/10.1186/s42408-024-00316-5

Stevens, J.T., Collins, B.M., Miller, J.D., North, M.P., Stephens, S.L., 2017. Changing spatial patterns of stand-replacing fire in California conifer forests. Forest Ecology and Management 406, 28–36. https://doi.org/10.1016/j.foreco.2017.08.051

U.S. Geological Survey, U.S. Dept. of Interior, and U.S. Department of Agriculture Forest Service 2026. Monitoring Trends in Burn Severity (MTBS). Available at: https://www.mtbs.gov. Accessed: 1 August 2022.

USDA Forest Service. 2026 FSGeodata Clearinghouse, Forest Activities Tracking System. Available at: https://data.fs.usda.gov/geodata/edw/datasets.php?dsetParent=Activities. Accessed 1 Aug 2022.

Van de Water, K.M., Safford, H.D., 2011. A Summary of Fire Frequency Estimates for California Vegetation before Euro-American Settlement. Fire Ecology 7, 26–58. https://doi.org/10.4996/fireecology.0703026

Vehtari, A., Gelman, A., Gabry, J., 2017. Practical Bayesian model evaluation using leave-one-out cross-validation and WAIC. Statistical Computing 27, 1413–1432. https://doi.org/10.1007/s11222-016-9696-4

Vinyeta, K., 2022. Under the guise of science: how the US Forest Service deployed settler colonial and racist logics to advance an unsubstantiated fire suppression agenda. Environmental Sociology 8, 134–148. https://doi.org/10.1080/23251042.2021.1987608

Waldrop, T.A., Yaussy, D.A., Phillips, R.J., Hutchinson, T.A., Brudnak, L., Boerner, R.E.J., 2008. Fuel reduction treatments affect stand structure of hardwood forests in Western North Carolina and Southern Ohio, USA. Forest Ecology and Management 255, 3117–3129. https://doi.org/10.1016/j.foreco.2007.11.010

Webster, K.M., Halpern, C.B., 2010. Long-term vegetation responses to reintroduction and repeated use of fire in mixed-conifer forests of the Sierra Nevada. Ecosphere 1, art9. https://doi.org/10.1890/ES10-00018.1

Westerling, A.L., 2016. Increasing western US forest wildfire activity: sensitivity to changes in the timing of spring. Philosophical Transactions of the Royal Society B: Biological Sciences 371, 20150178. https://doi.org/10.1098/rstb.2015.0178

Whitman, E., Batllori, E., Parisien, M.-A., Miller, C., Coop, J.D., Krawchuk, M.A., Chong, G.W., Haire, S.L., 2015. The climate space of fire regimes in north-western North America. Journal of Biogeography 42, 1736–1749. https://doi.org/10.1111/jbi.12533

Williams, A.P., Abatzoglou, J.T., Gershunov, A., Guzman-Morales, J., Bishop, D.A., Balch, J.K., Lettenmaier, D.P., 2019. Observed Impacts of Anthropogenic Climate Change on Wildfire in California. Earth's Future 7, 892–910. https://doi.org/10.1029/2019EF001210

Woolley, T., Shaw, D.C., Ganio, L.M., Fitzgerald, S., 2011. A review of logistic regression models used to predict post-fire tree mortality of western North American conifers. Int J Wildland Fire 21, 1–35. https://doi.org/10.1071/WF09039

Youngblood, A., Wright, C.S., Ottmar, R.D., McIver, J.D., 2008. Changes in fuelbed characteristics and resulting fire potentials after fuel reduction treatments in dry forests of the Blue Mountains, northeastern Oregon. Forest Ecology and Management 255, 3151–3169. https://doi.org/10.1016/j.foreco.2007.09.032

SUPPLEMENTARY INFORMATION (S1)

Table S1.1. Disaggregation of transect points sampled for each combination of treatments. The 'thin' category had some instances of multiple treatments (1,2,3 refer to the number of times the treatment was applied). At each transect point, four trees were sampled.

Thin	Pile	Masticate	Pile Burn	Rx Burn	Number of points sampled		
0	0	0	0	0	75	115	75
1	0	**1**	0	0	3	0	0
1	**1**	0	0	0	37	0	0
1	**1**	0	**1**	0	40	0	25
3	0	**1**	0	0	15	0	0
1	0	0	0	0	0	35	0
1	0	0	0	**1**	0	15	0
2	0	0	0	0	0	50	0
2	0	0	0	**1**	0	15	0
0	0	0	0	**1**	0	0	15
0	0	**1**	0	0	0	0	10
0	0	**1**	0	**1**	0	0	25
1	**1**	0	**1**	**1**	0	0	10

39

Table S1.2. Prior distributions specified for the Bayesian generalized additive mixed model of tree mortality as a function of treatment types. Normal (0, 0.5) prior on the intercept was not assigned to individual coefficients, so it applies uniformly to all population-level terms, including the penalized coefficient of the DBH$^+$ smooth. The exponential (4) sd prior with no group argument was used as the default for the Species-level intercept/slope and for FireID: TransectID and FireID: TransectID: Point standard deviations. The correlation between the Species-level intercept and DBH$^+$ slope retained the brms default. $^+$denotes that the variable was scaled.

Parameter class	**Model term**	**Prior**
Population-level (fixed) effects	All predictors (shared prior): Thin, Pile, Masticate, Pile Burn, Broadcast Burn, Years since last treatment$^+$, Distance to boundary edge$^+$, DBH$^+$	Normal (0, 0.5)
Intercept	Intercept (baseline log-odds of survival)	Normal (0.7, 0.5)
Smooth terms	Smoothing SD (sds) for DBH$^+$	Student-t (3, 0, 2.5)
Group-level (random) effects – SD		
	Species (intercept, DBH$^+$ slope)	Exponential (4)
	FireID: TransectID	Exponential (4)
	FireID: TransectID: Point	Exponential (4)
	FireID	Exponential (2)

Table S1.3. Prior distributions specified for the Bayesian generalized additive mixed model of tree mortality as a function of treatment types, with an interaction between pile and pile burns. Normal (0, 0.5) prior on the intercept was not assigned to individual coefficients, so it applies uniformly to all population-level terms, including the penalized coefficient of the DBH$^+$ smooth. The exponential (4) sd prior with no group argument was used as the default for the Species-level intercept/slope and for FireID: TransectID and FireID: TransectID: Point standard deviations. The correlation between the Species-level intercept and DBH$^+$ slope retained the brms default. $^+$denotes that the variable was scaled.

Parameter class	**Model term**	**Prior**
Population-level (fixed) effects	All predictors (shared prior): Thin, Pile, Masticate, Pile Burn, Broadcast Burn, Years since last treatment$^+$, Distance to boundary edge$^+$, DBH$^+$, Pile: Pile Burn	Normal (0, 0.5)
Intercept	Intercept (baseline log-odds of survival)	Normal (0.7, 0.5)
Smooth terms	Smoothing SD (sds) for DBH$^+$	Student-t (3, 0, 2.5)
Group-level (random) effects – SD		
	Species (intercept, DBH$^+$ slope)	Exponential (4)
	FireID: TransectID	Exponential (4)
	FireID: TransectID: Point	Exponential (4)
	FireID	Exponential (2)

Table S1.4. Prior distributions specified for the Bayesian generalized additive mixed model of tree mortality as a function of treatments, with data restricted to only the Dixie fire, and with an interaction between thins and broadcast burns. Normal (0, 0.5) prior on the intercept was not assigned to individual coefficients, so it applies uniformly to all population-level terms, including the penalized coefficient of the DBH⁺ smooth. The Thin: Broadcast Burn interaction was given its own, more tightly regularizing prior, normal (0, 0.3). The exponential (4) sd prior with no group argument was used for all group-level standard deviations (Species intercept/slope, TransectID, and TransectID: Point), since no group-specific overrides were set. The correlation between the Species-level intercept and dbh_scaled slope retained the brms default prior, LKJ (1).

Parameter class	**Model term**	**Prior**
Population-level (fixed) effects	All predictors (shared prior): Thin, Pile, Masticate, Pile Burn, Broadcast Burn, Years since last treatment⁺, Distance to boundary edge⁺, DBH⁺	Normal (0, 0.5)
	Thin: Broadcast Burn (interaction)	Normal (0, 0.3)
Intercept	Intercept (baseline log-odds of survival)	Normal (0.7, 0.5)
Smooth terms	Smoothing SD (sds) for DBH⁺	Student-t (3, 0, 2.5)
Group-level (random) effects – SD		
	Species (intercept, dbh slope)	Exponential (4)
	TransectID	Exponential (4)
	TransectID: Point	Exponential (4)

Table S1.5. Prior distributions specified for the Bayesian generalized additive mixed model of bole char height (log-transformed) as function of treatment types. The response variable, bole char height (m), is a log-transformed continuous measure modeled with a Gaussian family, so this model includes an explicit prior on the residual scale (sigma) in addition to the mean-structure priors. The normal (0, 0.5) prior on the intercept was not assigned to individual coefficients and so applies uniformly to all population-level terms, including the dbh_scaled smooth coefficient. The exponential (4) sd prior with no group argument was used as the default for the Species-level intercept/slope and for FireID: TransectID and FireID: TransectID: Point standard deviations. The correlation between the Species-level intercept and dbh_scaled slope retained the brms default prior.

Parameter class	**Model term**	**Prior**
Population-level (fixed) effects	All predictors (shared prior): Thin, Pile, Masticate, Pile Burn, Broadcast Burn, Years since last treatment^{+}, Distance to boundary edge^{+}, DBH^{+}	Normal (0, 0.5)
Intercept	Intercept (baseline log bole char height)	Normal (1.71, 0.5)
Smooth terms	Smoothing SD (sds) for DBH^{+}	Student-t (3, 0, 2.5)
Group-level (random) effects – SD		
	Species (intercept, DBH^{+} slope)	Exponential (4)
	FireID: TransectID	Exponential (4)
	FireID: TransectID: Point	Exponential (4)
	FireID	Exponential (2)
Residual scale	sigma (residual SD of log bole char height)	Normal (1.27, 0.5)

Table S1.6. Prior distributions specified for the Bayesian ordinal (cumulative-link) generalized additive mixed model of crown scorch as a function of treatment types. Here, *s*corch is an ordinal outcome modeled with a cumulative-link (proportional-odds) model; the three intercepts correspond to the K − 1 = 3 category thresholds. The Normal (0, 0.5) prior on class = "b" was not assigned to individual coefficients, so it applies uniformly to all population-level terms, including the penalized coefficient of the dbh_scaled smooth. The exponential (4) sd prior with no group argument was used as the default for the Species-level intercept and slope standard deviations, since no group-specific override was set for that term; FireID: TransectID and FireID: TransectID: Point were each given explicit Exponential (4) priors. The correlation between the Species-level intercept and dbh_scaled slope retained the brms default prior, LKJ (1).

Parameter class	**Model term**	**Prior**
Population-level (fixed) effects	All predictors (shared prior): Thin, Pile, Masticate, Pile Burn, Broadcast Burn, Years since last treatment^{+}, Distance to boundary edge^{+}, DBH^{+}	Normal (0, 0.5)
Ordinal thresholds (Intercepts)	Threshold 1 (none – low scorch)	Normal (−3.35, 0.5)
	Threshold 2 (low – moderate scorch)	Normal (−1.45, 0.5)
	Threshold 3 (moderate – complete torch)	Normal (−0.63, 0.5)
Smooth terms	Smoothing SD (sds) for DBH+	Student-t (3, 0, 2.5)
Group-level (random) effects – SD		
	Species (intercept, DBH^{+} slope)	Exponential (4)
	FireID: TransectID	Exponential (4)
	FireID: TransectID: Point	Exponential (4)
	FireID	Exponential (2)

Table S1.7. Prior distributions specified for the Bayesian ordinal (cumulative-link) generalized additive mixed model of crown torch as a function of treatment types. Here, torch is an ordinal outcome modeled with a cumulative-link (proportional-odds) model; the three intercepts correspond to the K − 1 = 3 category thresholds. All continuous predictors were standardized (mean = 0, SD = 1) prior to model fitting; priors are expressed on the logit scale. The Normal (0, 0.5) prior on the intercept was not assigned to individual coefficients, and applies uniformly to all population-level terms, including the penalized coefficient of the scaled DBH smooth. The exponential (4) sd prior with no group argument was used as the default for the Species-level intercept and slope standard deviations. The correlation between the Species-level intercept and DBH (scaled) slope retained the brms default prior.

Parameter class	**Model term**	**Prior**
Population-level (fixed) effects	All predictors (shared prior): Thin, Pile, Masticate, Pile Burn, Broadcast Burn, Years since last treatment^{+}, Distance to boundary edge^{+}, DBH^{+}	Normal (0, 0.5)
Ordinal thresholds (Intercepts)		
	Threshold 1 (none – low torch)	Normal (−0.51, 0.5)
	Threshold 2 (low – moderate torch)	Normal (0.37, 0.5)
	Threshold 3 (moderate – complete torch)	Normal (1.19, 0.5)
Smooth terms	Smoothing SD (sds) for DBH+	Student-t (3, 0, 2.5)
Group-level (random) effects – SD		
	Species (intercept, dbh slope)	Exponential (4)
	FireID	Exponential (2)
	FireID: TransectID	Exponential (4)
	FireID: TransectID: Point	Exponential (4)

Table S1.8. Prior distributions specified for the Bayesian generalized additive mixed model of postfire tree mortality as a function of all tree injury components. All continuous predictors were standardized (mean = 0, SD = 1) prior to model fitting; priors are expressed on the logit scale. The exponential (4) sd prior with no group argument was used as the default for the Species-level intercept and slope standard deviations. The correlation between the Species-level intercept and DBH (scaled) slope retained the brms default prior.

Parameter class	**Model term**	**Prior**
Intercept	Intercept (baseline log-odds)	Normal (1, 1)
Population-level (fixed) effects		
	Scorch: low	Normal (0, 1)
	Scorch: moderate	Normal (1, 1)
	Scorch: complete	Normal (4, 1)
	Torch: low	Normal (0, 1)
	Torch: moderate	Normal (3, 1)
	Torch: complete	Normal (4, 1)
Smooth terms (non-linear effects)		
	Bole char height, linear/penalized component	Normal (0, 1)
	DBH, linear/penalized component	Normal (0, 1)
	Smoothing SD (sds), shared across smooths	Student-t (3, 0, 2.5)
Group-level (random) effects — SD		
	Species (intercept, DBH slope)	Exponential (2)
	FireID	Exponential (4)
	FireID: TransectID	Exponential (4)
	FireID: TransectID: Point	Normal (1, 1)

Table S1.9. Posterior parameter estimates for the Bayesian mixed-effects model predicting tree mortality as a function of treatment types. Estimates are posterior means with 95% credible intervals (CI) and effective sample sizes (ESS) indicate MCMC convergence and precision. R-hat for all values was 1. Random effects account for non-independence among trees within the same fire, transect, and monitoring point, as well as species-level variation in intercepts and DBH slopes.

Parameter	Estimate	Estimated Error	Lower 95% CI	Upper 95% CI	Bulk ESS	Tail ESS
Smoothing Spline Hyperparameter						
Sd (DBH$^+$)	4.49	1.70	2.21	8.73	5132	5207
Multilevel Hyperparameters						
FireID: sd (Intercept)	0.68	0.58	0.02	2.10	1332	3185
FireID: TransectID: sd (Intercept)	3.78	0.43	3.02	4.71	2797	4667
FireID: TransectID: Point:sd (Intercept)	2.13	0.21	1.75	2.57	3287	5137
Species:sd (Intercept)	0.98	0.33	0.48	1.74	3592	4947
Species:sd (DBH+)	0.20	0.16	0.01	0.61	3821	3720
Species: Cor (Intercept, DBH+)	0.27	0.50	-0.79	0.97	7453	4984
Regression Coefficients						
Intercept	2.00	0.49	1.00	2.94	5044	5533
Thin	-0.78	0.26	-1.29	-0.28	5440	5984
Pile	-0.16	0.39	-0.93	0.60	7607	6140
Masticate	-0.08	0.42	-0.90	0.74	8371	5560
Pile Burn	-0.42	0.41	-1.23	0.38	8569	6373
Broadcast Burn	-0.89	0.40	-1.68	-0.10	7361	6392
Years since last treatment+	0.02	0.24	-0.45	0.49	4667	5868
Distance to boundary edge+	-0.04	0.21	-0.46	0.38	5214	5692
DBH$^+$	-0.08	0.51	-1.07	0.93	14256	5588

Table S1.10. Posterior parameter estimates for the Bayesian mixed-effects model predicting tree mortality as a function of treatment types, with an interaction term between piling and pile burning. Estimates are posterior means with 95% credible intervals (CI) and effective sample sizes (ESS) indicate MCMC convergence and precision. R-hat for all values was 1. Random effects account for non-independence among trees within the same fire, transect, and monitoring point, as well as species-level variation in intercepts and DBH slopes.

Parameter	Estimate	Estimated Error	Lower 95% CI	Upper 95% CI	Bulk ESS	Tail ESS
Smoothing Spline Hyperparameter						
Sd (DBH)+	4.55	1.74	2.27	8.90	5828	6230
Multilevel Hyperparameters						
FireID: sd (Intercept)	0.69	0.59	0.02	2.18	1401	3821
FireID: TransectID: sd (Intercept)	3.79	0.43	3.03	4.70	2667	4913
FireID: TransectID: Point:sd (Intercept)	2.12	0.21	1.72	2.56	2955	4583
Species:sd (Intercept)	0.96	0.32	0.47	1.72	3317	4969
Species:sd (DBH+)	0.21	0.17	0.01	0.63	3396	3840
Species: Cor (Intercept, DBH+)	0.28	0.50	-0.78	0.97	6896	4973
Regression Coefficients						
Intercept	2.03	0.50	1.01	3.02	4712	4899
Thin	-0.78	0.26	-1.29	-0.26	5344	6104
Pile	-0.10	0.39	-0.86	0.66	7880	6250
Masticate	-0.09	0.42	-0.91	0.73	7859	5726
Pile Burn	-0.31	0.43	-1.14	0.53	10133	5866
Broadcast Burn	-0.90	0.40	-1.68	-0.12	7040	6622
Years since last treatment+	0.01	0.24	-0.45	0.50	5000	5684
Distance to boundary edge+	-0.03	0.22	-0.47	0.40	5045	5664
Pile: Pile Burn	-0.32	0.43	-1.17	0.53	10319	6108
DBH+	-0.07	0.51	-1.04	0.92	15090	5667

Table S1.11. Posterior parameter estimates for the Bayesian mixed-effects model predicting tree mortality as a function of treatment types for only the Dixie fire, with an interaction term between thins and broadcast burns. Estimates are posterior means with 95% credible intervals (CI) and effective sample sizes (ESS) indicate MCMC convergence and precision. R-hat for all values was 1. Random effects account for non-independence among trees within the same fire, transect, and monitoring point, as well as species-level variation in intercepts and DBH slopes.

Parameter	Estimate	Estimated Error	Lower 95% CI	Upper 95% CI	Bulk ESS	Tail ESS
Smoothing Spline Hyperparameter						
Sd (DBH⁺)	5.36	2.33	2.38	11.25	4230	5412
Multilevel Hyperparameters						
FireID: sd (Intercept)	0.46	0.44	0.01	1.63	5617	4301
FireID: TransectID: sd (Intercept)	3.57	0.52	2.69	4.7	2854	4165
FireID: TransectID: Point:sd (Intercept)	1.95	0.30	1.42	2.58	3158	5064
Species: sd (Intercept)	0.47	0.31	0.02	1.16	2242	3017
Species: sd (DBH⁺)	0.18	0.17	0.01	0.63	4883	4133
Species: Cor (Intercept, DBH⁺)	-0.06	0.57	-0.95	0.94	7666	5403
Regression Coefficients						
Intercept	0.96	0.60	-0.22	2.14	5677	5727
Thin	-0.02	0.38	-0.78	0.72	6373	5957
Pile	-0.01	0.49	-0.96	0.97	11874	6208
Masticate	-0.01	0.50	-1.01	0.99	12275	6174
Pile Burn	0.01	0.50	-0.95	0.96	13327	5766
Broadcast Burn	-0.84	0.46	-1.72	0.06	8951	6289
Years since last treatment⁺	0.41	0.36	-0.28	1.11	6697	6555
Distance from boundary edge⁺	0.02	0.30	-0.59	0.62	5286	5771
Thin: Broadcast Burn	-0.41	0.27	-0.95	0.13	9128	6008
DBH⁺	-0.08	0.49	-1.00	0.90	12068	6247

Table S1.12. Posterior parameter estimates for the Bayesian mixed-effects model predicting bole char height (m) as a function of treatment types. Estimates are posterior means with 95% credible intervals (CI) and effective sample sizes (ESS) indicate MCMC convergence and precision. R-hat for all values was 1. Random effects account for non-independence among trees within the same fire, transect, and monitoring point, as well as species-level variation in intercepts and DBH slopes.

Parameter	Estimate	Estimated Error	Lower 95% CI	Upper 95% CI	Bulk ESS	Tail ESS
Smoothing Spline Hyperparameter						
Sd (DBH⁺)	2.00	0.77	0.94	3.83	3565	4394
Multilevel Hyperparameters						
FireID: sd (Intercept)	0.35	0.25	0.02	0.97	1920	3013
FireID: TransectID: sd (Intercept)	0.81	0.08	0.66	0.99	2548	4312
FireID: TransectID: Point: sd (Intercept)	0.53	0.02	0.48	0.57	3466	5107
Species: sd (Intercept)	0.15	0.07	0.03	0.32	3054	2551
Species: sd (DBH⁺)	0.08	0.07	0.00	0.27	2047	3820
Species: Cor (Intercept, DBH⁺)	0.24	0.52	-0.86	0.95	6161	5059
Regression Coefficients						
Intercept	1.82	0.23	1.37	2.30	4549	6063
Thin	-0.16	0.06	-0.28	-0.04	5074	5398
Pile	0.25	0.14	-0.03	0.53	4643	5731
Masticate	0.04	0.13	-0.23	0.29	5093	5515
Pile Burn	-0.37	0.16	-0.68	-0.07	4893	5172
Broadcast Burn	-0.38	0.12	-0.62	-0.14	4988	5983
Years since last treatment⁺	-0.06	0.06	-0.17	0.05	4826	5748
Distance from boundary edge⁺	-0.01	0.05	-0.10	0.08	5055	5845
DBH⁺	0.31	0.50	-0.70	1.28	18055	5635
Further Distributional parameters						
sigma	0.63	0.01	0.61	0.65	8572	6056

Table S1.13. Posterior parameter estimates for the Bayesian mixed-effects model predicting crown scorch (low/mod/high) as a function of treatment types. Estimates are posterior means with 95% credible intervals (CI) and effective sample sizes (ESS) indicate MCMC convergence and precision. R-hat for all values was 1. Random effects account for non-independence among trees within the same fire, transect, and monitoring point, as well as species-level variation in intercepts and DBH slopes.

Parameter	Estimate	Estimated Error	Lower 95% CI	Upper 95% CI	Bulk ESS	Tail ESS
Smoothing Spline Hyperparameter						
Sd (DBH^+)	4.88	1.87	2.26	9.40	4623	5348
Multilevel Hyperparameters						
FireID: sd (Intercept)	2.12	0.67	1.04	3.67	3557	3855
FireID: TransectID: sd (Intercept)	3.44	0.39	2.76	4.30	2474	4963
FireID: TransectID: Point: sd (Intercept)	1.76	0.13	1.51	2.03	2824	4831
Species: sd (Intercept)	0.66	0.22	0.32	1.18	5032	5813
Species: sd (DBH^+)	0.12	0.12	0.00	0.45	4363	4941
Species: Cor (Intercept, DBH^+)	0.04	0.55	-0.92	0.94	10587	5710
Regression Coefficients						
Intercept (none-low)	-5.81	0.37	-6.52	-5.07	9672	6511
Intercept (low-moderate)	-2.09	0.34	-2.76	-1.40	10909	6510
Intercept (moderate-complete)	0.27	0.35	-0.42	0.97	10507	6883
Thin	-0.50	0.21	-0.91	-0.10	4926	5474
Pile	-0.18	0.36	-0.89	0.52	8152	6940
Masticate	-0.04	0.38	-0.79	0.68	7969	6450
Pile Burn	-0.57	0.39	-1.35	0.15	8117	6500
Broadcast Burn	-0.91	0.36	-1.60	-0.20	6325	5394
Years since last treatment+	-0.14	0.21	-0.54	0.26	5123	5582
Distance to boundary edge+	-0.2	0.18	-0.56	0.16	4338	5839
DBH^+	-0.09	0.49	-1.05	0.88	16280	5274

Table S.1.14. Posterior parameter estimates for the Bayesian mixed-effects model predicting crown torch (low/mod/high) as a function of treatment types. Estimates are posterior means with 95% credible intervals (CI) and effective sample sizes (ESS) indicate MCMC convergence and precision. R-hat for all values was 1. Random effects account for non-independence among trees within the same fire, transect, and monitoring point, as well as species-level variation in intercepts and DBH slopes.

Parameter	Estimate	Estimated Error	Lower 95% CI	Upper 95% CI	Bulk ESS	Tail ESS
Smoothing Spline Hyperparameter						
Sd (DBH$^+$)	3.30	1.48	1.36	6.98	3333	4506
Multilevel Hyperparameters						
FireID: sd (Intercept)	1.13	0.58	0.10	2.43	783	978
FireID: TransectID: sd (Intercept)	3.55	0.35	2.94	4.30	1714	3123
FireID: TransectID: Point: sd (Intercept)	2.02	0.13	1.79	2.27	2465	4392
Species:sd (Intercept)	0.49	0.19	0.15	0.92	3223	2589
Species:sd (DBH$^+$)	0.30	0.19	0.02	0.74	2033	2477
Species: Cor (Intercept, DBH$^+$)	0.12	0.50	-0.87	0.91	3106	4125
Regression Coefficients						
Intercept (none-low)	-2.94	0.34	-3.61	-2.28	6034	6057
Intercept (low-moderate)	-0.10	0.34	-0.76	0.55	6590	6262
Intercept (moderate-complete)	2.41	0.34	1.73	3.08	6587	6153
Thin	-0.59	0.24	-1.05	-0.12	3657	4976
Pile	0.04	0.34	-0.64	0.71	4826	6001
Masticate	-0.40	0.37	-1.11	0.34	5043	5860
Pile Burn	-0.60	0.37	-1.34	0.13	4768	5659
Broadcast Burn	-1.14	0.37	-1.86	-0.39	4018	5112
Years since last treatment+	-0.45	0.20	-0.85	-0.06	3234	4532
Distance to boundary edge+	-0.44	0.18	-0.78	-0.10	3333	4742
DBH$^+$	-0.12	0.49	-1.06	0.83	11339	5552

Table S1.15. Posterior parameter estimates for the Bayesian mixed-effects model predicting tree mortality as a function of tree injury components. Estimates are posterior means with 95% credible intervals (CI) and effective sample sizes (ESS) indicate

MCMC convergence and precision. R-hat for all values was 1. Random effects account for non-independence among trees within the same fire, transect, and monitoring point, as well as species-level variation in intercepts and DBH slopes.

Parameter	Estimate	Estimated Error	Lower 95% CI	Upper 95% CI	Bulk ESS	Tail ESS
Smoothing Spline Hyperparameter						
sd (Bole char height$^+$)	2.80	1.63	0.50	6.69	3410	3120
sds (DBH$^+$)	3.24	1.55	1.16	7.09	6026	5178
Multilevel Hyperparameters						
FireID: sd (Intercept)	0.37	0.34	0.01	1.27	4660	5040
FireID: TransectID: sd (Intercept)	1.36	0.23	0.96	1.85	4547	5745
FireID: TransectID: Point: sd (Intercept)	0.39	0.32	0.01	1.13	1355	3568
Species: sd (Intercept)	0.73	0.32	0.22	1.47	3934	3976
Species: sd (DBH$^+$)	0.22	0.19	0.01	0.73	5063	4917
Species: Cor (Intercept, DBH$^+$)	0.10	0.54	-0.88	0.96	8848	5769
Regression Coefficients						
Intercept	-3.11	0.70	-4.53	-1.79	5883	5716
Scorch (none-low)	-0.54	0.52	-1.56	0.47	6703	5881
Scorch (low-moderate)	-0.09	0.53	-1.14	0.95	6614	6444
Scorch (moderate-complete)	6.42	0.58	5.31	7.57	5565	6219
Torch (none-low)	1.03	0.38	0.28	1.79	10570	6988
Torch (low-moderate)	2.91	0.59	1.76	4.10	11926	6933
Torch (moderate-complete)	2.94	0.72	1.58	4.40	12772	5914
Years since last treatment$^+$	0.29	0.26	-0.21	0.79	7627	6556
Distance to boundary edge$^+$	0.06	0.21	-0.36	0.47	7783	6605
Bole char height $^+$	0.43	0.99	-1.52	2.36	12382	5627
DBH$^+$	-0.19	1.01	-2.12	1.77	18961	5867

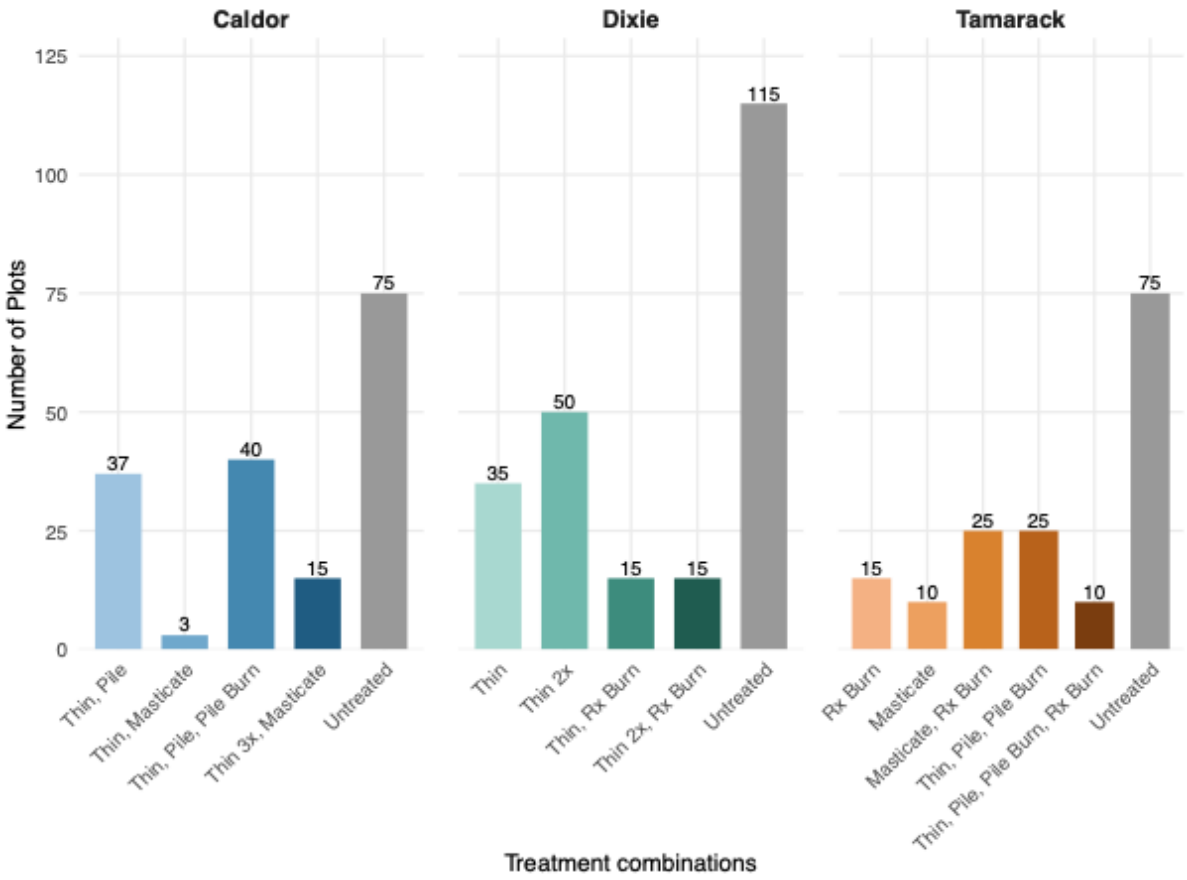


Figure S.1.1. Combinations of treatment types for each fire, with number of plots (here referring to the 10 sampling points along a given transect) sampled listed above the bar. Rx burn = broadcast burn. Thin 2x = thinned two times, Thin 3x = thinned three times.

CHAPTER 2. QUANTIFYING POST-FIRE LIVE TREE PRESENCE AND SPATIAL VARIATION USING SENTINEL-2 TIME SERIES

A version of this chapter was published as Saberi, S.J., van Mantgem P.J., Wright, M.C., Wong, C.Y., Latimer, A.M. and D.J.N. Young. 2026. Quantifying post-fire live tree presence and spatial variation using Sentinel-2 time series. Forest Ecology and Management.

DOI: https://doi.org/10.1016/j.foreco.2025.123461

ABSTRACT

Accurate mapping of post-fire surviving trees is important for tracking forest recovery and prioritizing land management decisions. Satellite-based remote sensing is an effective method to assess post-fire forest conditions. Traditionally, differenced satellite-derived burn severity indices are computed by differencing one year pre- and post-fire spectral reflectance values. Differenced burn severity indices are useful for quantifying and mapping the magnitude of ecological change, but their application to detecting and mapping post-fire live trees may not be as appropriate, particularly for delayed tree mortality. Delayed tree mortality ("delayed mortality") is a phenomenon where trees that initially survive fire then die over an extended period (between one and five years), and it can be challenging to measure and predict. In this study, we demonstrate the potential of mapping delayed mortality using readily available remotely sensed imagery alone. We used random forest models to detect post-fire live trees using 10-m resolution Sentinel-2 data at one-, three-, and five-years post-fire for four fires in the southern Sierra Nevada, California, USA. Using imagery from the National Agriculture Imagery Program (NAIP; 60-cm resolution), we manually classified live tree presence in 6000 Sentinel-2 pixels (500 pixels for each fire-year combination) to calibrate and validate models. Sentinel-2 based model accuracies ranged from 65% to 86% with F-scores ranging from 0.52 to 0.86, and their predictions of live pixel area were on average 44% lower than inferred from more traditional indices such as relative differenced normalized burn ratio (RdNBR). This work represents a promising first step in using freely available post-fire spectral reflectance imagery to detect live trees over an extended period to support post-fire management.

INTRODUCTION

In forest ecosystems, fire is a key process that can affect vegetation structure, function, abundance, species composition, and spatial distribution (Bowman et al. 2009). Some forests such as yellow pine-mixed conifer in the Sierra Nevada of California are adapted to fire such that they rely on frequent surface fire to clear the understory and maintain heterogeneity in structure and species composition (Safford and Stevens 2017). Over a century of fire suppression, land use change, loss of cultural burning by Indigenous peoples who stewarded the land, and warmer temperatures due to anthropogenic climate change has led to a 'fire deficit' in many forest types that results in an increase in large fires and area burned at high severity (here referring to 75% or more tree mortality) in recent decades (Westerling 2016, Seidl et al. 2017, Parks and Abatzoglou 2020, Williams et al. 2023). Beyond affecting fire regimes, environmental changes have the potential to alter post-fire forest recovery and reorganization. Throughout forested biomes worldwide, larger and higher-severity fires can lead to 'tipping points' where forested ecosystems convert to non-forests such as shrublands or woodlands (Adams 2013, Coop et al. 2016, Hart et al. 2019). Monitoring post-fire forest response is important for understanding recovery or transition trajectories particularly as fire regimes continue to change. Areas within a fire perimeter containing mature seed-bearing trees that remain alive after fire (also known as 'fire refugia' or unburned islands, Meddens et al. 2016) are particularly important to track because they serve as the seed source for future forest reestablishment for obligate seeding species, such as most conifers (Meddens et al. 2018).

An element of post-fire forest response that is particularly important to account for is delayed mortality. Delayed mortality is the phenomenon whereby some trees that initially survive fire die over an extended post-fire period, usually between one and five years (van Mantgem et al. 2011, Hood et al. 2018). Direct, proximate causes of tree death include tissue damage from the heat of the fire and do not account for other stressors (Hood et al. 2018). Indirect causes of tree death are more challenging to predict and can include pre-fire stress from competition, drought, disease, or heightened post-fire bark beetle populations (McDowell et al. 2008, Hood et al. 2018, Shearman et al. 2023). Delayed post-fire tree mortality has parallels with tree mortality in forests in the absence of fire, the causes of which are often complex and controlled by multiple mechanisms (Stephenson et al. 2011, Das et al. 2016). For example, if, after a given fire delayed mortality is not widespread and most trees that survive post-fire continue to stay alive, (and remain vigorous enough to produce viable seeds) they may contribute to continued forest persistence. Post-fire forest persistence can depend on the assumption that live seed-bearing trees are close enough to total mortality patches such that seed dispersal and subsequent regeneration can occur (Coop et al. 2020). Alternatively, if delayed mortality is widespread and most trees that initially survive a fire subsequently die, there may not be enough seed sources for forests to persist.

Field-based methods to directly assess fire-caused tree injuries using metrics like cambium kill and crown volume kill have been developed and translated into species-specific predictive models of immediate mortality (Hood et al. 2007), but the required field sampling is labor- and cost-intensive and not easily scalable to broad spatial extents.

Moreover, measurements of fire-caused tree injury may not be predictive of delayed mortality (Shearman et al. 2023). Remotely sensed data are a useful alternative to field-based data as they allow for assessments across broad spatial extents (e.g., entire fire perimeters or administrative boundaries). Extensive research on immediate post-fire effects on forest vegetation has been conducted using Landsat data (which is freely available and dates to 1972, https://landsat.usgs.gov, accessed 9/4/2025), primarily using normalized burn ratio (NBR)-based indices. These indices use the shortwave and near-infrared bands, which can provide information about vegetation moisture content (Key and Benson 2006, Miller and Thode 2007). Higher values of differenced Normalized Burn Ratio (dNBR) correspond to increased exposure of mineral soil and ash, increased char and consumption of downed fuels, and decreased aboveground green biomass and vegetation cover (Key and Benson 2006). Differenced NBR-based indices, particularly RdNBR (relative differenced normalized burn ratio), are useful in determining where there has been high proportional forest loss (Miller and Thode 2007). A popular source for RdNBR data is the Monitoring Trends in Burn Severity (MTBS) program, which provides RdNBR layers at 30-m resolution from 1984 to the present, usually on a two-year time delay (Eidenshink et al. 2007, Kolden et al. 2015, Picotte et al. 2020). Importantly, RdNBR is not designed to capture post-fire condition (e.g., identify areas of surviving trees), but to quantify relative changes from pre- to post-fire (e.g., percentage forest loss). In analyses focused specifically on post-fire condition (e.g., prevalence of surviving trees) as opposed to change, using purely post-fire spectral information is likely to be more relevant. In addition, the interpretation of RdNBR can be confounded by post-fire regrowth. For example, if a tree

dies due to fire but a shrub within the same pixel rapidly (re)establishes, RdNBR values could register minimal or no change and lead to the misinterpretation that there was no fire-caused tree mortality.

There have been efforts to track both immediate post-fire and delayed mortality with remote sensing methods using either high-resolution, proprietary satellite data (Dixon et al. 2023, Busby et al. 2024) or other NBR-change-based metrics (Reilly et al. 2023), but these methods can either be cost prohibitive or relatively coarse in spatial and temporal grain (i.e., 30-meter pixels and only two temporal markers). Challenges with coarser spatial resolution include specificity around individual trees: a single surviving tree might only represent a fraction of a 30-meter pixel and therefore not be clearly detected based on the pixel's spectral signature.

Research Objectives and Hypotheses

The objective of this study is to evaluate the potential to predict post-fire live tree presence/absence from 1 to 5 years post-fire using strictly post-fire Sentinel-2 (Phiri et al. 2020) imagery and to ask both methodological and ecological questions. Our study extends the findings of Wong et al. (2025) from immediate post-fire assessments to longer post-fire time intervals. Methodologically, we ask: 1) can tree survival and mortality be reliably predicted up to five years post-fire? 2) What combination of training data years balances accuracy and bias? 3) How do the inferences from a RdNBR-based mortality product (where a non-high severity pixel is assumed to contain live trees) compare to our product based on strictly post-fire Sentinel-2 imagery? Ecologically, we ask: 1) based on

the final model, how prevalent is delayed mortality in the southern Sierra Nevada mountains of California, and are these trends consistent across different fires and years? 2) What is the total live area per fire and how does this change over time? We hypothesized that the Sentinel-2-based model will be able to predict post-fire live tree patterns with accuracies either in the same range or better than the current prevailing method of using NBR-based indices such as RdNBR that quantify change as opposed to state. The comparison of our random forest-based product to RdNBR provides land managers and end users with information concerning the applicability of RdNBR to predict post-fire live tree presence over time.

METHODS

Study Area

Study fire perimeters were constrained by the availability dates of the source data for reflectance and photo interpretation (Sentinel-2 from the European Space Agency (https://sentinels.copernicus.eu/sentinel-data-access/sentinel-products/sentinel-2-data-products/collection-1-level-1c, accessed 5/1/2025), and National Agriculture Imagery Program (NAIP, https://wildlife.ca.gov/Data/GIS/Map-Services, accessed 5/1/2024) from the United States Department of Agriculture, respectively (Maxwell et al. 2017). Sentinel-2 is available since 2015, while NAIP imagery is available in California during even years only during this study's 2015–2022-time frame. Available resources constrained our focus to California counties in the Sierra Nevada that contained recently federally designated disaster wildfires: Alpine, Amador, El Dorado, Lassen, Placer, Plumas, and Tulare. We then

queried the CalFire FRAP (California Department of Forestry and Fire Protection Fire and Resource Assessment Program) Historical Fire Perimeter GIS database (https://www.fire.ca.gov/what-we-do/fire-resource-assessment-program/fire-perimeters, accessed 9/4/2025) for fires greater than 5,000 acres between 2015 and 2020 to allow for enough post-fire years of data. We further narrowed the list of fires that fit the search criteria by removing fires with over 50% of their perimeter having reburned in subsequent years, because this interferes with tracking mortality that cannot be disentangled from individual fire events. Additionally, we screened remaining fires by the Existing Vegetation Type (EVT) from the LANDFIRE database (https://www.landfire.gov/data/FullExtentDownloads, accessed 4/24/2024) to remove fires dominated primarily by grassland or shrubland. This screening process resulted in four fires for analysis: the 2015 Cabin and Rough Fires, and the 2017 Pier and Schaeffer Fires, located in the Sequoia and Sierra National Forests, respectively (Figure 2.1, Table 2.1).

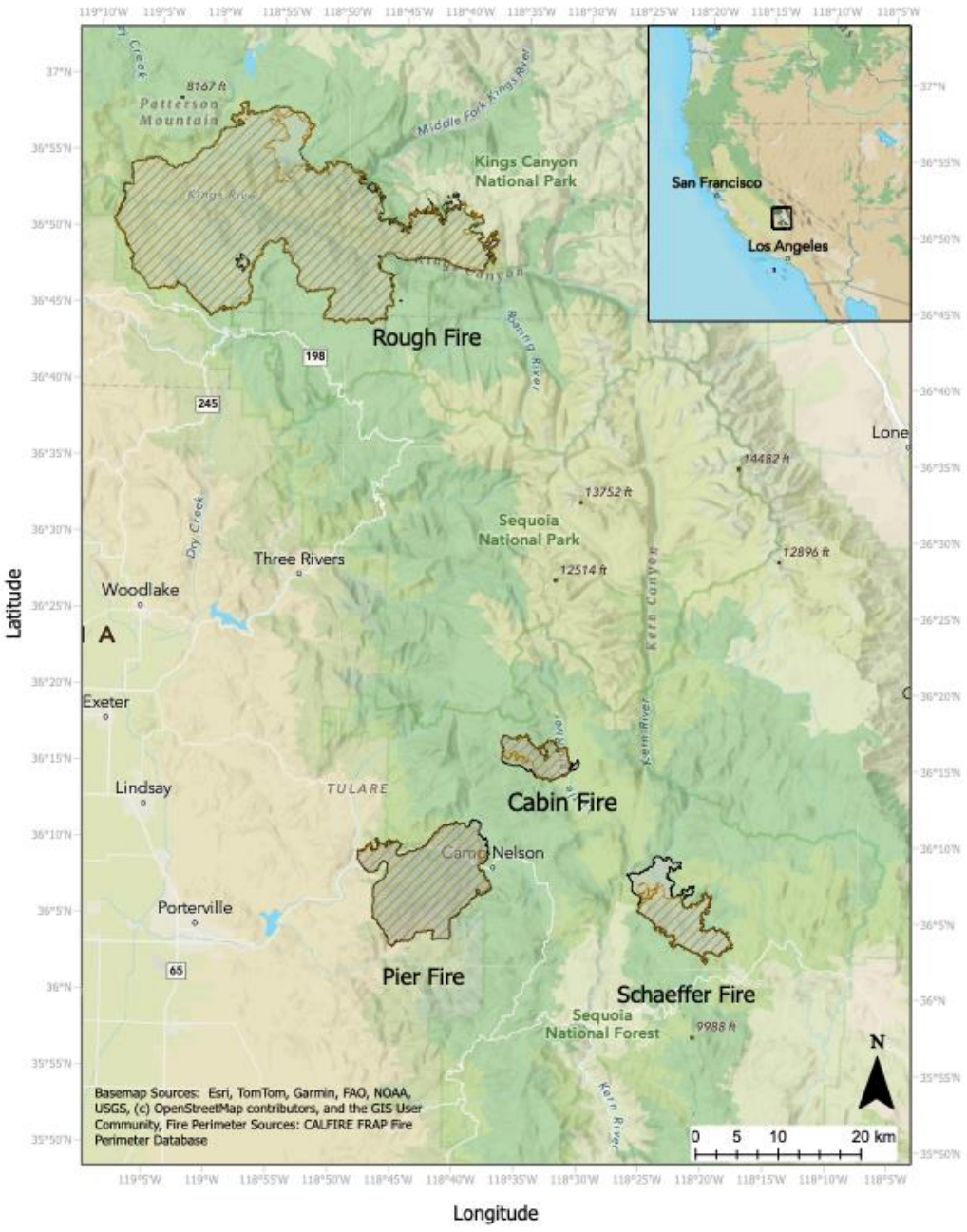


Figure 2.1. Map showing the four fires in this study (full fire perimeter outlined in gray, analyses area that masks out reburned areas shown in brown hatches), which are in the Sierra and Sequoia National Forests. The Rough fire also burned into Kings Canyon National Park, representing six percent of the fire's total burn area.

Table 2.1. Information about size, ignition and containment date for each the study fires.

Fire	Size (hectares)	Ignition Date	Containment Date	Duration (Days)
Rough	59231	7/31/2015	11/5/2015	97
Cabin	2925	6/18/2015	10/22/2015	126
Pier	14822	8/29/2017	11/29/2017	92
Schaeffer	6515	6/24/2017	7/31/2017	37

The yellow pine and mixed conifer forests of the southern Sierra Nevada of California is an area of high fire activity and are departed from pre-European settlement estimates of fire return intervals (Fites-Kaufman et al. 2007, Safford and Van de Water 2014). Yellow pine and mixed conifer forests in the Sierra Nevada have a mean fire return interval of about 11 years (Van de Water and Safford 2011). The climate in this region is primarily Mediterranean with warm dry summers and cool, wet winters. Dominant species include red fir (*Abies magnifica*) and lodgepole pine (*Pinus contorta*) at high elevations, yellow pines including ponderosa pine (*Pinus ponderosa*) and Jeffrey pine (*Pinus jeffreyi*), sugar pine (*Pinus lambertiana*), white fir (*Abies concolor*), incense cedar (*Calocedrus decurrens*) at mid-elevations, and black oak (*Quercus kellogii*) at lower elevations.

Sentinel-2 Data Acquisition

Sentinel-2 data acquisition and processing were conducted in the cloud-based Google Earth Engine (GEE) environment (Gorelick et al. 2017). We accessed one-year, three-year, and five-year post-fire imagery for each fire to correspond with available NAIP imagery (2016, 2018, 2020, and 2022). We used the Sentinel L1C data because L2A data

were not available for all years of interest. Notably, L2A data have bands that include information about cloud probability and snow probability, as well as cloud masks, while L1C data simply contain the cirrus cloud band from which these masks are calculated; we completed cloud masking by reclassifying the QA60 bitmask band using the values identified as clouds. After cloud masking, we applied an algorithm to the L1C data that processed it to the L2A level (Yin et al. 2022), which takes the raw TOA (top of atmosphere) data and applies an atmospheric correction to produce a BOA (bottom of atmosphere) product. The Yin algorithm generally follows the same steps as the 'sen2cor' processor provided by the European Space Agency (Main-Knorn et al. 2017) but allows for the entire workflow to stay within the GEE environment. Then we computed a composite image from cloud-free pixels in June and July (which correspond to peak growing months) for each of the individual year post-fire images. Lastly, we resampled bands not natively in 10-m resolution (Bands 1,5,6,7,11,12) to 10-m resolution using bilinear interpolation so that all final spectral bands were at the same resolution. Final images were then exported from the GEE environment so they could be used for modeling in R version 4.4.1 (R Core Team 2024).

Photo interpretation

The methods for photo interpretation and data analysis follow that of Wong et al. (2025). For photo interpretation, 60-cm resolution NAIP imagery was accessed from the California Fish and Wildlife Map Services ArcGIS server connection (CDFW Map Services 2024). To create a stratified sample of points for each fire, we first used k-means clustering to define ten classes of similar pixels based on all bands of a single image. K-means clustering partitions *n* observations into *k* clusters (in this case clustering of pixels

across all bands) where each observation belongs to the cluster with the nearest mean, such that the within-cluster sum of squares is minimized. This algorithm is designed to capture structure or similarity inherent to a dataset (Hartigan and Wong 1979). Note that polygons used for each fire were modified to exclude reburn areas. We used Generalized Random Tessellation Stratified (GRTS) sampling across each fire to create 500 spatially balanced points with a minimum distance of 100 meters between each sample point. Since the analysis spanned three years (one, three-, and five-years post-fire) for each fire, this resulted in 500 sampling points per year for 1500 points total per fire, and a total of 6000 sampling points for all four fires. The pixels containing each sample point were converted to polygons and then overlaid onto corresponding NAIP imagery for each year. Each pixel polygon was visually classified into one of the following classes: 1) Does not contain live vegetation, 2) Contains a live tree, with or without live understory vegetation, 3) Borderline live tree (touching border but not within a focal pixel) 4) Contains live understory vegetation but does not contain live trees and 5) Undetermined classification (Figure S1.1). Class 5 was used to improve the certainty of what was contained in the polygons (by avoiding guessing) and reduce uncertainty caused by shadows. The data for the photo-interpreted classifications are found in Saberi et al. (2025).

Random Forest Models

Before beginning modeling, the five classes described in the photo interpretation section were converted into two classes. Classes 1, 3 and 4 were turned into “not live tree” while class 2 remained as a “live tree” class, and pixels marked as class 5 (undetermined, representing 1.33% of all pixels) were removed from the analysis. We used the

'randomForest' package in R version 4.4.1 (Liaw and Wiener 2002) to create, test, and validate random forest classification models. For each fire and year combination, each photo-interpreted polygon was matched to its corresponding Sentinel-2 pixel and the corresponding band values were extracted (Figure 2.2, S2.2, S2.3). In the exploration stage, multiple models were tested with different temporal subsets and different combinations of explanatory variables. For example, we tested predicting a given year by training the model with only its matching year of data (i.e., predict one-year post-fire by training with only one-year post-fire data), different combinations of data from year one, year three, and year five as well as predicting a given year with training data from all three years of available data (Table S2.1). We used a leave-one-fire-out (LOFO) cross-validation approach to test cross-site performance. With the LOFO validation method, we iteratively pooled all the pixels from three of the four fires together as training data to test against the withheld fire. This process was repeated such that the pixels from each fire were used both in training and testing (in separate iterations). Then, we analyzed the accuracy (fraction of true positives and true negatives relative to all cases), precision (fraction of true positives relative to true positives and false positives), and recall (fraction of true positives relative to true positives and false negatives) of each candidate model to select the final model, where any given year of post-fire live tree presence was predicted using input spectral data (all Sentinel-2 bands) from all three years of available data. The final model was favored due to its high accuracy over multiple time steps and a modest decrease in precision and recall when compared to the models trained on temporal subsets (Figure 2.3, Table S2.2). For each fire and year combination, the final model was applied to the pixels corresponding to the entire

fire perimeter to produce prediction maps (Figure 2.4, S2.4), where each pixel is treated as 'live' or 'dead'. We did not attempt to resolve information at a sub-pixel level. For each model, we reported the F-score, which is a metric that combines both precision and recall. The F-score is bounded between values of 0 and 1, a value of 1 means there is perfect precision and recall, while a value below 0.5 indicates poor model performance. We compared prediction maps from our strictly post-fire imagery (at 10-m resolution) against the change-based burn severity index RdNBR (at 30-m resolution). We calculated RdNBR at one, three-, and five-years post-fire in the GEE environment following methods from Parks et al. 2018. While it can be argued that a Sentinel-2 derived RdNBR product could produce a more direct comparison to the maps derived from our Sentinel-2-based random forest models (as both products would be at 10 m resolution), we calculated RdNBR using Landsat imagery as that metric was developed for this sensor. In addition, the Landsat-based 30-m data product is widely used by land managers and end users, often downloaded from the MTBS website (Key and Benson 2006, Eidenshink et al. 2007, Picotte et al. 2020). While they have different spatial resolutions, the differences in inference from these two products informs prospective users of the applicability of each to assessments of post-fire live vegetation over time. We applied the thresholds from Miller et al. 2009 to count any pixel value above the 'high severity' class threshold (defined at a value of 572, corresponding to 75% canopy cover loss) as 'dead' and any pixel value below the 'high severity' class threshold as 'live' to produce binary maps of live and dead trees which we compare to our Sentinel-2 derived predictions (Figure 2.5, S2.5) via fire-level summary statistics (e.g., percent of fire with live tree cover). After obtaining the results of the random

forest modeling and RdNBR thresholding, we extracted monthly precipitation averages from PRISM (PRISM Climate Group 2025). We then summed monthly averages to get the total for the water year (Oct-Sep) in the approximate centroid of each fire perimeter. We also extracted 30-year precipitation normal for each fire perimeter.

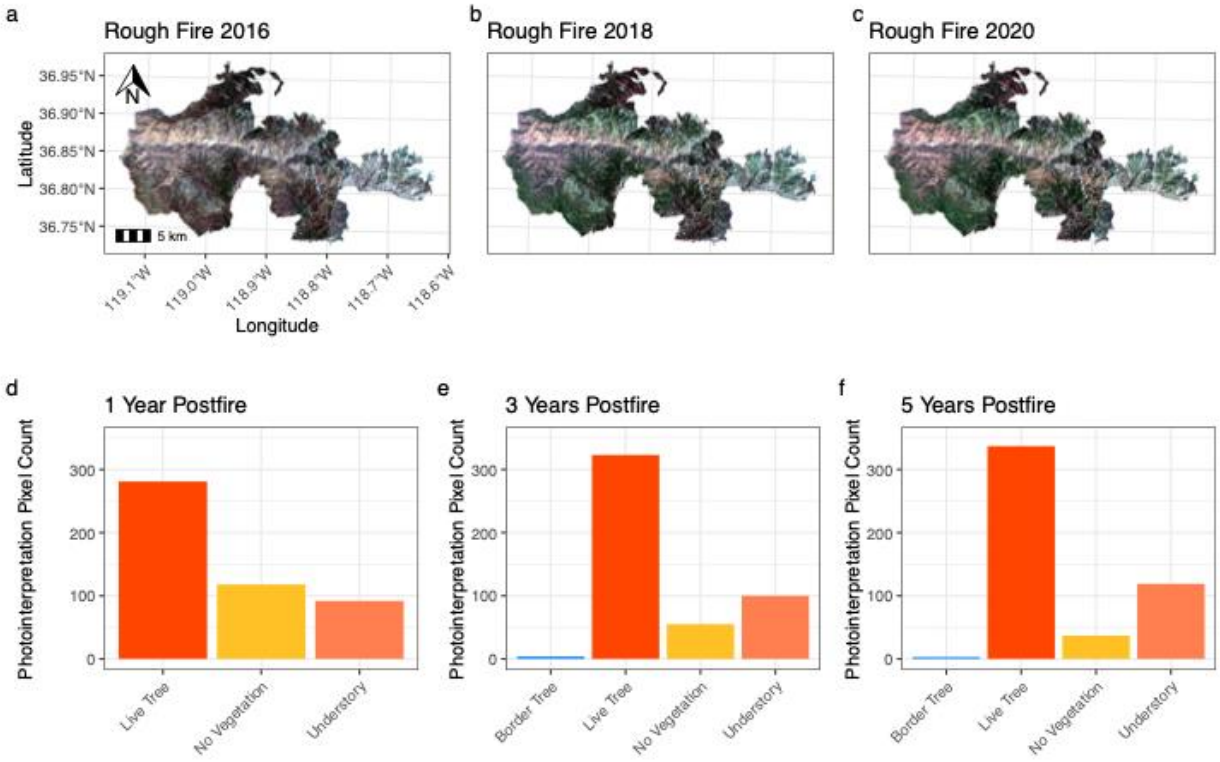


Figure 2.2. Panels a-c: true color Sentinel-2 imagery for the 2015 Rough fire, One, three-, and five-years post-fire. Fire perimeter from California Department of Forestry and Fire Protection Fire and Resource Assessment Program, Historical Fire Perimeter GIS database (https://www.fire.ca.gov/what-we-do/fire-resource-assessment-program/fire-perimeters, accessed 9/4/2025). Panels d-f show the counts of photo-interpreted pixel classes for each timestep, with the same pixels interpreted at each timestep. Note that border trees were dropped from the analyses

Table 2.2. Live and dead tree predictions summarized across the study fires produced from all-bands, all-years Sentinel-2 random forest models.

Fire	Post -fire Year	Total Live Area Km^2	Total no live Area Km^2	Percent Live Area	Percent no Live Area	Average Dist. to Live Pixel (meters)	Percent of pixels > 100 m from a live pixel
Rough	1	287.67	306.26	48.43	51.57	16.80	2.23
Rough	3	392.62	133.07	66.11	33.89	8.20	0.73
Rough	5	374.73	138.30	63.09	36.91	9.58	0.75
Cabin	1	10.41	14.29	42.16	57.84	24.92	6.95
Cabin	3	11.73	12.97	47.50	52.50	12.45	0.89
Cabin	5	12.57	12.13	50.89	49.11	10.38	0.43
Pier	1	82.19	62.67	56.74	43.26	19.29	4.78
Pier	3	104.57	40.29	72.19	27.81	7.21	0.65
Pier	5	84.21	60.64	58.13	41.87	11.83	1.23
Schaeffer	1	11.56	36.55	24.02	75.98	37.45	9.01
Schaeffer	3	15.09	33.02	31.37	68.63	28.93	5.73
Schaeffer	5	9.50	38.61	19.75	80.25	29.89	4.57

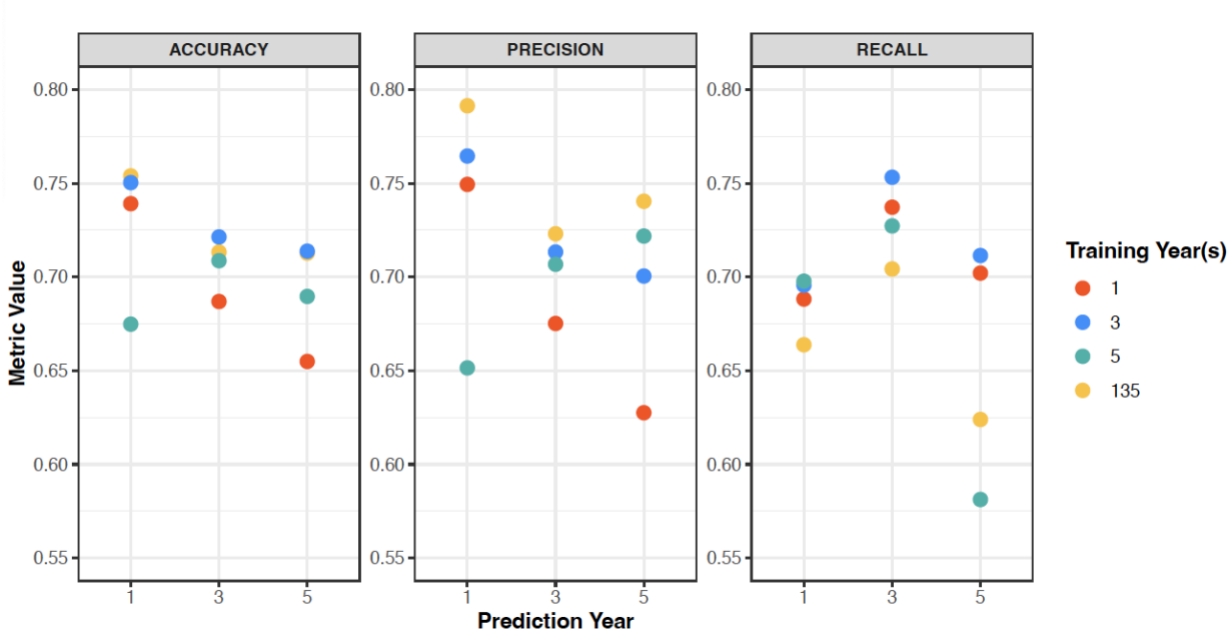


Figure 2.3. Accuracy, precision, and recall for each candidate model (individual training years versus all training years). Training years refer to the years post-fire from which the Sentinel-2 imagery was obtained, with years 135 meaning all years combined.

RESULTS

Analysis of the candidate random forest models led us to select the models that had training data from all years. This was because although accuracy decreased by 0.04 between Year 1 and Year 3, it stayed the same between Year 3 and Year 5. In addition, these models had higher initial precision and recall that did not fluctuate too drastically over the subsequent time steps and indicate shifting bias. The decision was also influenced by the assumption that including training information from all-time points inclusive and prior to the prediction year would allow for the random forest model more opportunity to 'learn' patterns that are relevant across multiple years. The final random forest models showed relatively high accuracies, mostly above 70%. The lowest accuracy for an individual fire-

year model combination was 65% (Cabin Fire, three years post-fire) and the highest was 86% (Pier Fire, one-year post-fire), with an average of 73% (Table S1). For the Rough, Cabin, and Pier Fires, accuracy in models decreased slightly between the Year 1 and Year 3 time points, with the Rough Fire model showing a 0.02 decrease in accuracy and the Cabin and Pier Fire models showing a 0.08 and 0.09 decrease. The Schaeffer Fire model had a 0.02 increase in accuracy between Year 1 and Year 3, as well as a 0.03 increase in accuracy between Year 3 and Year 5. The Pier Fire models were the only ones that decreased between both time steps.

The predictions from the final models also showed a similar trend for each fire over time: between Year 1 and Year 3, the live tree pixels increased for all four fires. In all fire perimeters except the Schaeffer fire, there was a net gain in percentage of live tree pixels by Year 5. There was variation in the direction of change for the live percentage between Year 3 and Year 5: the Rough Fire, Pier Fires, and Schaeffer Fires showed a slight decrease while the Cabin Fire showed a slight increase. Ultimately, proportion live change (in either direction) was never greater than 0.18. (Figure 2.4, Table 2.2) The slight increase at year three may represent post-fire tree recovery or re-greening of scorched trees, and the decrease at year five may indicate the eventual death of the re-greened trees (Figure 2.4, Table 2.2). However, the same trend of increased live tree abundance after Year 1 were apparent in our sample of photo-interpreted NAIP imagery for the Cabin, Pier, and Rough Fires (Figure S2.1). The absolute percent changes in live tree pixel abundance were smaller for the photo-interpreted pixels than the modeled pixels. For most of the individual models, precision tended to be higher than recall, indicating that the model is keeping false-positive

rates low at the cost of overlooking some live trees by classifying them as dead (Table S2.1). Eight of the twelve models showed F-scores of 0.6 or higher (the highest being 0.86), indicating that generally the random forest models are an effective binary classifier.

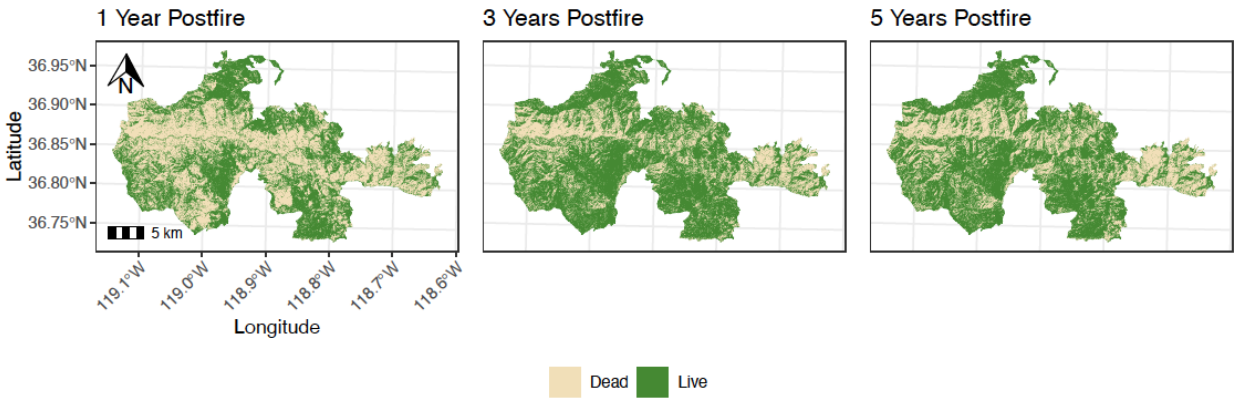


Figure 2.4. Predictions of live and dead pixels (10-m resolution) at one, three-, and five-years post-fire from all Sentinel-2 bands random forest model for the Rough Fire. Fire perimeter from California Department of Forestry and Fire Protection Fire and Resource Assessment Program, Historical Fire Perimeter GIS database (https://www.fire.ca.gov/what-we-do/fire-resource-assessment-program/fire-perimeters, accessed 9/4/2025).

The random forest models predicted less total area of pixels containing live trees than did the thresholded RdNBR maps (Figures 2.4,2.5, S2.4 and S2.5, Tables 2.2 and 2.3). For example, the Sentinel-2-based random forest model predicted that the total area of live pixels one year after the Cabin Fire was approximately 10.41 $km^{2,}$ while the thresholded traditional RdNBR maps predict the total area to be nearly triple, or 29.79 km^2. The difference in live area could simply be a function of the thresholding and coarser pixel size, and we would require truthing of RdNBR pixels, which was outside the scope of this study, to determine whether RdNBR is overpredicting live tree pixels. The trend of RdNBR thresholded maps suggesting a larger area containing live pixels was consistent across all

fires and time periods. Notably, both methods showed very low percentages of pixels containing no live trees (heretofore referred to as 'dead pixel' and in figures) greater than 100 meters away from the nearest live pixel: an average of 3.16 percent across all fires for the random forest models and an average of 1.96 percent for the RdNBR thresholded maps. In line with the larger estimates of pixels containing live trees from the RdNBR thresholded maps, the average distance of a dead pixel to the nearest live pixel is on average shorter than the estimates from the random forest generated maps (for example, 1.45 meters away versus 24.92 meters away for the Cabin Fire, Tables 2.2 and 2.3). Across all fires, the average distance of a dead pixel to the nearest live pixel was 18.08 meters for the random forest generated maps versus 7.29 meters for the thresholded RdNBR maps. For the relative precipitation comparison, we found the centroid of the Rough Fire and Cabin Fire saw about 3.6 and 3.5 times more rain in water year 2017 than in water year 2015, respectively (Figure 2.6).

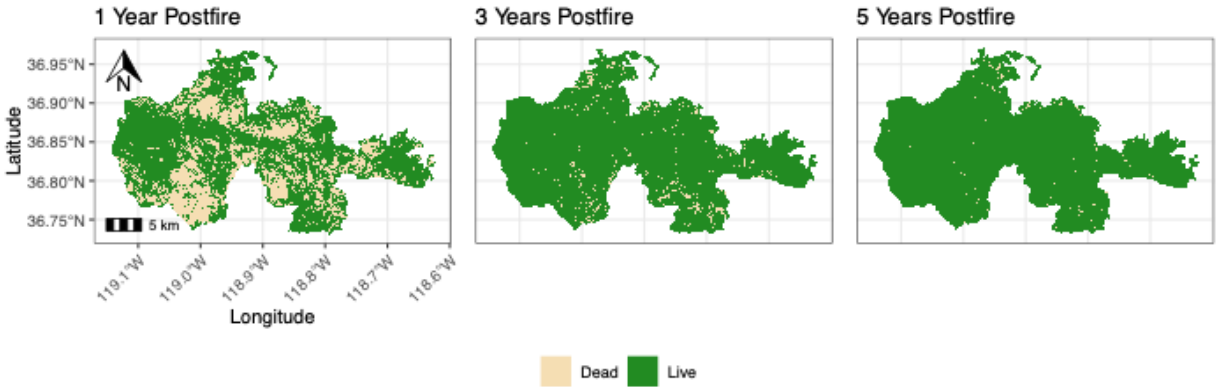


Figure 2.5. Predictions of live and dead pixels (30-m resolution) at one, three-, and five-years post-fire from thresholded Landsat-derived RdNBR maps for the Rough Fire. Fire perimeter from California Department of Forestry and Fire Protection Fire and Resource Assessment Program, Historical Fire Perimeter GIS database (https://www.fire.ca.gov/what-we-do/fire-resource-assessment-program/fire-perimeters, accessed 9/4/2025).

Table 2.3. Predicted estimates of live and dead area, as well as average distance to nearest live pixel and percent of pixels greater than 100 meters from a Landsat-based and thresholded RdNBR cutoff product.

Fire	Post-fire Year	Total Live Area Km^2	Total Dead Area Km^2	Percent Live Area	Percent Dead Area	Average Dist. to Live Pixel (meters)	Percent of Pixels > 100 m from a Live Pixel
Rough	1	512.36	234.55	68.59	31.4	25.87	8.15
Rough	3	718.30	28.68	96.16	3.84	1.45	0.05
Rough	5	739.81	7.25	99.04	0.97	0.47	0.00
Cabin	1	29.79	1.50	95.22	4.78	1.45	0.00
Cabin	3	26.95	4.33	86.15	13.85	6.00	0.64
Cabin	5	29.79	1.50	95.22	4.78	1.45	0.00
Pier	1	128.66	52.14	71.16	28.84	25.28	8.60
Pier	3	174.14	6.67	96.31	3.69	1.45	0.13
Pier	5	180.46	0.35	99.808	0.192	0.05	0.00
Schaeffer	1	37.19	23.44	61.34	38.66	23.48	5.92
Schaeffer	3	59.63	1.00	98.357	1.643	0.49	0.00
Schaeffer	5	60.55	0.08	99.87	0.13	0.03	0.00

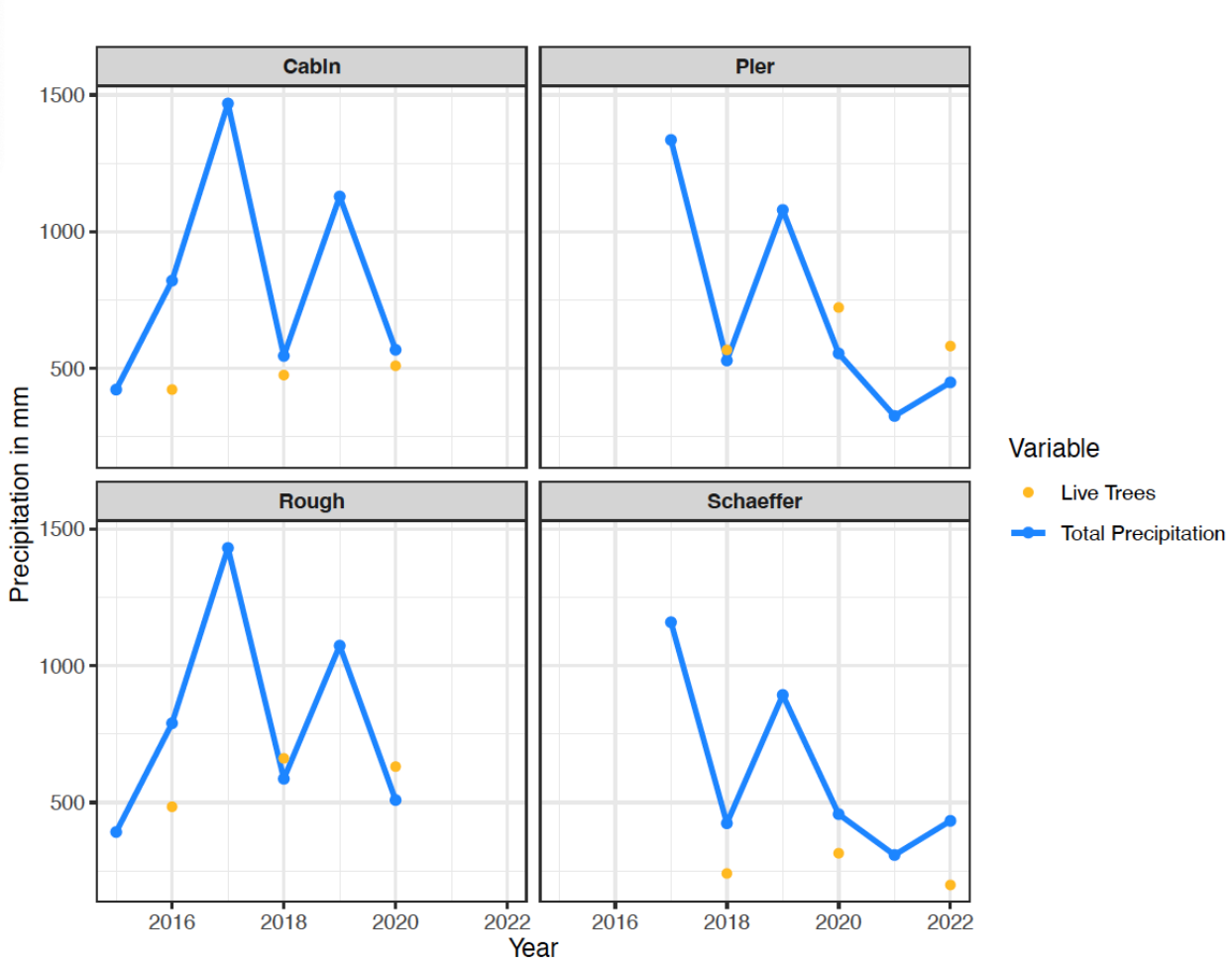


Figure 2.6. Total precipitation for the water (Oct – Sep) year for each fire shown in blue. Yellow dots represent the proportion of live trees out of 1000 so they can be meaningfully depicted on the same y axis.

DISCUSSION

Detection of delayed mortality up to five years post-fire can be performed relatively accurately with the application of random forest models using spectral bands from strictly postfire Sentinel-2 imagery. By observing and predicting how live tree cover changed from postfire Year 1 to Years 3 and 5 across four fires, this study revealed a substantial amount of green-up occurring after fire in forested areas in most fires. Three of the four case study fires used in this investigation showed an increase in percentage of live area between Year 1 and Year 3 post-fire, while there was more variation in directional change between Year 3 and Year 5. The initial increase in percentage live followed by subsequent decrease in some cases suggests vegetation recovery that could be tree recovery (e.g., green needle flushing of fire-injured trees) or shrub recovery. Given that this investigation was done using only spectral data, it can be difficult to parse out the true source of the greening without employing more complex methods such as spectral unmixing (Quintano et al. 2012). However, our photo-interpreted NAIP imagery sample showed similar increases in live tree prevalence between Year 1 and Years 3-5 (Figure S2.6), and model precision (percentage of predicted live-tree pixels that contained live trees) only dropped by 5-7 percentage points between Year 1 and Years 3-5 (Figure 2.3, Table S2.2), suggesting that much, if not most of the predicted increases in green tree abundance may represent real recovery of tree canopies (the only exception being the Schaeffer Fire). In the conifer forests that comprise most of our study area, high-severity fire disturbance is often followed by strong shrub establishment, often reaching near 100% shrub cover within 5 years post-fire (Coppoletta et al. 2015). The fact that our models retained accuracies of 68-74% through year 5 post-

fire, despite presumably high shrub abundance, implies that the model had relatively high skill in distinguishing live shrubs from live trees. Confidence in tree recovery being captured over understory green up is increased by the fact that spectral reflectance is highly correlated to actual tree cover (Cilek et al. 2021) in forested areas. Existing discrepancies may arise from the fact that the photo interpreted pixels were only a random subsample of the broader landscape for which predictions were made, and thus some degree of random deviations may be expected.

Above-average precipitation in the first post-fire year may be an important cause of the green up (presumably primarily green tree recovery) predicted by our models and observed in the human-interpreted NAIP imagery. Two of the fires in this analysis, the Cabin and Rough Fires, burned in the summer of 2015, and the following water year (specifically, water year 2017) was exceptionally wet (Pile et al. 2019) (Figure 2.6). The Cabin and Rough Fires had and 1.4 and 2 times more precipitation than 30-year precipitation normals. Similarly, the trends for percentage live pixels in the Schaeffer and Pier fires shadow the total precipitation patterns for the years of interest. The Cabin and the Rough Fires also had large areas of high burn severity one year post fire, which is in congruence with the finding that drought prior to fire increases tree mortality after fire (Cansler et al. 2024).

Another potential explanation for the apparent transitions of trees from dead to live is that green needles were initially eliminated by fire but later regrew. For example, ponderosa pine, a dominant species in the study system, has thick bark and large branches, and its buds can survive fire even if foliage is scorched (Hood et al. 2010). Green needle flushing at various timesteps post-fire has been observed in yellow pines including

ponderosa (Reed and Hood 2024). Questions that arise include: how did these trees recover from fire-caused injury, and what was the cause of death of the trees that ultimately died? One potential determinant of these outcomes is the trees' reserves of nonstructural carbohydrates (NSCs), which play an important role in tree functions including metabolism, growth, and recovery from disturbance (Hartmann and Trumbore 2016). In times of stress (such as from drought or fire-caused injury), trees can draw from NSC reserves and if they cross a critical threshold, mortality can occur (Barker Plotkin et al. 2021). NSC dynamics are starting to be linked to crown injury metrics (such as scorch), which is a strong predictor of tree mortality (Reed and Hood 2024). NSC dynamics may also partially explain patterns of susceptibility to bark beetle mortality, at least in cases where beetle populations are below outbreak conditions (Stephenson et al. 2019). A better understanding of exactly how NSC dynamics are impacted by compounding disturbances in coniferous forests would help to resolve these possibilities and provide useful information for managers. Characterization and understanding of post-fire tree stress that moves beyond the binary of 'live' or 'dead' has been identified as a research need (Varner et al. 2009), and labeling trees or pixels beyond this binary classification in remote sensing studies may help to uncover trends and/or mechanisms that are currently obscured.

Other potential drivers of vegetation and/or spectral recovery (or lack thereof) are post-fire management intervention and natural seedling regeneration. We examined the Forest Service Activity Tracking System (FACTS, https://data-usfs.hub.arcgis.com/datasets/activity-project-areas-nepa-feature-layer/about, accessed 9/5/2025) database to see what, if any, post-fire activities had been implemented within

each of the four fire perimeters. In the footprint of the Schaeffer Fire, approximately 29 ha were harvested for timber in 2021 (4 years after fire), along the very southern edge of the fire footprint along roads. Within the Pier Fire footprint, there was some scattered piling and burning of fuels post fire. Within the footprint of the Rough Fire, post-fire tree planting was implemented in about 156 ha in numerous small patches throughout the southern edge of the fire perimeter between 2016 and 2018. No management activities were conducted in the perimeter of the Cabin Fire. While these management activities did not cover a large area (proportional to each fire footprint), they could have contributed to vegetation recovery, as fuel burning or timber harvest creates openings in the forest floor that can then be occupied by newly establishing vegetation, including naturally recruiting tree seedings (Rhoades and Fornwalt 2015). Examination of post-fire monitoring data, if collected, could help to determine the extent to of natural regeneration and link it to spectral recovery.

Notably, the random forest models derived from strictly post-fire Sentinel imagery predicted a lower proportion of pixels containing live trees compared to thresholded RdNBR maps in which the non-high-severity classes are interpreted to contain live trees, a common practice in fire ecology (Miller and Thode 2007, Miller et al. 2009, Belote et al. 2015, Walker et al. 2019). The higher estimate of live tree pixel area, and lower estimate of distance to live tree pixels, by the RdNBR-based method may be a function of the coarser spatial resolution (30m) of Landsat-derived RdNBR itself. As stated earlier, Landsat-derived RdNBR was used in this study in a deliberate effort to gain insight into the management implications of using the index in its perhaps most common form: the 30 m-resolution

Landsat-based layers provided by the MTBS program. RdNBR, although widely used, has some shortcomings in biological interpretation stemming from the underlying algebra (Parks et al. 2014). For example, in low biomass environments, pre-fire NBR values can be low due to sparse vegetation, leading to a small denominator value, and subsequently produce extreme values of RdNBR that can be difficult to interpret (Parks et al. 2014). RBR, or the relativized burn ratio, does not have the same mathematical limitations as RdNBR, but it is not available through MTBS. Given that RdNBR can be difficult to interpret even when used as originally intended (as a metric of change as opposed to state), it is likely to be even more challenging to interpret when used outside its intended scope (i.e., to map a post-fire state, such as live tree presence) and therefore, post-fire-only spectral data (instead of a differenced index) may produce more accurate results. Furthermore, the links between tree physiological dynamics and fire-induced tree injury discussed earlier may be better informed by post-fire imagery instead of differenced indices, because the ability to quantify tree status at different time points may help to better identify 'tipping points' where trees go from injured and/or recovering to dead.

LIMITATIONS

While our work demonstrates that this model framework (which is extended beyond one year as presented in Wong et al. 2025) reliably predicts live trees at one, three, and five years post-fire, there are some caveats. Due to constraints on study fire selection, only two distinct fire years (2015 and 2017) were considered in this study. The potential for year effects like precipitation as discussed above may affect spectral signals of live tree

presence in ways that may not transfer to other years. Additionally, longer-term post-fire processes such as bark sloughing or bark beetle outbreaks may affect the spectral differentiation between live and dead trees. Future studies could address this limitation by including fires from additional years, potentially relying on purpose-collected ground-based validation data rather than interpretation of NAIP imagery, which is only available biennially. Future research that collects field data could also help in quantifying the uncertainty in differentiating between actual tree recovery and understory vegetation recovery, In addition to potential year effects, there was variability in the proportion of conifer forest within each fire perimeter. Portions of our focal fires were dominated by non-conifer vegetation, and it is possible that if this analysis were restricted to areas that only contained coniferous forest, higher model accuracies would result. However, running this analysis on the diverse array of vegetation occurring across these post-fire landscapes, as we did, is more realistic because it represents true conditions and does not artificially inflate model performance by restricting to specific vegetation types with particularly clear spectral signals. Additionally, tree crowns can be smaller than the 10 m pixel size used to produce the random forest prediction maps. It is challenging to predict heterogeneous within-pixel vegetation from a spectral reflectance-only approach; a potential alternative is to use finer-grain data (as in Sebastian et al. 2024), but such data is generally proprietary and cost-prohibitive at large spatial extents. Furthermore, the spectral-based approach means that we cannot differentiate trees from shrubs. Without field-mapped trees, it can be challenging to differentiate tree from shrub growth, although texture metrics or spectral unmixing from Sentinel could help. Lidar data can potentially help to more accurately map

live trees and differentiate forest structure, but while available on broad spatial extents through the USGS 3DEP program (https://www.usgs.gov/3d-elevation-program, accessed 9/5/2025), it is rarely available on repeat timescales necessary for post-fire analysis (Jeronimo et al. 2018, Ostergren et al. 2019).

Potential directions for future research include employing spectral unmixing methods or using freely available spectral data and pairing it with uncrewed aerial vehicle (UAV) field surveys to identify individual trees or tree approximate objects (TAO) (Bao et al. 2024). Additionally, explicitly classifying shrubs, understory vegetation, and trees (as opposed to simply live tree or no live tree as we have done here) may aid the model in distinguishing the spectral source of green-up, as would including climate data and seasonality data (in the form of multiple images per year) in the classifier. Such an approach would be a natural next step in this line of research. Finally, the decision to resample six bands from Sentinel-2 (Band 1 was 60-m, all other resampled bands were 20-m) to 10-m resolution using GEE's default bilinear interpolation method could have introduced some imprecision to the input dataset, but it allowed us to use the remaining bands (Bands 2, 3, 4, and 8) at their native 10-m resolution; theoretically, the random forest model could learn to place greater importance on the more spatially precise bands while still using the spatially coarser bands to provide important context.

The limitations of RdNBR, our thresholded comparison product, also merit discussion. As more research is conducted on broad-scale burn severity assessments, much of it relies on MTBS products such as RdNBR. MTBS contains several sources of error which include phenological offsets that are manually set by analysts, as well as subjective

classification thresholds (Kolden et al. 2015). Researchers who calculate RdNBR on their own in GEE can apply phenological offsets in a scripted manner using logic developed in Parks et al. 2018, but the lack of standardized classification thresholds remains. Perhaps most widely used are thresholds for the Sierra Nevada from a field-validated study in 2009 (Miller et al. 2009), while more recent and statistically robust regional models and thresholds have come out of the interior Pacific Northwest (Saberi and Harvey 2023), as well as the Southwest (Reiner et al. 2022) of the United States. Challenges remain when methodological refinements to burn severity indices are applied in new locations, as strengths of correlations can vary (Cansler et al. 2012). Despite these challenges, RdNBR has a high correspondence to more ecologically interpretable fire-effect measures such as canopy cover or basal area loss (Saberi and Harvey 2023). Further studies of the relationship between RdNBR and empirical forest condition would help to determine how best to interpret remotely sensed post-fire indices in different contexts.

CONCLUSION

This study is the first of its kind to use strictly postfire spectral data to model live trees with random forests at one, three-, and five-years post-fire across four fires in the southern Sierra Nevada. We compared the area of pixels containing live trees from predictive maps produced by random forest models to predictive maps produced by thresholded RdNBR and found that the random forest models predicted a much smaller area of live pixels per fire, and longer average distances to the nearest live pixel. Percentage live area increased by Year 3 in three out of four fires and either increased slightly or

decreased between Year 3 and Year 5, suggesting that delayed tree mortality was not common at this time step. Challenges with this study include the fact that the fires were from only two years (2015 and 2017), and unusually high precipitation in the 2017 water year may have caused more easily detectable green up for the 2015 fires. In addition, questions remain about the source of observed trends such as injured trees recovering and then dying later, which reflects a knowledge gap in our understanding of mechanisms of tree stress and subsequent mortality. This study is still one of the first to utilize freely available imagery to model delayed tree mortality using non-differenced spectral information at multiple time steps. These methods could support a cost effective and reliable decision support tool for predicting post-fire tree mortality and live tree presence through time and space and help forest managers prioritize restoration efforts, allocate resources, and adapt intervention strategies to changing environmental conditions and risk scenarios.

ACKNOWLEDGEMENTS

We thank Kara Sanghera for her invaluable help in tree photo interpretation and David Russell for helpful machine learning discussions. Funding for this project is provided by the Robert T. Stafford Disaster Relief and Emergency Assistance Act (42 U.S.C. 5121 et seq.) and supplemental funding acts for Federal disaster relief activities. Any use of trade, firm, or product names is for descriptive purposes only and does not imply endorsement by the US government.

REFERENCES

Adams, M.A., 2013. Mega-fires, tipping points and ecosystem services: Managing forests and woodlands in an uncertain future. Forest Ecology and Management, The Mega-fire reality 294, 250–261. https://doi.org/10.1016/j.foreco.2012.11.039

Bao, S.G., Wang, W.J., Liu, Z., Zhang, H.K., Wang, L., Ma, J., Sun, H., Ba, S., Wang, Y., He, H.S., 2024. Revealing post-megafire spectral and compositional recovery in the Siberian boreal forest using Landsat time series and regression-based unmixing approach. Remote Sensing of Environment 311, 114307. https://doi.org/10.1016/j.rse.2024.114307

Barker Plotkin, A., Blumstein, M., Laflower, D., Pasquarella, V.J., Chandler, J.L., Elkinton, J.S., Thompson, J.R., 2021. Defoliated trees die below a critical threshold of stored carbon. Functional Ecology 35, 2156–2167. https://doi.org/10.1111/1365-2435.13891

Belote, T.R., Larson, A.J., Dietz, M.S., 2015. Tree survival scales to community-level effects following mixed-severity fire in a mixed-conifer forest. Forest Ecology and Management 353, 221–231. https://doi.org/10.1016/j.foreco.2015.05.033

Bowman, D.M.J.S., Balch, J.K., Artaxo, P., Bond, W.J., Carlson, J.M., Cochrane, M.A., D'Antonio, C.M., DeFries, R.S., Doyle, J.C., Harrison, S.P., Johnston, F.H., Keeley, J.E., Krawchuk, M.A., Kull, C.A., Marston, J.B., Moritz, M.A., Prentice, I.C., Roos, C.I., Scott, A.C., Swetnam, T.W., van der Werf, G.R., Pyne, S.J., 2009. Fire in the Earth System. Science 324, 481–484. https://doi.org/10.1126/science.1163886

Busby, S., Evers, C., Holz, A., 2024. Patterns, drivers, and implications of postfire delayed tree mortality in temperate conifer forests of the western United States. Ecosphere 15, e4805. https://doi.org/10.1002/ecs2.4805

California Department of Forestry and Fire Protection. Historical Fire Perimeters (Firep22_1, released April 2023). Fire Resource Assessment Program. Available at: https://www.fire.ca.gov/what-we-do/fire-resource-assessment-program/fire-perimeters. Accessed 5 September 2025.

California Department of Fish and Wildlife. NAIP Data. Available at: https://wildlife.ca.gov/Data/GIS/Map-Services. Accessed 1 May 2024.

Cansler, C.A., McKenzie, D., 2012. How Robust Are Burn Severity Indices When Applied in a New Region? Evaluation of Alternate Field-Based and Remote-Sensing Methods. Remote Sensing 4, 456–483. https://doi.org/10.3390/rs4020456

Cilek, A., Berberoglu, S., Donmez, C., Sahingoz, M., 2022. The use of regression tree method for Sentinel-2 satellite data to mapping percent tree cover in different forest types. Environmental Science and Pollution Research 29, 23665–23676. https://doi.org/10.1007/s11356-021-17333-5

Cansler, C.A., Wright, M.C., Van Mantgem, P.J., Shearman, T.M., Varner, J.M., Hood, S.M., 2024. Drought before fire increases tree mortality after fire. Ecosphere 15, e70083. https://doi.org/10.1002/ecs2.70083

Coop, J.D., Parks, S.A., McClernan, S.R., Holsinger, L.M., 2016. Influences of prior wildfires on vegetation response to subsequent fire in a reburned Southwestern landscape. Ecological Applications 26, 346–354. https://doi.org/10.1890/15-0775

Coop, J.D., Parks, S.A., Stevens-Rumann, C.S., Crausbay, S.D., Higuera, P.E., Hurteau, M.D., Tepley, A., Whitman, E., Assal, T., Collins, B.M., Davis, K.T., Dobrowski, S., Falk, D.A., Fornwalt, P.J., Fulé, P.Z., Harvey, B.J., Kane, V.R., Littlefield, C.E., Margolis, E.Q., North, M., Parisien, M.-A., Prichard, S., Rodman, K.C., 2020. Wildfire-Driven Forest Conversion in Western North American Landscapes. BioScience 70, 659–673. https://doi.org/10.1093/biosci/biaa061

Coppoletta, M., Merriam, K.E., Collins, B.M., 2016. Post-fire vegetation and fuel development influences fire severity patterns in reburns. Ecological Applications 26, 686–699. https://doi.org/10.1890/15-0225

Das, A.J., Stephenson, N.L., Davis, K.P., 2016. Why do trees die? Characterizing the drivers of background tree mortality. Ecology 97, 2616–2627. https://doi.org/10.1002/ecy.1497

Dixon, D.J., Zhu, Y., Brown, C.F., Jin, Y., 2023. Satellite detection of canopy-scale tree mortality and survival from California wildfires with spatio-temporal deep learning. Remote Sensing of Environment 298, 113842. https://doi.org/10.1016/j.rse.2023.113842

Eliades, F., Sarris, D., Bachofer, F., Michaelides, S., Hadjimitsis, D., 2024. Understanding Tree Mortality Patterns: A Comprehensive Review of Remote Sensing and Meteorological Ground-Based Studies. Forests 15, 1357. https://doi.org/10.3390/f15081357

European Space Agency. Copernicus Sentinel-2 Collection 1 MSI Level 1C (L1C). Available at: https://sentinels.copernicus.eu/sentinel-data-access/sentinel-products/sentinel-2-data-products/collection-1-level-1c. Accessed 1 May 2025.

European Space Agency. Sentinel-2 Level 1C data. Available through Google Earth Engine as collection "Copernicus/S2_Harmonized." Accessed 1 May 2025.

Gorelick, N., Hancher, M., Dixon, M., Ilyushchenko, S., Thau, D., Moore, R., 2017. Google Earth Engine: Planetary-scale geospatial analysis for everyone. Remote Sensing of Environment, Big Remotely Sensed Data: Tools, Applications and Experiences 202, 18–27. https://doi.org/10.1016/j.rse.2017.06.031

Hart, S.J., Henkelman, J., McLoughlin, P.D., Nielsen, S.E., Truchon-Savard, A., Johnstone, J.F., 2019. Examining forest resilience to changing fire frequency in a fire-prone region of boreal forest. Global Change Biology 25, 869–884. https://doi.org/10.1111/gcb.14550

Hartigan, J.A., Wong, M.A., 1979. Algorithm AS 136: A K-Means Clustering Algorithm. Journal of the Royal Statistical Society. Series C (Applied Statistics) 28, 100–108. https://doi.org/10.2307/2346830

Hartmann, H., Trumbore, S., 2016. Understanding the roles of nonstructural carbohydrates in forest trees – from what we can measure to what we want to know. New Phytologist 211, 386–403. https://doi.org/10.1111/nph.13955

Hood, S.M., McHugh, C.W., Ryan, K.C., Reinhardt, E., Smith, S.L., 2007. Evaluation of a post-fire tree mortality model for western USA conifers. International Journal of Wildland Fire 16, 679–689. https://doi.org/10.1071/WF06122

Hood, S.M., Smith, S.L., Cluck, D.R., 2010. Predicting mortality for five California conifers following wildfire. Forest Ecology and Management 260, 750–762. https://doi.org/10.1016/j.foreco.2010.05.033

Hood, S.M., Varner, J.M., Mantgem, P. van, Cansler, C.A., 2018. Fire and tree death: understanding and improving modeling of fire-induced tree mortality. Environ. Res. Lett. 13, 113004. https://doi.org/10.1088/1748-9326/aae934

Key, C.H., Benson, N.C., 2006. Landscape Assessment (LA). *FIREMON: Fire effects monitoring and inventory system* 164 LA-1.

Kolden, C.A., Smith, A.M., Abatzoglou, J.T., 2015. Limitations and utilisation of Monitoring Trends in Burn Severity products for assessing wildfire severity in the USA. International Journal of Wildland Fire 24, 1023–1028.

Jeronimo, S.M.A., Kane, V.R., Churchill, D.J., McGaughey, R.J., Franklin, J.F., 2018. Applying LiDAR Individual Tree Detection to Management of Structurally Diverse Forest Landscapes. Journal of Forestry 116, 336–346. https://doi.org/10.1093/jofore/fvy023

LANDFIRE. 2024. Existing Vegetation Type Layer, LANDFIRE 2.4.0, U.S. Department of the Interior, Geological Survey, and U.S. Department of Agriculture. Accessed 24 April 2024 at https://www.landfire/data/FullExtentDownloads

Liaw, A. and Wiener, M., 2002. Classification and regression by randomForest. R news, 2(3), pp.18-22.

Main-Knorn, M., Pflug, B., Louis, J., Debaecker, V., Müller-Wilm, U., Gascon, F., 2017. Sen2Cor for Sentinel-2, in: Image and Signal Processing for Remote Sensing XXIII. Presented at the Image and Signal Processing for Remote Sensing XXIII, SPIE, pp. 37–48. https://doi.org/10.1117/12.2278218

Maxwell, A.E., Warner, T.A., Vanderbilt, B.C., Ramezan, C.A., 2017. Land cover classification and feature extraction from National Agriculture Imagery Program (NAIP) Orthoimagery: A review. Photogrammetric Engineering & Remote Sensing 83, 737–747. https://doi.org/10.14358/PERS.83.10.737

McDowell, N., Pockman, W.T., Allen, C.D., Breshears, D.D., Cobb, N., Kolb, T., Plaut, J., Sperry, J., West, A., Williams, D.G., Yepez, E.A., 2008. Mechanisms of plant survival and mortality during drought: why do some plants survive while others succumb to drought? New Phytologist 178, 719–739. https://doi.org/10.1111/j.1469-8137.2008.02436.x

Meddens, A.J.H., Kolden, C.A., Lutz, J.A., Smith, A.M.S., Cansler, C.A., Abatzoglou, J.T., Meigs, G.W., Downing, W.M., Krawchuk, M.A., 2018. Fire Refugia: What Are They, and Why Do They Matter for Global Change? BioScience 68, 944–954. https://doi.org/10.1093/biosci/biy103

Miller, J.D., Thode, A.E., 2007. Quantifying burn severity in a heterogeneous landscape with a relative version of the delta Normalized Burn Ratio (dNBR). Remote Sensing of Environment 109, 66–80. https://doi.org/10.1016/j.rse.2006.12.006

Miller, J.D., Knapp, E.E., Key, C.H., Skinner, C.N., Isbell, C.J., Creasy, R.M., Sherlock, J.W., 2009. Calibration and validation of the relative differenced Normalized Burn Ratio (RdNBR) to three measures of fire severity in the Sierra Nevada and Klamath Mountains, California, USA. Remote Sensing of Environment 113, 645–656. https://doi.org/10.1016/j.rse.2008.11.009

Mitas, L., Mitasova, H., 1999. Spatial interpolation. In: Longley, P., Goodchild, M.F., Maguire, D.J., Rhind, D.W. (Eds.), *Geographical Information Systems: Principles, Techniques, Management and Applications*. Hoboken, New Jersey, USA, Wiley, 481–492.

Ostergren, C.L., Decker, D., and Carswell, W.J., Jr., 2019. The 3D Elevation Program—Supporting California's economy (ver. 1.1, June 2019): U.S. Geological Survey Fact Sheet 2019-3029, 2 p., https://doi.org/10.3133/fs20193029

Parks, S.A., Dillon, G.K., Miller, C., 2014. A New Metric for Quantifying Burn Severity: The Relativized Burn Ratio. Remote Sensing 6, 1827–1844. https://doi.org/10.3390/rs6031827

Parks, S.A., Holsinger, L.M., Voss, M.A., Loehman, R.A., Robinson, N.P., 2018. Mean Composite Fire Severity Metrics Computed with Google Earth Engine Offer Improved Accuracy and Expanded Mapping Potential. Remote Sensing 10, 879. https://doi.org/10.3390/rs10060879

Parks, S.A., Abatzoglou, J.T., 2020. Warmer and Drier Fire Seasons Contribute to Increases in Area Burned at High Severity in Western US Forests From 1985 to 2017. Geophysical Research Letters 47, e2020GL089858. https://doi.org/10.1029/2020GL089858

Phiri, D., Simwanda, M., Salekin, S., Nyirenda, V.R., Murayama, Y., Ranagalage, M., 2020. Sentinel-2 Data for Land Cover/Use Mapping: A Review. Remote Sensing 12, 2291. https://doi.org/10.3390/rs12142291

Picotte, J.J., Bhattarai, K., Howard, D., Lecker, J., Epting, J., Quayle, B., Benson, N., Nelson, K., 2020. Changes to the Monitoring Trends in Burn Severity program mapping production procedures and data products. Fire Ecology 16, 16. https://doi.org/10.1186/s42408-020-00076-y

Pile, L., Meyer, M., Rojas, R., Roe, O., Smith, M., 2019. Drought Impacts and Compounding Mortality on Forest Trees in the Southern Sierra Nevada. Forests 10, 237. https://doi.org/10.3390/f10030237

Quintano, C., Fernández-Manso, A., Shimabukuro, Y.E., Pereira, G., 2012. Spectral unmixing. International Journal of Remote Sensing 33, 5307–5340. https://doi.org/10.1080/01431161.2012.661095

PRISM Climate Group, Oregon State University. 2014. Available at: https://prism.orgeonstate.edu/explorer. Accessed 5 April 2025.

R Core Team. 2024. R: A language and environment for statistical computing. R Foundation for Statistical Computing. Available at: https://www.R-project.org/

Reed, C.C., Hood, S.M., 2024. Nonstructural carbohydrates explain post-fire tree mortality and recovery patterns. Tree Physiology 44, tpad155. https://doi.org/10.1093/treephys/tpad155

Reilly, M.J., Zuspan, A., Yang, Z., 2023. Characterizing post-fire delayed tree mortality with remote sensing: sizing up the elephant in the room. Fire Ecology 19, 64. https://doi.org/10.1186/s42408-023-00223-1

Reiner, A.L., Baker, C., Wahlberg, M., Rau, B.M., Birch, J.D., 2022. Region-Specific Remote-Sensing Models for Predicting Burn Severity, Basal Area Change, and Canopy Cover Change following Fire in the Southwestern United States. Fire 5, 137. https://doi.org/10.3390/fire5050137

Rhoades, C.C., Fornwalt, P.J., 2015. Pile burning creates a fifty-year legacy of openings in regenerating lodgepole pine forests in Colorado. Forest Ecology and Management 336, 203–209. https://doi.org/10.1016/j.foreco.2014.10.011

Saberi, S.J., Harvey, B.J., 2023. What is the color when black is burned? Quantifying (re)burn severity using field and satellite remote sensing indices. Fire Ecology 19, 24. https://doi.org/10.1186/s42408-023-00178-3

Saberi, S.J., Latimer, A.M., Young, D.J., Wong, C.Y., van Mantgem, P.J., Wright, M.C., 2025. Data describing the presence of live trees for three years in Sentinel-2 pixels across four fires in California, USA: U.S. Geological Survey data release, https://doi.org/10.5066/P13LSPGV.

Safford, H.D., Water, K.M.V. de, 2014. Using fire return interval departure (FRID) analysis to map spatial and temporal changes in fire frequency on national forest lands in California. Res. Pap. PSW-RP-266. Albany, CA: U.S. Department of Agriculture, Forest Service, Pacific Southwest Research Station. 59 p 266. https://doi.org/10.2737/PSW-RP-266

Safford, H.D., Stevens, J.T., 2017. Natural range of variation for yellow pine and mixed-conifer forests in the Sierra Nevada, southern Cascades, and Modoc and Inyo National Forests, California, USA.

Seidl, R., Thom, D., Kautz, M., Martin-Benito, D., Peltoniemi, M., Vacchiano, G., Wild, J., Ascoli, D., Petr, M., Honkaniemi, J., Lexer, M.J., Trotsiuk, V., Mairota, P., Svoboda, M., Fabrika, M., Nagel, T.A., Reyer, C.P.O., 2017. Forest disturbances under climate change. Nature Climate Change 7, 395–402. https://doi.org/10.1038/nclimate3303

Shearman, T.M., Varner, J.M., Hood, S.M., van Mantgem, P.J., Cansler, C.A., Wright, M., 2023. Predictive accuracy of post-fire conifer death declines over time in models based on crown and bole injury. Ecological Applications 33, e2760. https://doi.org/10.1002/eap.2760

Stephenson, N.L., van Mantgem, P.J., Bunn, A.G., Bruner, H., Harmon, M.E., O'Connell, K.B., Urban, D.L., Franklin, J.F., 2011. Causes and implications of the correlation between forest productivity and tree mortality rates. Ecological Monographs 81, 527–555. https://doi.org/10.1890/10-1077.1

Stephenson, N.L., Das, A.J., Ampersee, N.J., Bulaon, B.M., Yee, J.L., 2019. Which trees die during drought? The key role of insect host-tree selection. Journal of Ecology 107, 2383–2401. https://doi.org/10.1111/1365-2745.13176

United States Department of Agriculture. National Agriculture Imagery Program. Available at: https://map.dfg.ca.gov/arcgis/services, Accessed 1 June 2025.

U.S. Geological Survey. Landsat surface reflectance data products. Available at: https://landsat.usgs.gov/, Accessed 4 September 2025.

U.S. Geological Survey. 3D Elevation program. Available at: https://www.usgs.gov/3d-elevation-program, Accessed 5 September 2025.

Walker, R.B., D. Coop, J., M. Downing, W., A. Krawchuk, M., L. Malone, S., W. Meigs, G., 2019. How Much Forest Persists Through Fire? High-Resolution Mapping of Tree Cover to Characterize the Abundance and Spatial Pattern of Fire Refugia Across Mosaics of Burn Severity. Forests 10, 782. https://doi.org/10.3390/f10090782

Westerling, A.L., 2016. Increasing western US forest wildfire activity: sensitivity to changes in the timing of spring. Philosophical Transactions of the Royal Society B: Biological Sciences 371, 20150178. https://doi.org/10.1098/rstb.2015.0178

Williams, J.N., Safford, H.D., Enstice, N., Steel, Z.L., Paulson, A.K., 2023. High-severity burned area and proportion exceed historic conditions in Sierra Nevada, California, and adjacent ranges. Ecosphere 14, e4397. https://doi.org/10.1002/ecs2.4397

Wong, C.Y.S., Wright, M.C., Van Mantgem, P.J., Latimer, A.M., Young, D.J.N., 2025. Sentinel imagery detects the presence of live trees following large wildfires in California. Environmental Research Ecology. https://doi.org/10.1088/2752-664X/add5fd

Van de Water, K.M., Safford, H.D., 2011. A Summary of Fire Frequency Estimates for California Vegetation before Euro-American Settlement. Fire Ecology 7, 26–58. https://doi.org/10.4996/fireecology.0703026

van Mantgem, P.J., Stephenson, N.L., Byrne, J.C., Daniels, L.D., Franklin, J.F., Fulé, P.Z., Harmon, M.E., Larson, A.J., Smith, J.M., Taylor, A.H., Veblen, T.T., 2009. Widespread Increase of Tree Mortality Rates in the Western United States. Science 323, 521–524. https://doi.org/10.1126/science.1165000

van Mantgem, P.J., Stephenson, N.L., Knapp, E., Battles, J., Keeley, J.E., 2011. Long-term effects of prescribed fire on mixed conifer forest structure in the Sierra Nevada, California. Forest Ecology and Management 261, 989–994. https://doi.org/10.1016/j.foreco.2010.12.013

Varner, M.J., Putz, F.E., O'Brien, J.J., Kevin Hiers, J., Mitchell, R.J., Gordon, D.R., 2009. Post-fire tree stress and growth following smoldering duff fires. Forest Ecology and Management 258, 2467–2474. https://doi.org/10.1016/j.foreco.2009.08.028

Yin, F., Lewis, P.E., Gómez-Dans, J.L., 2022. Bayesian atmospheric correction over land: Sentinel-2/MSI and Landsat 8/OLI. Geoscientific Model Development 15, 7933–7976. https://doi.org/10.5194/gmd-15-7933-2022

SUPPLEMENTARY INFORMATION (S2)

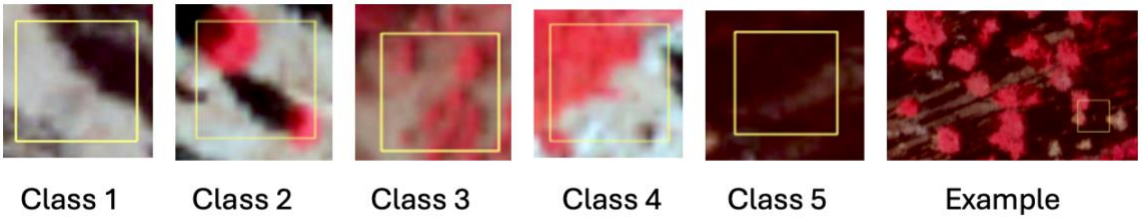


Figure S2.1. Representative photos of how different classes might look in false-color NAIP imagery, at a scale of 1:500. Pixels (10-m by 10-m) are delineated by the yellow square, and classes are: 1) Does not contain live vegetation, 2) Contains a live tree, with or without live understory vegetation, 3) Borderline live tree (touching border but not within a focal pixel, see upper right corner) 4) Contains live understory vegetation but does not contain live trees and 5) Undetermined classification. Class 5 in this example shows a zoomed-in view of the forest obscured by shadows. The “Example” photo at far right shows a zoomed-out false-colored NAIP imagery with the pixel area shown as a yellow square.

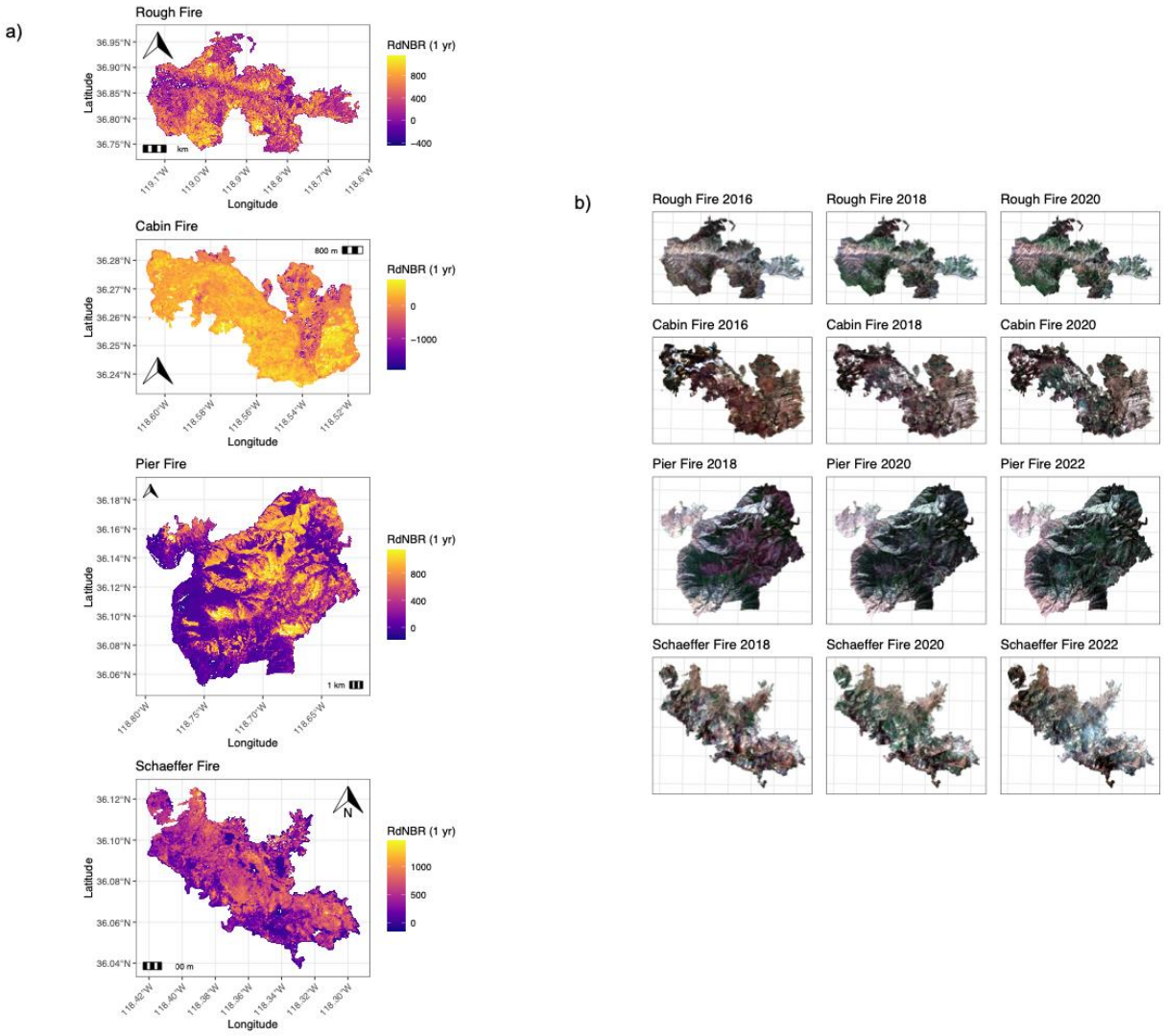


Figure S2.2. A) RdNBR for each fire, calculated one year post fire. B) True color composites from Sentinel-2 imagery for each fire and year combination. In all panels, fire perimeters come from California Department of Forestry and Fire Protection Fire and Resource Assessment Program, Historical Fire Perimeter GIS database (https://www.fire.ca.gov/what-we-do/fire-resource-assessment-program/fire-perimeters, accessed 9/4/2025).

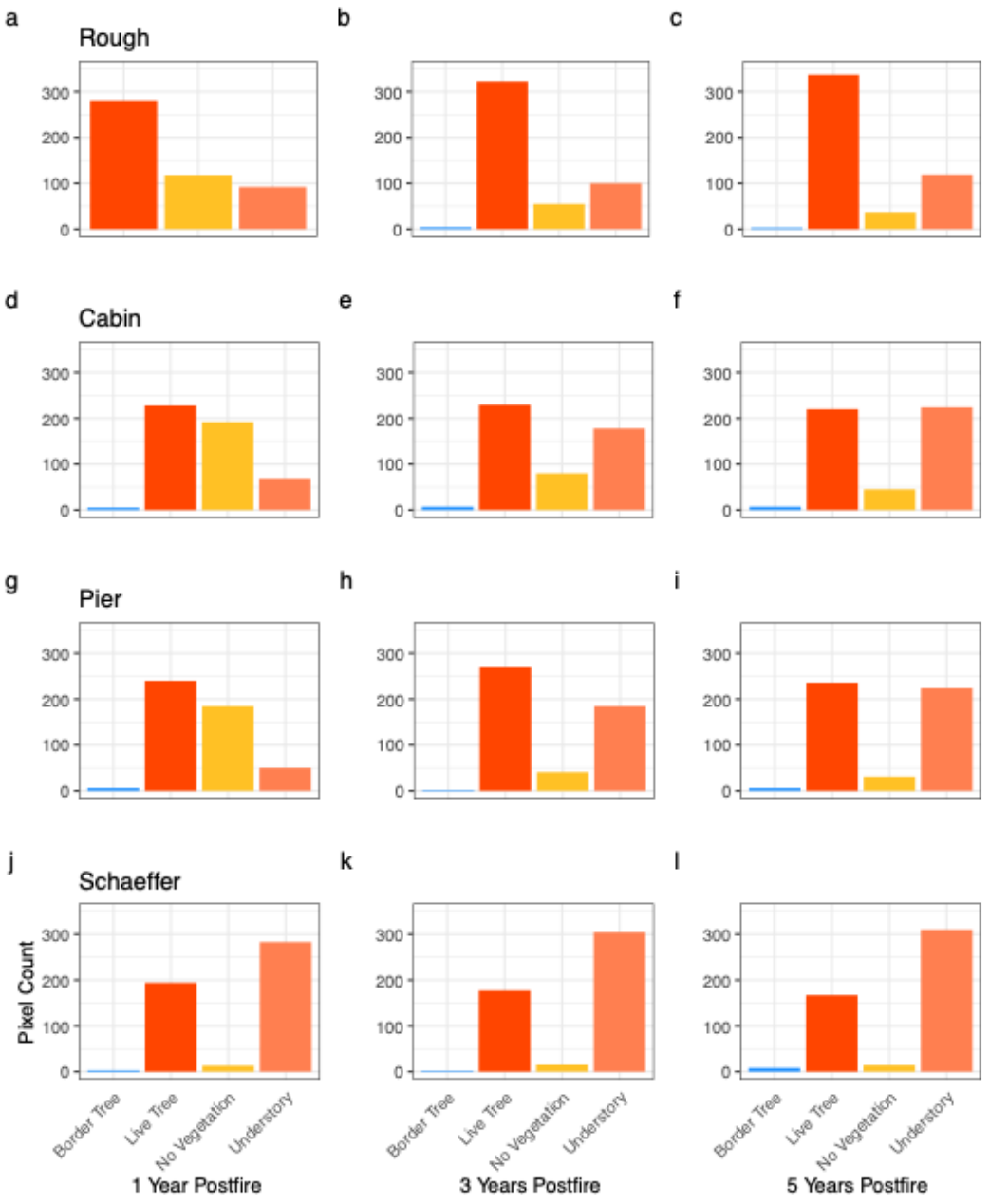


Figure S2.3. Counts of photo-interpreted pixels of each class for each post-fire image and year combination. Note that border trees were removed from the dataset for analyses, and that the Year 1 Rough Fire dataset did not contain any border trees.

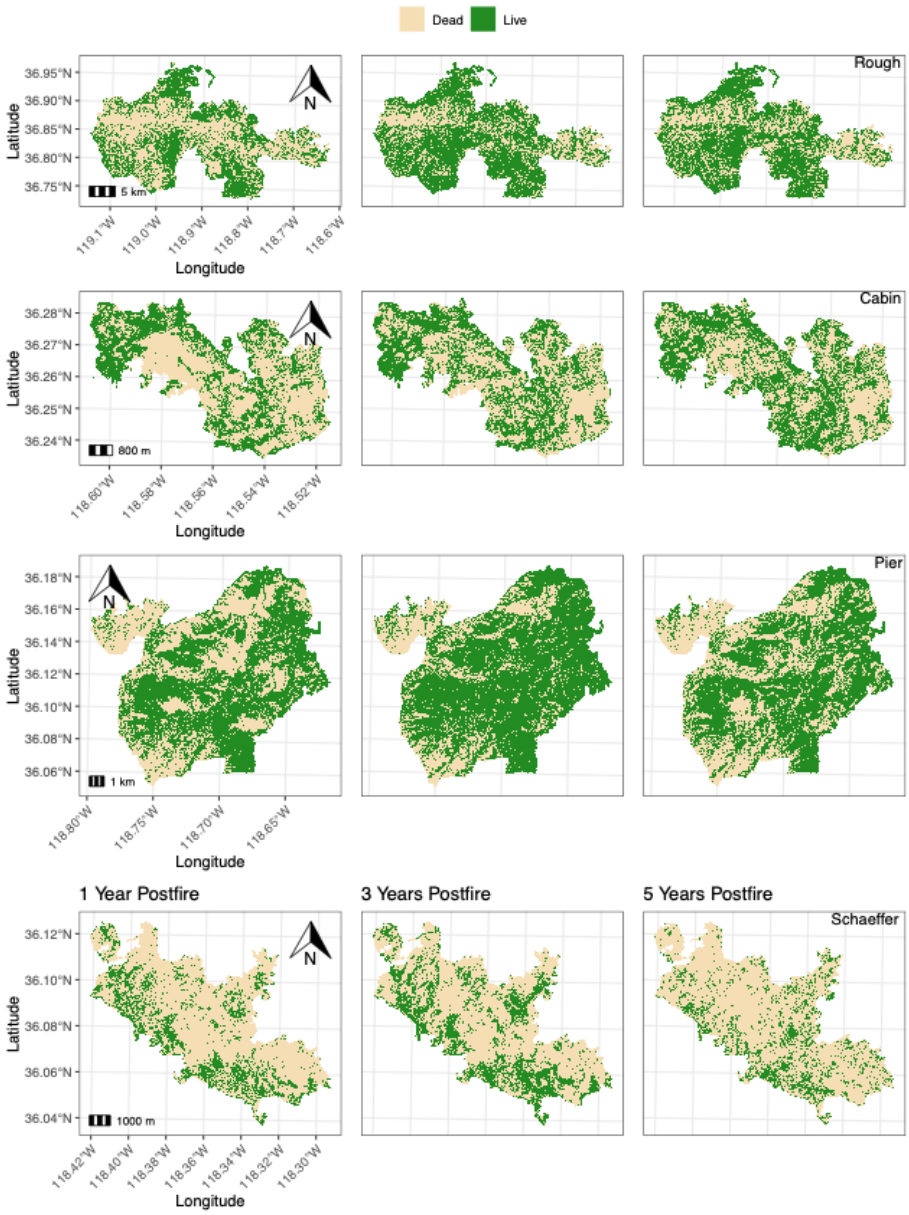


Figure S2.4. Prediction maps of live and dead pixels for all four fires (The top row is a reproduction of the Rough fire predictions as shown in the main manuscript) as estimated from the all-bands Sentinel-2 random forest models. Fire perimeters come from California Department of Forestry and Fire Protection Fire and Resource Assessment Program, Historical Fire Perimeter GIS database (https://www.fire.ca.gov/what-we-do/fire-resource-assessment-program/fire-perimeters, accessed 9/4/2025).

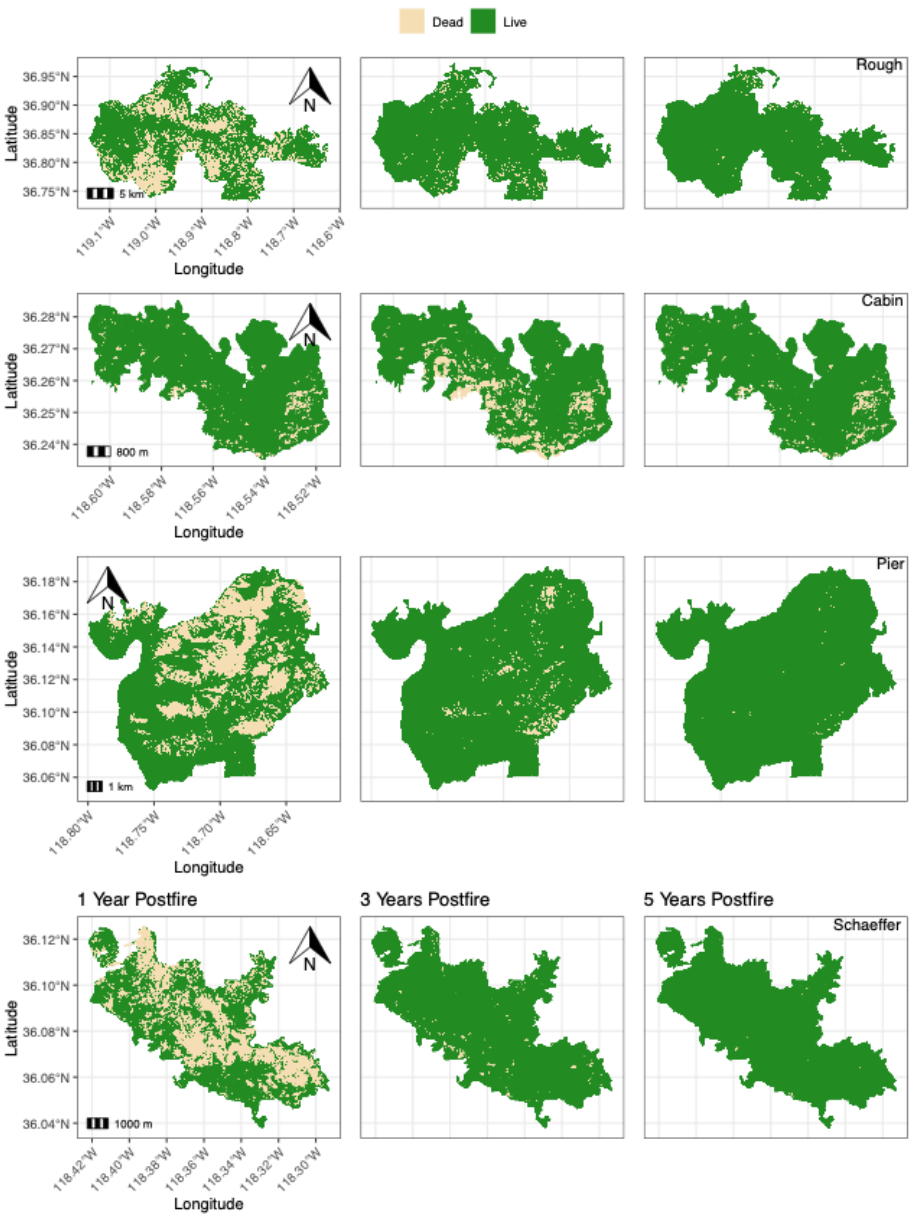


Figure S2.5. Prediction maps of live and dead pixels for all four fires (The top row is a reproduction of the Rough fire predictions as shown in the main manuscript) as estimated from thresholding RdNBR maps. Fire perimeters come from California Department of Forestry and Fire Protection Fire and Resource Assessment Program, Historical Fire Perimeter GIS database (https://www.fire.ca.gov/what-we-do/fire-resource-assessment-program/fire-perimeters, accessed 9/4/2025).

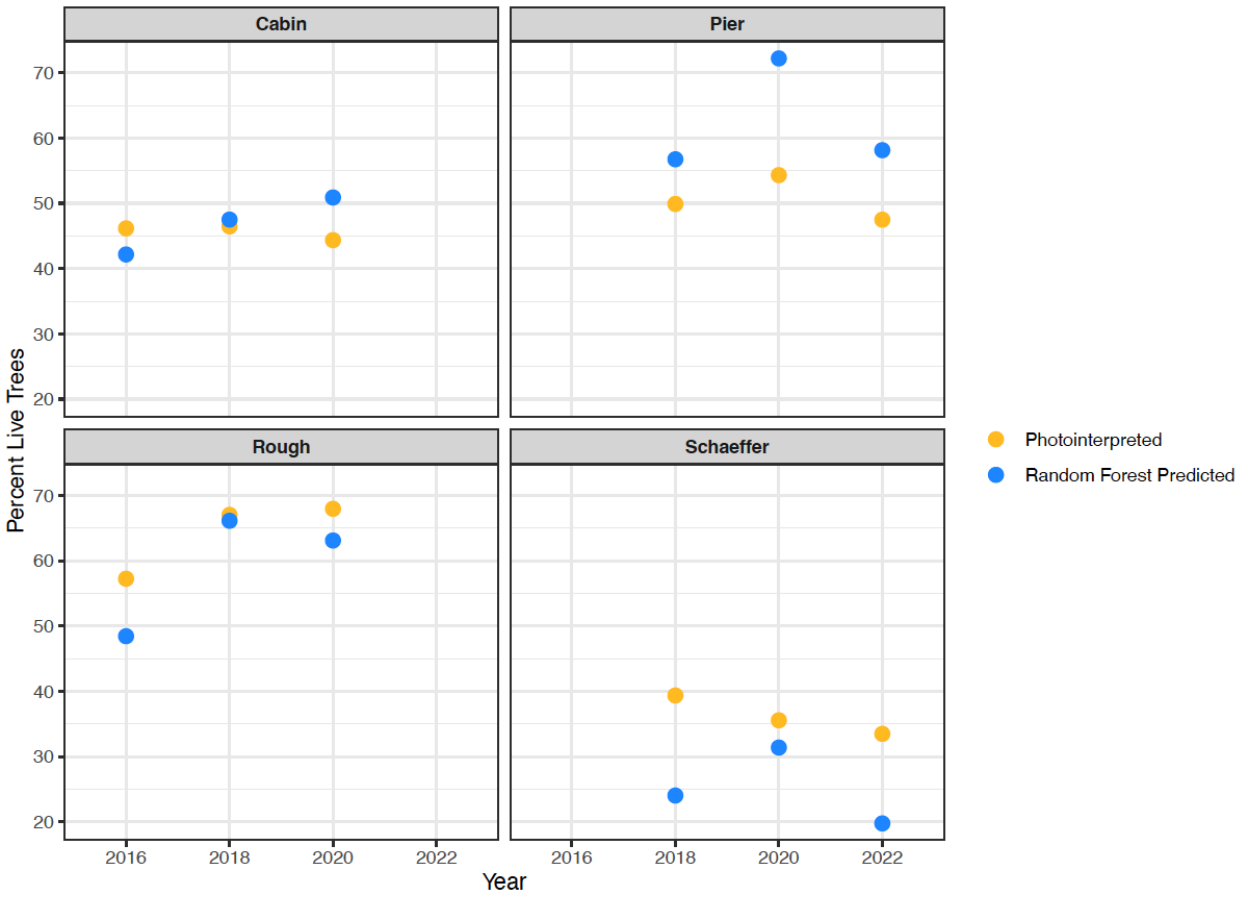


Figure S2.6. Change in percentage of live trees over time per fire as derived from photo-interpreted NAIP imagery shown in yellow dots. Blue dots represent the change in percentage of live trees over time as derived from the random forest model predictions.

Table S2.1. Proportions of true and false positives, true and false negatives, as well as accuracy, precision, recall, and F-score for the photo-interpreted dataset. Predicted live and predicted dead for each fire-year model also reflects only the truthed (where truth = photo interpretation) data.

Fire	Post-fire Year	True +	True -	False +	False -	Accuracy	Precision	Recall	F-score	Predicted Live	Predicted Dead
Rough	1	0.42	0.32	0.11	0.15	0.74	0.79	0.74	0.76	0.54	0.46
Rough	3	0.53	0.20	0.13	0.14	0.72	0.80	0.79	0.79	0.66	0.34
Rough	5	0.49	0.22	0.10	0.19	0.70	0.82	0.72	0.77	0.59	0.41
Cabin	1	0.26	0.47	0.07	0.20	0.73	0.79	0.57	0.66	0.33	0.67
Cabin	3	0.24	0.42	0.12	0.23	0.65	0.67	0.51	0.58	0.35	0.65
Cabin	5	0.24	0.44	0.11	0.21	0.68	0.68	0.53	0.60	0.35	0.65
Pier	1	0.42	0.44	0.06	0.07	0.86	0.88	0.85	0.86	0.48	0.52
Pier	3	0.46	0.31	0.14	0.09	0.77	0.76	0.84	0.80	0.60	0.40
Pier	5	0.36	0.37	0.15	0.11	0.74	0.71	0.77	0.74	0.52	0.48
Schaeffer	1	0.17	0.51	0.10	0.22	0.68	0.64	0.43	0.52	0.27	0.73
Schaeffer	3	0.21	0.49	0.15	0.14	0.70	0.58	0.59	0.59	0.36	0.64
Schaeffer	5	0.12	0.61	0.05	0.21	0.73	0.69	0.36	0.47	0.17	0.83

Table S2.2. Accuracy, precision, and recall values for twelve candidate models (inclusive of all fires). Training years 135 means that all years of data were included in the training dataset (Year 1, Year 3, and Year 5).

Prediction Year	Training Year(s)	Accuracy	Precision	Recall
1	135	0.75	0.79	0.66
3	135	0.71	0.72	0.70
5	135	0.71	0.74	0.62
1	1	0.74	0.75	0.69
3	1	0.69	0.68	0.74
5	1	0.65	0.63	0.70
1	3	0.75	0.76	0.70
3	3	0.72	0.71	0.75
5	3	0.71	0.70	0.71
1	5	0.67	0.65	0.70
3	5	0.71	0.71	0.73
5	5	0.69	0.72	0.58

Data Availability: Photo interpretation data are found in Saberi et al. (2025). All other data are publicly available.

CHAPTER 3. DRIVERS OF CONIFER REGENERATION IN SUCCESSIVELY BURNED AREAS IN THE CENTRAL SIERRA NEVADA

Saba J. Saberi, Hugh D. Safford, Derek J.N. Young, Andrew M. Latimer

ABSTRACT

Repeated high severity fire that is not within an ecosystem's historical fire regime can pose risk of type conversion to an alternate stable state. California's mixed conifer forests, which historically burned frequently and at low severity, are now burning at much higher severity. A combination of fire suppression and removal of indigenous land stewardship has led to dense, homogenous forests which, when combined with hot and dry conditions, contribute to high severity fire. Large fires with large patches of high burn severity raise concerns for regeneration failure, particularly when fires occur in quick succession (< 30 years), referred to as short interval reburns. Despite the increase of reburns, it is difficult to study their impacts on forest succession as sampling overlapping areas that have burned in multiple fires is an opportunistic endeavor. In this study, we took advantage of the 2021 Caldor fire reburning the 2004 Freds fire, the 2011 Long fire, and the 2019 Caples fire in the Central Sierra Nevada to investigate the effects of short term reburns on conifer regeneration. Using generalized linear mixed models with a log link (Tweedie distribution), we found that for pine species, the time between fires, or reburn interval, was a significant predictor of post-fire seedling density, while distance to seed source was a significant predictor for shade tolerant species. For shade tolerant species seedlings (0 year), reburn interacted with shrub cover to influence seedling density such that increased shrub cover corresponded with slightly increased seedling density, suggesting a nurse effect. Due to the over dispersed nature of seedling data, the correlation between observed and fitted values was low, but binarizing the data at a cutoff of 175 seedlings/ha showed strong predictive capability. Overall, a higher shade tolerant species

density compared to pine species density post-fire was reflective of the biological legacy of shade tolerant species dominance. The results of this study suggest that the incorporation of reburn history and reburn intervals into existing post-fire regeneration planning tools may aid land managers in identifying areas with high reforestation need.

INTRODUCTION

The severity and size of wildland fires in western North America have increased over the past several decades, in part due to hotter, drier conditions resulting from climate change and fuel accumulation from historical fire suppression (Westerling et al. 2016, Abatzoglou and Williams 2016). Increased high severity fire can affect forest successional pathways and, in extreme cases, drive transitions to alternative stable states (Harvey et al. 2016a). Many areas throughout fire-adapted coniferous forests of western North America are likely to experience repeat fire, or reburns, due to increased fire frequency. Repeat forest fires can act as linked disturbances in that the first fire can impact the probability of occurrence or severity of the second (Parks et al. 2014, Harvey et al. 2016a, Stevens-Rumann et al. 2016, Coppoletta et al. 2016, Collins et al. 2018, Tortorelli et al. 2024). For example, an initial fire can consume fuel and kill less fire-resistant vegetation, reducing the probability of a second fire. Alternatively, the initial fire can shift vegetation from obligate seeding conifers to resprouting species while simultaneously creating fuel for the second fire, eliminating seedlings and seed sources (Coop et al. 2020). A reburn *per se* does not necessarily raise concerns of forest regeneration failure or state transition. However, short interval reburns, or fires occurring more frequently than an area's natural fire return

interval, may not allow time for vegetation regrowth and seed establishment ('immaturity risk') and can be the impetus for transition to non-forest and erosion of resilience among other drivers, making them an important topic of study (Turner et al. 2019).

Departures from historical fire regimes and forest structure affect the impacts reburns can have on postfire forest succession. The historical fire regime of mixed conifer forests in California was characterized by frequent, low severity fire that clears the understory of fuel and opens the canopy (Safford and Stevens 2017, Bohlman et al. 2021). Historically, fires burned at low to moderate severities, killed only a small percentage of canopy trees, produced diverse forest structure at fine scales and maintained pine dominance in areas that would otherwise undergo succession to shade-tolerant species dominance (Safford and Stevens 2017). At broader spatial scales, forest structure and species composition were variable, and the proportion experiencing high severity fire was below ten percent (Stephens et al. 2015). Fire suppression since the early 1900s has led to an increase in density, canopy cover, homogenization, and often dominance by relatively fire-intolerant species like white fir and incense cedar (Stephens et al. 2015). Currently, low- and mid-elevation forests are burning at much higher severities than during pre-European settlement (Mallek et al. 2013, Williams et al. 2023). This increase in high severity fire is partially attributable to historic fire suppression policies that altered forest structure and composition such that stands are dense, dominated by middle-aged tree cohorts, and have an increased abundance of shade-tolerant and fire-sensitive species (Welch et al. 2016). The impact of short interval reburns in these altered forests is dependent on the severity of fires and the forest type. For example, two severe fires in quick succession can

lead to immaturity risk (Enright et al. 2015) and subsequent type conversion to non-forest. Alternatively, initial low-to-moderate severity fires in dry forests of the Cascades and Sierra Nevada can have a moderating effect on reburns that last ~13 years (Tortorelli et al. 2024).

Since fire-sensitive fir species can regenerate in high shade conditions, their continued dominance in historically pine-dominated areas further exacerbates forest homogenization and erodes resilience to future fire (Steel et al. 2021). Furthermore, large patches with very high tree mortality include interior areas far from seed sources, and the resulting low seed availability may drive regeneration failure (Paudel and Markwith 2023). Conifer dispersal distances are short, with the majority of conifer seedling recruitment occurring within 60 meters of the nearest living tree (Welch et al. 2016), although longer distance recruitment at 200 m has been observed (Rother and Veblen 2016, Kemp et al. 2016).

Previous work on single burns (as opposed to short interval reburns) has identified multiple variables that influence postfire conifer recruitment. An influential variable includes long-term climate, wherein high precipitation is associated with high seedling establishment (Young et al. 2019, Shive et al. 2018, Stewart et al. 2021, Paudel et al. 2022). However, the effects of such top-down drivers of recruitment often differ by species, and within-stand differences in species' spatial distribution can also play a role (North et al. 2005). Climatic patterns can alter interspecific relationships, which affect regeneration. For example, decreased snowpack and warmer temperatures reduce the negative impacts that competing shrubs would have with ponderosa pine seedlings under ambient conditions (Werner et al. 2019). In addition, climate-driven shifts in seedling recruitment

are often insufficient to produce tree community reorganization in response to postfire drought or other individual weather events, in part because regeneration is largely constrained to the local reproductive species pool (Young et al. 2019). Constraints on recruitment can also vary by species based on seed availability or microsite condition. For example, seed availability declines towards upper range edges due to low numbers of parent trees (Kroiss and HilleResLambers 2015). In harsher conditions (such as high-elevation subalpine or very dry low-elevation environments), abiotic conditions might be bigger constraints on recruitment than in more mesic environments, where biotic interactions may more strongly affect recruitment (Bell et al. 2014).Another major driver of seedling recruitment is topography, which is linked to moisture availability: south-facing slopes and ridges often experience the highest moisture deficit, and the narrow range of topo-climatic conditions that seedlings can withstand can make areas inhospitable to recruitment (Dyer 2009, Littlefield 2019).

There has been some research in regeneration outcomes after short-interval fire, herein defined as a reburn within 30 years (although definitions vary within the literature), with varying results. For example, in the wet and warm Klamath-Siskiyou forests, post-fire regeneration was not particularly limited by short-interval fires, perhaps due to complex fire severity patterns that produced enough proximate seed sources and a climate that provides adequate moisture availability (Donato et al. 2009). In the Central Cascades, high severity fire and short-interval fires resulted in more fire-adapted pine regeneration, suggesting a possible transition of dominant conifer type that is more adapted to frequent fire (Busby et al. 2020). In contrast, research in the Northern Rockies and New Mexico

suggests that short interval fires in dry conifer forest post-fire seedling density (Larson et al. 2013, Stevens-Rumann and Morgan 2016, Coop et al. 2016). Some inquiries into drivers of reburns show that postfire vegetation and fuel development after an initial burn can shape the severity of a subsequent burn (Coppoletta et al. 2016). High severity fire can produce high shrub cover and substantial amounts of downed woody debris, which can in turn act as fuel in a subsequent fire that burns with high severity (Parks et al. 2018a, Lydersen et al. 2019), potentially eliminating most seedlings that recruited in the meantime. Coarse woody debris can aid in producing microclimates that are more hospitable to seedlings than exposed conditions where seedlings are seldom found (Gray et al. 2005) but reburns that remove such biological legacies leave few structures that can aid regeneration (Turner et al. 2019). Short interval reburns are increasing at a multidecadal scale in some regions (Buma et al. 2022), but there is a lack of research into how reburns may affect regeneration, particularly in mixed conifer forests. Reburns in areas burning repeatedly at low severity may act as a mechanism of forest resilience, but high severity reburns may erode resilience by way of recruitment failure.

Research Questions and Hypotheses

In this study, we resurveyed 93 plots in a large existing network that had been established after previous fires and then reburned in the 2021 Caldor Fire. Using species-level seedling data, we aimed to fill key knowledge gaps about post-reburn tree regeneration by asking the following questions: First, does fire history (e.g., the presence, severity, or years between successive fires) substantially drive conifer regeneration success or failure after a second fire, or are broader factors such as climate and

topography stronger determinants of postfire seedling density? We hypothesize that the presence and severity of an initial fire will be a strong driver of post-second-fire seedling density, as will the reburn interval (number of years between fires or YBF), since these variables affect pre-second-fire fuel loads and determine the surviving trees that could provide seed sources. For example, a high severity initial fire first may kill most or all trees, a short interval between fires may not allow for any regenerated trees to reach seed-bearing age, such that there is regeneration failure after a second fire. Alternatively, an initial low severity fire might leave behind high fuel loads that produce a high severity subsequent fire which kills all mature seed bearing trees and causes regeneration failure. We expect drivers that affect microsite conditions (which are particularly important to seedling establishment) such as a slope, slope position, and aspect may also play a significant, but more minor, role in determining post-second-fire seedling densities. Then, we ask: Do any differences exist when looking at only pine species versus shade tolerant species? We expect shade tolerant species density to be higher than pine species density post-reburn due to the high proportion of shade tolerant species in mixed conifer forests which result from fire exclusion. Given shade tolerant species abundance, it is likely that the nearest seed source post-fire is of a shade tolerant species, and the biological inertia is difficult to overcome in two successive fires Lastly, although there is a growing body of research on reburn patterns and mechanisms, drivers of regeneration in short-interval reburns have yet to be specifically examined in the literature, and this study would be the first of its kind.

METHODS

The study area is within the perimeter of the Caldor Fire, located in the Eldorado National Forest and the Lake Tahoe Basin Management Unit of the US Forest Service. The Caldor Fire was ignited on August 14, 2021, and by its containment in October reached a total area of approximately 90,000 ha. Due to its large size, the Caldor Fire burned over several areas that had previously burned in recent years, including the 2019 Caples Fire, the 2011 Long Fire, and the 2004 Freds Fire, which comprise the reburn areas of this study (Figure 3.1). Note that the Caples Fire was a prescribed fire that transitioned to a wildfire, and except for some spot fires, most of Caples Fire area either burned at low severity or not at all in the Caldor Fire. Lower elevations in the Caldor burn area are dominated by mixed conifer forest containing tree species such as ponderosa pine (*Pinus ponderosa*), sugar pine (*Pinus lambertiana*), incense cedar (*Calocedrus decurrens*), white fir (*Abies concolor*), and black oak (*Quercus kelloggii*), while higher elevations are dominated primarily by red fir (*Abies magnifica*), lodgepole pine (*P. contorta*) and Jeffrey pine (*P. jeffreyi*) (van Wagtendonk et al. 2018).

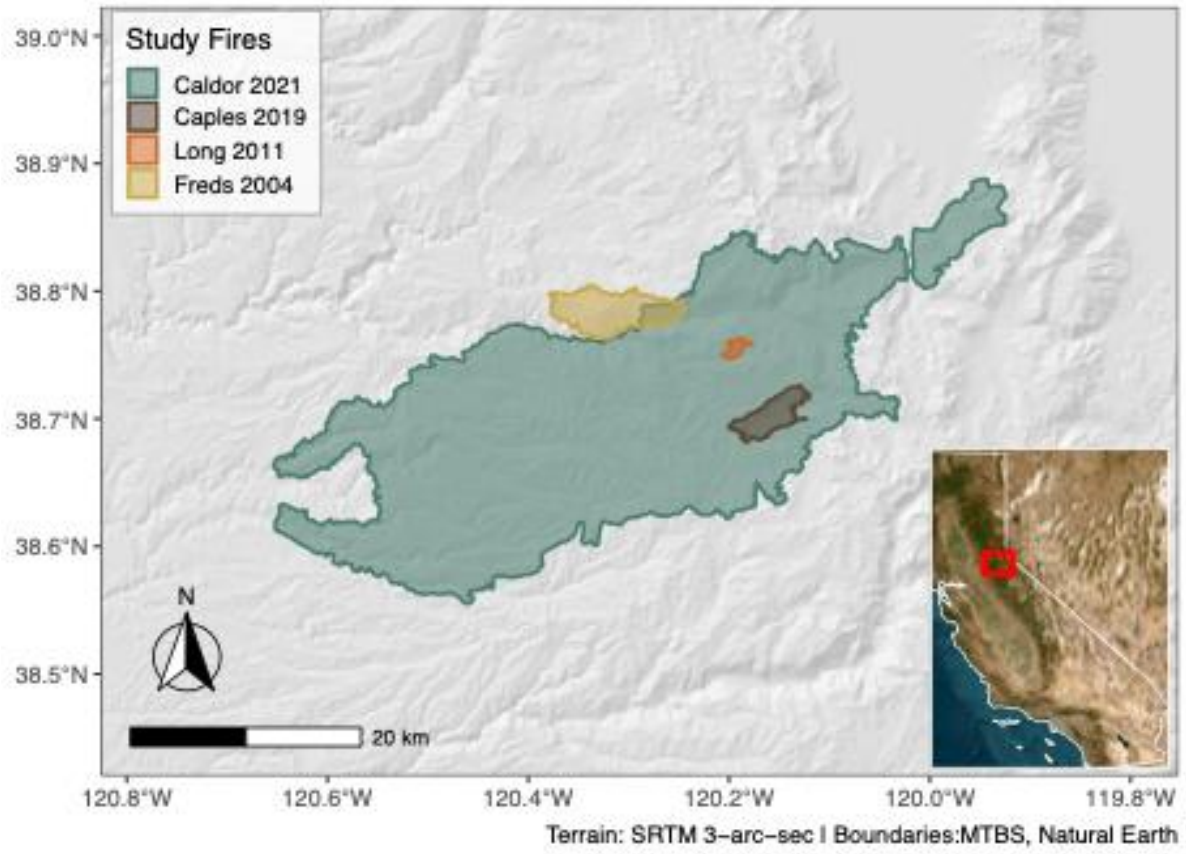


Figure 3.1. Map of study fires, with the Caldor fire shown in green, and the 3 reburn fires (Caples, Long, and Freds) in brown, orange, and yellow, respectively.

Table 3.1. Description of four sampled fires (one control and three reburns), along with biotic and abiotic plot characteristics. Percent high severity was derived from the acreage of burn severity table in published MTBS maps, except in the case of the Long fire, where RdNBR was calculated manually and classified into low, moderate, and high burn severity (>75%).

Fire	Year	Reburned by Caldor	Ignition Date	Hectares Burned	Percent High Severity	#Plots Sampled	Elevation (m)	HLI	Basal Area (m2/ha)
Caldor	2021	Control	14-Aug	91,961	30%	26	1276-2102	0.79-1	4.6-55.1
Caples	2019	Yes	10-Oct	1,420	2%	25	1786-2268	0.76-1	0-82.5
Long	2011	Yes	9-Sep	483	<1%	17	2046-2288	0.86-1	4.6-59.7
Freds	2004	Yes	13-Oct	3,298	25%	25	1312-2129	0.45-1	0-45.9
Total						93			

Field Measurements

The plots in this study leveraged an established post-fire monitoring plot network that we initiated throughout the Caldor fire perimeter in 2022. The Common Stand Exam (USDA Forest Service, 2015) plots from the original monitoring plot network were placed on a 400m grid spanning a gradient of burn severity as determined using classified RdNBR values (Miller and Thode 2007), in addition to a gradient of elevation, slope, and forest structure (Table 3.1). In 2023, we expanded the plot network and collected data for this study on the same grid for plots burned in only the Caldor (n=25) and the Caples and Caldor reburn (n=26). The plots from the Long and Caldor reburn (n=17) were revisits of those established in Miller et al. 2018, and the plots from the Freds and Caldor reburn (n=25) were revisits of a subset of established plots from Welch et al. 2016; plot locations were identified through personal communications and placed as close as possible to the existing GPS coordinates. Initial plans were to compare the initial survey data to the post-reburn data, but limitations with the fixed-area plot design led me to select a variable-radius design and thus forego the comparison. Additionally, note that Miller et al. 2018 reports the Long fire occurring in 2009, but it occurred in 2011, which we confirmed through cross validation of CalFIRE records and inspection of Sentinel-2 data pre- and post- fire dates in Google Earth Engine.

To collect detailed information on seedlings and avoid artificially inflating the dataset with zeroes, we used a variable-radius protocol modified from Young et al. 2025. Each seedling was identified to species, classified as either “0 year” or “≥1 year”), and tallied as follows: we first scanned the NE quadrant of the circle plot to a 4m radius. If there

were fewer than 10 seedlings of the species, we expanded to the entire circular plot within the 4m radius. If after expansion to the 4m radius circle and there were still fewer than 10 seedlings of the species, the plot was expanded to 6m. If there were fewer than 3 seedlings of the species in the 6m radius plus, the plot was expanded to an 8m radius. Finally, if there were fewer than 3 seedlings in the 8m radius plot, we expanded to a 10m radius for that species. We recorded all seedlings found within the final selected plot size. Note that we did not age seedlings but wanted to distinguish between seedlings of the year and older seedlings since we sampled 2 years post-Caldor Fire. Seedlings classified as ≥1 year were those that had lost their cotyledons and that had not reached breast height or 1.37 meters. In addition to identifying and counting each seedling found in up to a 10m circle plot, we also recorded the distance (in meters) to the nearest seed source for each species. We used a laser rangefinder to measure the three nearest mature seed-bearing trees for each species from plot center and selected the closest of the three during data cleaning. In each the 10m plot, we measured tree basal area by species using a basal area gauge, percent shrub cover using ocular estimation, percent canopy volume of green and black foliage using ocular estimation, and the dbh (cm) of an 'average' tree in the 10m plot.

Additional Data Collection

In addition to field measurements, we collected other relevant predictor variables. We used the 'prism' R package (v 0.3.0) to obtain 30 year normals (1991-2020) for maximum vapor pressure deficit, mean temperature, and mean precipitation (PRISM Climate Group 2026) at 800-meter resolution. RdNBR values quantifying the severity of the Caldor Fire and each of the previous fires were calculated in Google Earth Engine using

methods from Parks et al. 2018b. RdNBR was not taken from data packages published on MTBS because the Long Fire was missing from the MTBS database due to its small size (<1000 acres is the threshold for Western state). Since RdNBR had to be calculated independently for the Long Fire, we calculated it for all fires to maintain method consistency. Additionally, the MTBS RdNBR product is calculated subjectively since technicians manually set unburned offsets (Kolden et al. 2015) and scripted calculation of RdNBR in Google Earth Engine allowed for reproducibility. Elevation was not recorded in the field and instead extracted from the USGS 3DEP program's 1 meter resolution Digital Elevation Model (DEM) as available on Google Earth Engine. The DEM was also used to calculate missing slope and aspects. Heat load index (HLI, unitless) was calculated using methods from McCune and Keon 2002.

Data Analysis

Seedling counts were converted to density (seedlings per hectare, by species) by accounting for the search radius for each species per plot. Seedling densities by species were then aggregated to the level of 'pines' which included ponderosa pine, Jeffrey pine, sugar pine, lodgepole pine, and to the level of 'shade-tolerants' which includes incense cedar, Douglas-fir, white fir, and red fir. Non-coniferous species such as *Populus* species and *Quercus* species were excluded from this analysis. We used generalized linear mixed models with the 'glmmTMB' package to model pine and shade-tolerant seedling density. Pines and shade-tolerants were modeled separately since we counted almost 6 times more shade-tolerant seedlings (n=3709) in the field than pine seedlings (n=634) and wanted to separate signals by niche occupancy. First, we ran a correlation matrix on the

predictor variables as well as a variable inflation factor analysis using the 'corr' and 'vif' packages to identify highly correlated variables and remove them from the analysis (those with a correlation coefficient >0.5 and/or VIF >10). The final fixed effect variables included in the models were: distance to nearest seed source (meters), HLI (unitless), mean temperature (degrees Celsius), precipitation (mm), RdNBR of the first fire (unitless), RdNBR of the second fire (unitless, no reburn plots did not have a value for this variable), shrub cover (percent), mean tree dbh (cm), shrub cover, basal area of overstory trees within the plot (m^2 per hectare), green foliage volume (percent), and time between fires (years, no reburn plots were set at 0). All continuous predictor variables were scaled and centered. We included Fire ID as a random effect to capture variability in unmeasured differences between the four fires.

The seedling densities were over-dispersed and contained many zeroes, so we used a log link with a Tweedie distribution. The Tweedie distribution can be used to improve fit of data with a high proportion of zeroes but otherwise continuous positive values (Tweedie 1984, Foster and Bravington 2012, Tortorelli et al. 2020). Note that densities were used instead of counts to account for the variable radius method (although an area offset can account for variable plot size in a negative binomial regression, we opted to use the Tweedie distribution as it was appropriate for my data structure. For the pines and the shade tolerant models, we modeled seedlings at 0 year, ≥1 year, and all years, for a total of 6 models. We also ran additional models post hoc with an interaction term between all the predictor variables to see if interactions existed between the first and second burn severities as well as reburn interval. We used the 'emmeans' package to visualize predicted

seedling density as a function of a given predictor while holding all other predictors at their mean value. We calculated the correlation between observed and fitted values to assess model fit, in addition to calculating the AUC (area under the receiver operating curve). which is a statistical diagnostic that measures a model's ability to distinguish between two classes. Values for AUC range from 0.0 to 1.0, and a value of 0.5 is equivalent to random guessing. We binarized the data at replacement density (175 seedlings/ha) (Welch et al. 2016). This threshold is subjective, as it comes from the Pacific Southwest Regional Silviculturist's assessment that 70 mature trees/acre (175 trees/hectare) was sufficient stocking in most YMPC forests at the time of the publication of Welch et al. 2016. While many foresters in the state might not agree with this standard and prefer standards of 200 trees/acre (494 trees/hectare), this lower 'replacement density' thresholds represents a more liberal cutoff that reflects the natural range of variation in mixed conifer forests (Young et al. 2020).

RESULTS

Replacement Density

Among the four sampled fires, between 64% and 88% of plots had stand replacement density (175 seedlings/ha) of seedlings regardless of age (Figure 3.2). The control plots (no reburn) had the highest proportion of plots with replacement density for seedlings of all years, while the reburn plots from the Freds and Long Fires had higher proportions of replacement density for ≥1 year seedlings (70% and 64%, respectively). Only 12% of Freds reburn plots had enough 0 year seedlings for stand replacement. Of the 93

sampled plots, 20 plots had no pines, 21 plots had no shade tolerant species, and 10 plots had zero seedlings of any species.

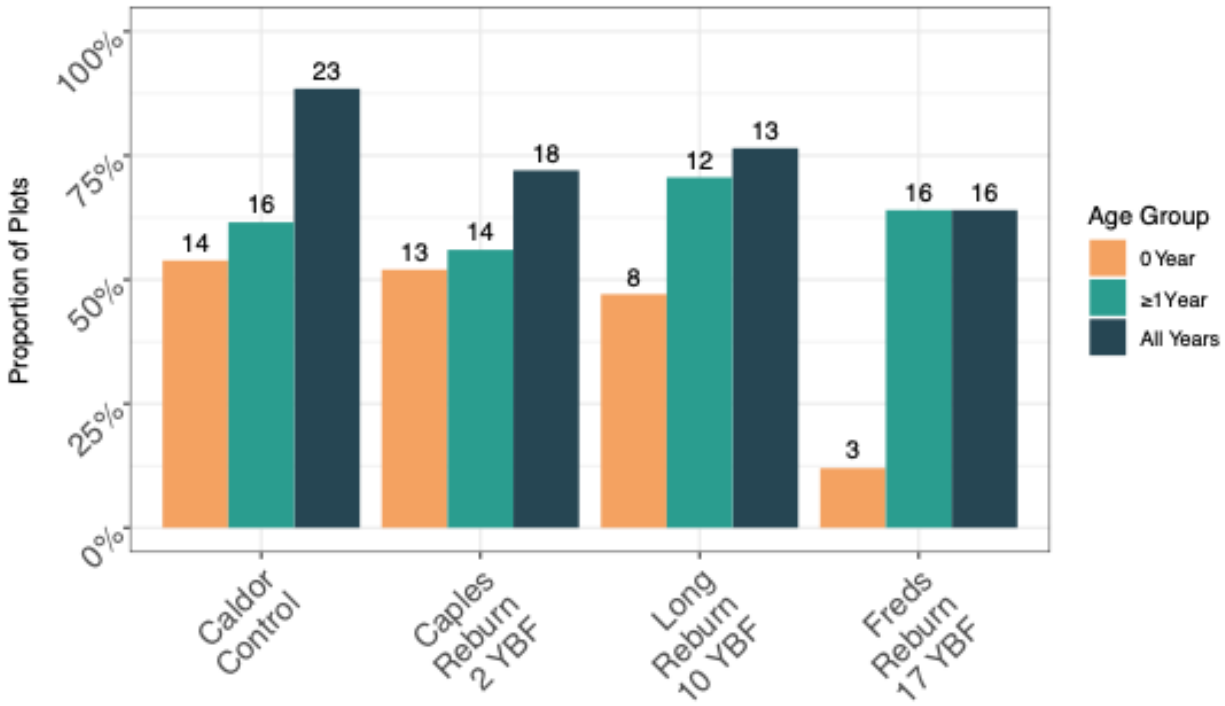


Figure 3.2. Proportion of 93 sampled plots hat reached replacement density, or approximately 175 seedlings/hectare, divided by age groups. YBF stands for Years Between Fires. Total sample size per fire is Caldor (n=26), Caples Reburn (n=23), Long Reburn (n= 17), Freds Reburn (n=25).

Pines versus Shade Tolerant Species

There were marked differences in predictor strength between the pine and shade tolerant models. Reburn interval (the number of years between fires) was a statistically significant predictor for the pine models, but not the shade-tolerant models. Increased reburn interval and percent shrub cover corresponded to a decreasing estimate of seedling density (Figures 3.3, 4). For the 0 year pine model, the strongest predictors were shrub cover (*b*= -0.808, p=0.018,) (Figure 3) followed by reburn interval (*b*= -0.639, p = 0.015)

(Figure 3.4), while predictors with moderate strength included mean tree dbh (b=0.466, p = 0.339) and basal area (b= *0.342,* p = 0.076) (Table 3.2). Note that all coefficient estimates (b) for the slope of each variable are on the log scale and represent values when controlling for differences between fires. Larger mean tree dbh and larger basal areas corresponded to increased seedling density. For the ≥1 year pine model, directionality of predictor variable coefficient estimates remained the same, but predictor strength and statistical significance varied slightly. The strongest predictor was reburn interval ($p < 0.01$), then shrub cover (b=-0.529, p=0.051) (Table 3.2). Basal area and percent green volume were slightly weaker predictors with greater statistical significance than shrub cover, (b=0.493, p=0.018 and b=-0.472, p=0.032, respectively) (Table 3.2). Results for the all years pine model were similar, with the strongest statistically significant predictors as follows (in decreasing absolute value of effect size): reburn interval (b=-0.722, $p < 0.01$), shrub cover (b=-0.609, p=0.015), basal area (b=0.392, p=0.016), and mean tree dbh (b=.355, p=0.051) (Figure 3.3, Table 3.2). Shrub cover had the largest effect size for all three pine models (Figure 3.5). For all the pine models, percent deviance explained was low and ranged from 1.7% - 3% while the correlation between fitted and observed values was around 10% (Figure 3.6, Table 3.3). Given the pine models' overestimation at observed values of zero and underestimation at observed values above zero, We calculated AUC values at a threshold of 175 seedlings/ha and obtained values 0.72, 0.71, and 0.66 for the pine 0 year, ≥ 1 year, and all years models, respectively (Table 3.3).

Table 3.2. Results of the GLMMs for pine and shade tolerant seedling densities. **** indicates p < 0.001, *** indicates p < 0.01, ** indicates p < 0.05, and * indicates p < 0.1.(YBF = Years between fires).

		Inter-cept	Dist. to seed source (m)	Heat Load Index	Precip (mm)	1st fire RdNBR	2nd fire RdNBR	Perc. (%) shrub cover	Mean tree dbh (cm)	Basal area (m^2/ha)	Perc. (%) green vol.	YBF
Pine year 0												
	Estimate	2.032	0.168	0.168	-0.301	-0.329	-0.245	-0.808	0.466	0.342	0.216	-0.639
	Std. Error	0.236	0.235	0.259	0.212	0.267	0.236	0.343	0.220	0.193	0.243	0.263
	z value	8.619	0.714	0.650	-1.418	-1.232	-1.040	-2.357	2.122	1.775	0.890	-2.426
	p value	<0.001 ***	0.475	0.516	0.156	0.218	0.299	0.018 4**	0.033 9**	0.076*	0.373	0.0153 **
Pine year 1+												
	Estimate	2.057	-0.152	0.111	0.266	0.183	0.231	-0.529	0.175	0.493	-0.472	-0.783
	Std. Error	0.196	0.236	0.195	0.218	0.257	0.230	0.272	0.205	0.209	0.220	0.212
	z value	10.517	-0.644	0.570	1.221	0.711	1.004	-1.945	0.855	2.359	-2.149	-3.697
	p value	<0.001 ***	0.520	0.569	0.222	0.477	0.315	0.052 *	0.392	0.018 **	0.032 **	<0.001 ***
All pines												
	Estimate	2.892	0.050	0.187	-0.042	-0.127	-0.039	-0.609	0.355	0.393	-0.098	-0.722
	Std. Error	0.175	0.192	0.194	0.175	0.220	0.186	0.250	0.182	0.165	0.191	0.199
	z value	16.481	0.263	0.963	-0.241	-0.578	-0.212	-2.433	1.955	2.392	-0.514	-3.627

	p value	<0.001 ***	0.793	0.336	0.809	0.563	0.832	0.015 **	0.051 *	0.017 **	0.608	<0.001 ***
Shade toler-ants		-2.637	-6.798	0.178	-0.035	-1.141	-0.420	-0.707	0.217	0.491	0.030	0.473
	Estimate											
	Std. Error	1.685	4.043	0.314	0.455	0.756	0.729	0.644	0.441	0.278	0.470	0.486
year 0	z value	-1.565	-1.682	0.568	-0.077	-1.510	-0.575	-1.098	0.491	1.763	0.064	0.975
	p value	0.118*	0.093*	0.570	0.939	0.131	0.565	0.272	0.623	0.078*	0.949	0.330
Shade toler-ants		4.997	-0.087	-0.542	1.164	-0.809	0.532	-0.541	0.511	0.876	0.545	-0.252
	Estimate											
	Std. Error	0.649	0.280	0.202	0.275	0.313	0.407	0.350	0.228	0.210	0.236	0.664
year 1+	z value	7.699	-0.311	-2.677	4.235	-2.589	1.307	-1.543	2.242	4.168	2.310	-0.379
	p value	<0.001 ***	0.756	0.007 **	<0.001 ***	0.010 **	0.191	0.123	0.025 **	<0.001 ***	0.021 **	0.705
All shade toler-ants		5.012	-0.083	-0.537	1.163	-0.808	0.527	-0.545	0.509	0.874	0.551	-0.249
	Estimate											
	Std. Error	0.641	0.276	0.200	0.272	0.308	0.401	0.345	0.225	0.207	0.232	0.657
	z value	7.821	-0.300	-2.682	4.282	-2.624	1.317	-1.581	2.260	4.224	2.374	-0.380
	P value	<0.001 ***	0.764	0.007 **	<0.001 ***	0.009 **	0.188	0.114	0.024 **	<0.001 ***	0.018 **	0.704

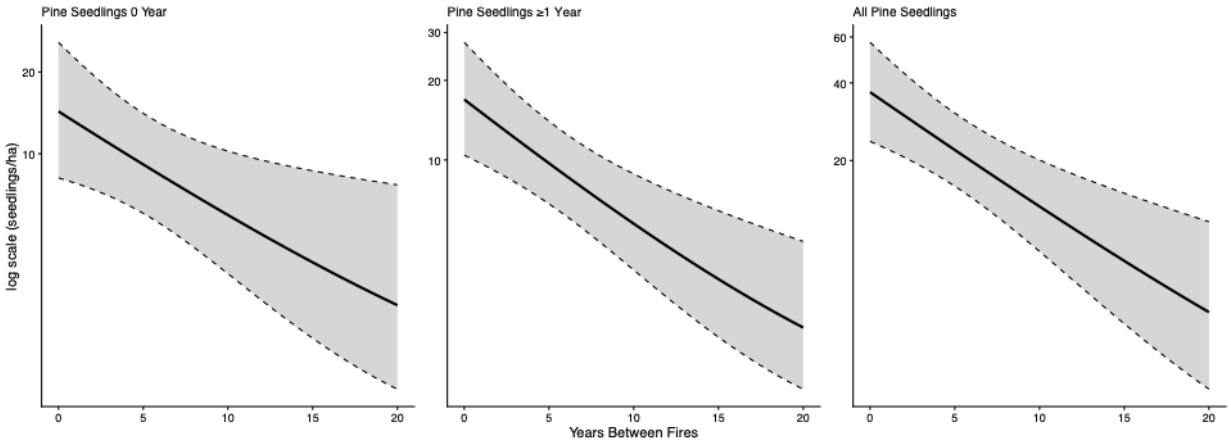


Figure 3.3. Marginal response curves for seedling densities for each of the pine seedling models as a function of reburn interval or years between fires, holding all other predictors constant at their mean values.

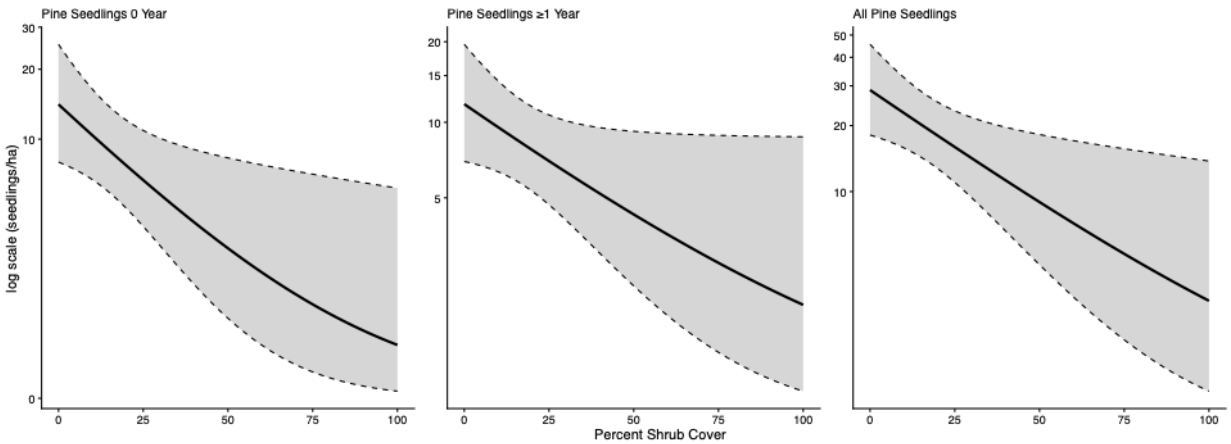


Figure 3.4. Marginal response curves for seedling densities for each of the three pine seedling models as a function of percent shrub cover, holding all other predictors constant at their mean values.

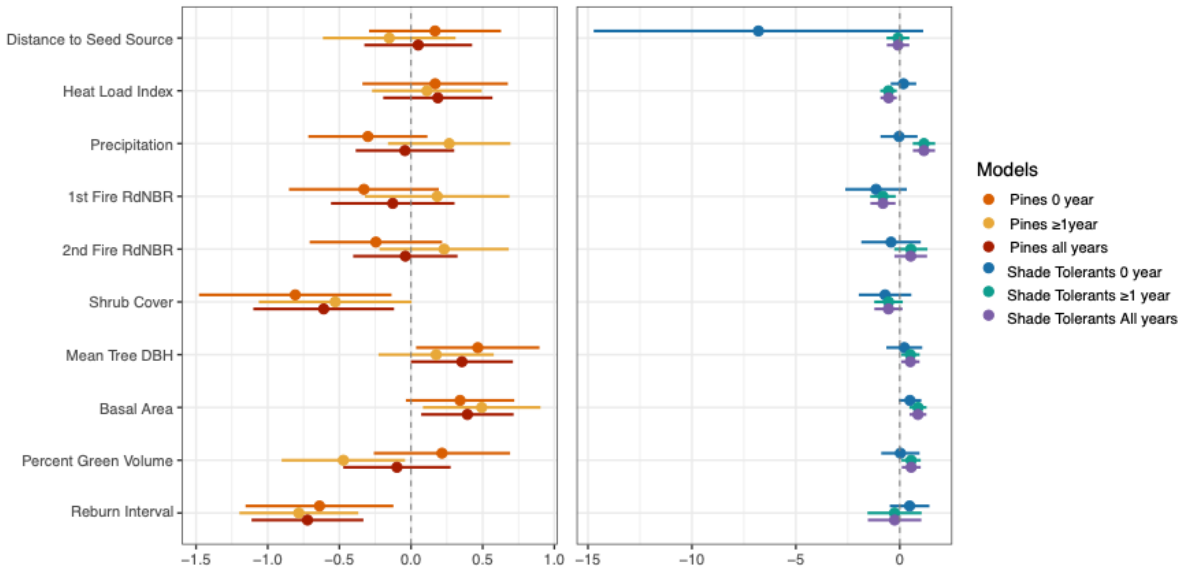


Figure 3.5. Dot and whisker plots showing effect sizes for coefficients in the six different models.

The shade tolerant seedling models had different significant predictors and effect sizes for predictors than the pine models. The model for 0 year shade tolerant seedlings was overwhelmingly driven by distance to the nearest seed source ($p < 0.1$) and basal area was also a strong predictor ($b = 0.491$, $p = 0.076$) (Figures 3.5 and 3.7). The models for ≥1 and all years for shade tolerant species were different from the 0 year model, but very similar to each other. For both ≥1 year and all years shade tolerant models, climatic and topographic variables were more significant predictors than reburn history. The strongest predictor was precipitation (30 year normals) ($b=1.16$, $p<0.001$), followed by basal area ($b=0.87$, $p<0.001$), RdNBR of the first fire ($b=-0.81$, $p<0.001$), percent green volume ($b=0.55$, $p<0.05$), heat load index ($p < 0.01$), and mean tree dbh ($b=0.51$, $p<0.05$) (Figure 3.7, Table 3.2). Unlike the pine models, reburn interval was not statistically significant and had a small effect size ($b=-0.25$, Figure 3.5, Table 3.2). Percent shrub cover had a slightly smaller

effect size in the shade tolerant models (around 0.55, compared to 0.61 and 0.81 in pine models), but was not statistically significant (Figure 3.5). While percent deviance explained for the shade tolerant models was also low (3-5%), the correlation between observed and fitted values was slightly stronger, at 14% for the 0 year shade tolerant model, and 19% for the ≥ 1 year and all years model (Figure 3.6, Table 3.3). AUC values for the shade tolerant 0 year, ≥1 year, and all years models were 0.88, 0.67, and 0.67, respectively (Table 3.3).

Table 3.3. Percent deviance explained and area under the receiver operating characteristic curve (AUC-ROC) for each of the pine and shade tolerant GLMMs.

Model	Percent deviance explained	AUC (at a threshold of 175 seedlings/ha)
Pine 0 year	2.83	0.72
Pine ≥1 year	1.43	0.71
All pines	1.71	0.66
Shade tolerants 0 year	5.13	0.88
Shade tolerant ≥1 year	3.12	0.67
All shade tolerants	3.11	0.67

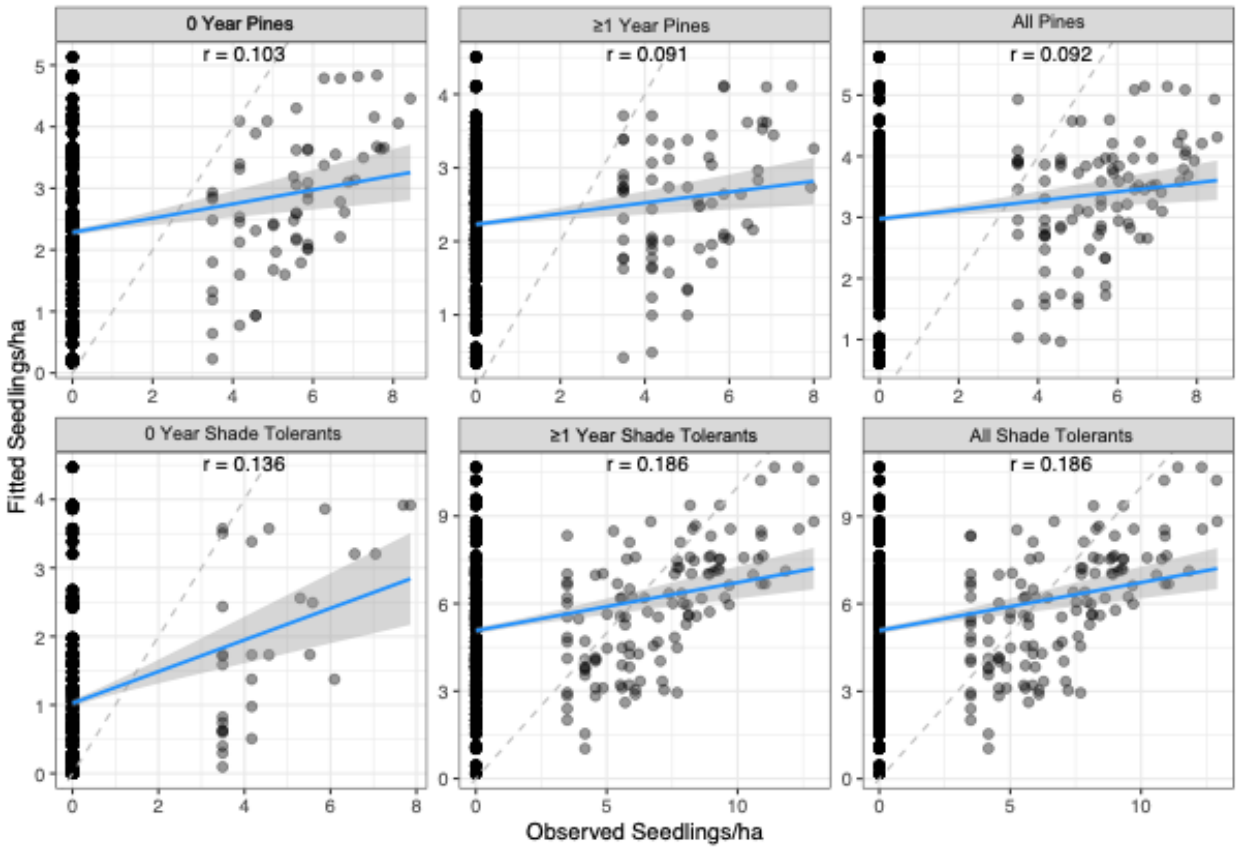


Figure 3.6. Observed versus fitted values of seedling density for each of the six models, along with the correlation coefficient, r. The grey dotted line represents the 1:1 line, while the blue lines and grey ribbons show the trend line and affiliated 95% confidence intervals.

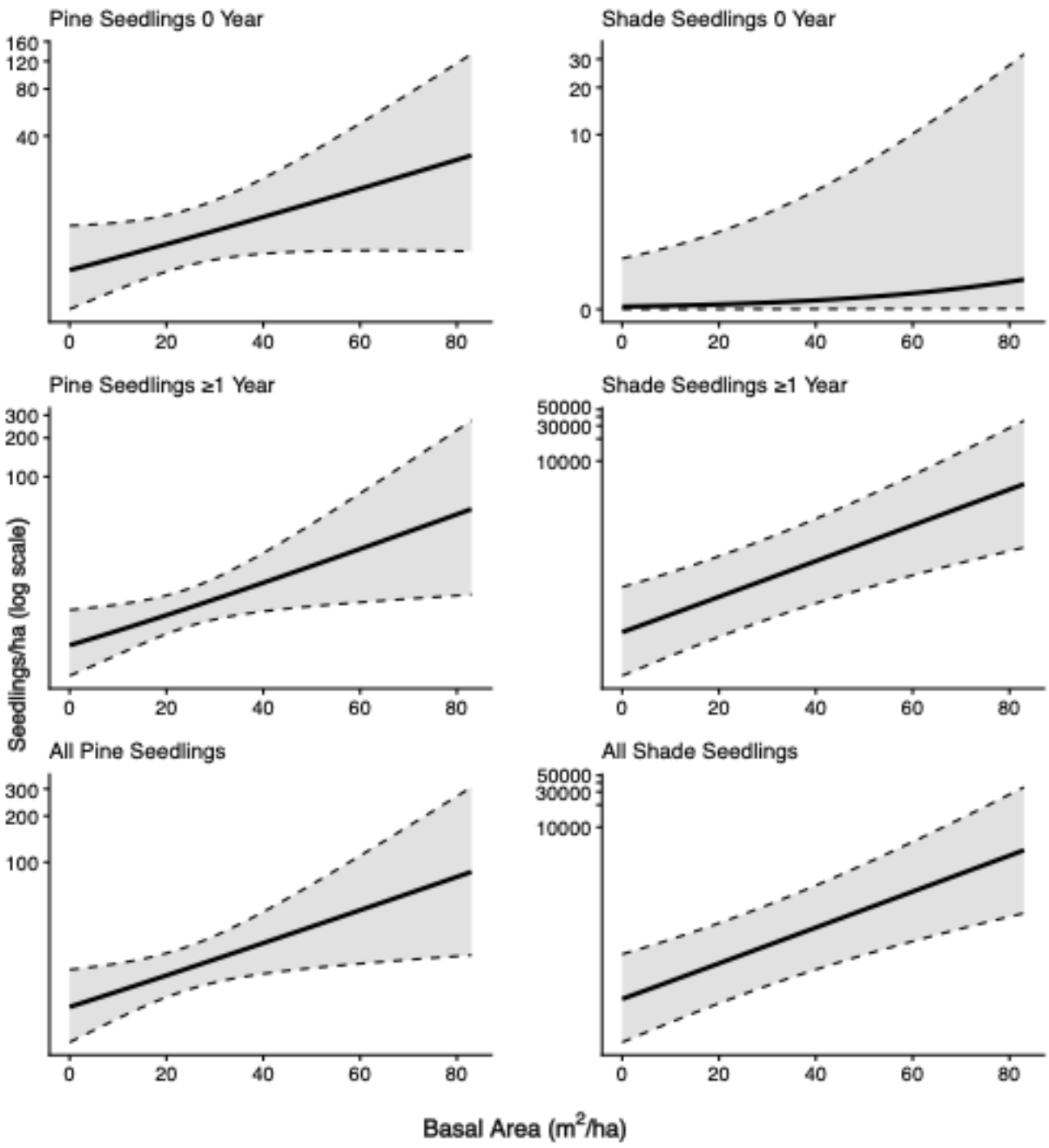


Figure 3.7. Marginal response curves for seedling densities for each of the six seedling models as a function of overstory tree basal area (m^2/ha), holding all other predictors constant at their mean values.

Reburn interval influences interacting predictors in shade-tolerant models

While reburn interval was not a strong or statistically significant predictor on its own, post-hoc analysis showed the slopes of other predictors to vary based on reburn interval when it was introduced as an interaction term.. Specifically, for the 0 year shade tolerant model, there was a significant interaction between percent shrub cover and reburn interval (Figure 3.8a, Table3. 4). For the Caldor control (0 YBF), the slope of the curve describing the relationship between percent shrub cover and seedling density was nearly flat between 0 and 20% shrub cover but then increased as shrub cover increased. For the Caples reburn (2 YBF), the slope remained flat across all values of percent shrub cover. Conversely, for longer times between fires (10 years for the Long reburn and 17 for the Freds reburn), seedling density decreased as shrub cover increased, then leveled out to zero at around approximately 10% shrub cover (Figure 3.8a). The other significant interaction term was between reburn interval and basal area, specifically for the ≥ 1 year and all years shade tolerant models (Figure 3.8b, c). Both models had the same trend: a higher starting intercept of seedling density for the Caldor control (0 YBF) and Caples reburn (2 YBF) with a slightly positive slope, and a lower starting intercept for the Long (10 YBF) and Freds (17 YBF) reburns, with a stronger positive slope. All four lines intersect at a basal area of approximately 37 m^2/ha, and the confidence intervals have significant overlap. The pine models were also examined for statistically significant interaction terms but did not have any.

Table 3.4. Results of GLMMs for shade tolerant species models with interaction term for reburn interval. **** indicates p < 0.001, *** indicates p < 0.01, ** indicates p < 0.05, and * indicates p < 0.1. (YBF= Years between fires)

		Inter-cept	**Dist. to seed source (m)**	**Heat Load Index**	**Precip. (mm)**	**1st fire RdNBR**	**2nd fire RdNBR**	**Perc. (%) shrub cover**	**Mean tree dbh (cm)**	**Basal area (m^2/ha)**	**Perc. (%) green volume**	**YBF**	**Interac-tion term with YBF**
Shade tolerants													*shrub cover*
	Estimate	-3.018	-5.429	0.169	-0.137	-1.204	-0.151	-1.909	-0.093	0.547	0.059	-1.108	-2.680
year 0	Std Error	1.597	3.720	0.304	0.476	0.579	0.715	0.896	0.413	0.273	0.451	0.944	1.216
	z value	-1.889	-1.460	0.555	-0.288	-2.079	-0.212	-2.131	-0.225	2.004	0.131	-1.174	-2.204
	p value	0.059 *	0.144	0.579	0.774	0.038 **	0.832	0.033 **	0.822	0.045 **	0.896	0.241	0.028**
													basal area
Shade tolerants	Estimate	5.016	-0.115	-0.441	1.106	-0.884	0.496	-0.610	0.456	0.836	0.445	-0.383	0.391
year 1+	Std Error	0.629	0.285	0.208	0.268	0.312	0.404	0.347	0.224	0.210	0.238	0.648	0.207
	z value	7.973	-0.404	-2.124	4.127	-2.836	1.227	-1.757	2.038	3.981	1.865	-0.590	1.890
	p value	<0.001 ****	0.686	0.034 **	<0.001 ****	0.005 ***	0.220	0.079 *	0.042 **	<0.001 ****	0.062*	0.555	0.059*

												Basal area
All shade tolerants	Estimate	5.030	-0.111	-0.437	1.108	-0.883	0.491	-0.614	0.453	0.834	0.451	-0.379	0.390
	Std Error	0.621	0.280	0.205	0.265	0.307	0.397	0.342	0.221	0.207	0.235	0.641	0.205
	z value	8.102	-0.397	-2.129	4.178	-2.872	1.236	-1.795	2.048	4.030	1.921	-0.591	1.904
	p value	<0.001****	0.691	0.033**	<0.001****	0.004****	0.217	0.073*	0.041*	<0.001****	0.055	0.554	0.057*

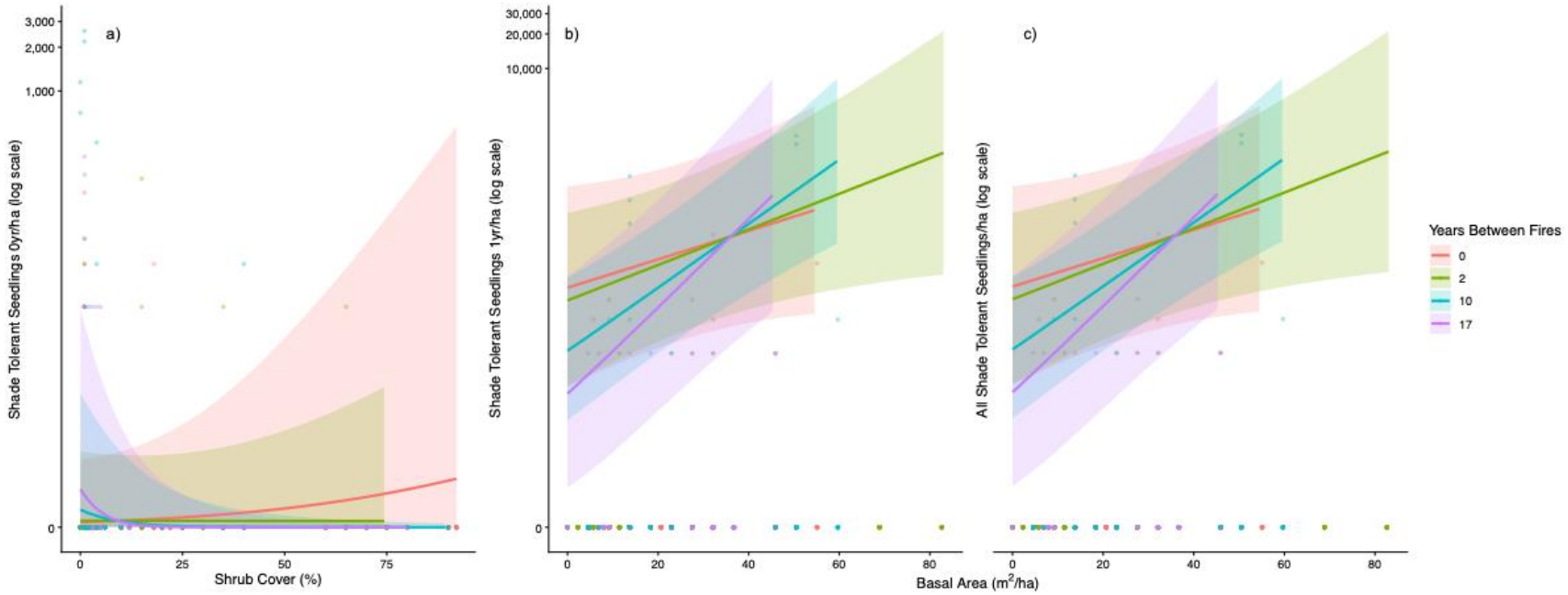


Figure 3.8 Marginal response curves for shade tolerant seedlings. (a) predicted 0 year seedlings as a function of the interaction between percent shrub cover and reburn interval; (b) predicted ≥ 1 year seedlings as a function of the interaction between basal area and reburn interval; (c) all year seedlings as a function of the interaction between basal area and reburn interval.

DISCUSSION

Replacement Density

We assessed seedling density post-fire in a control fire and three reburns and found a smaller proportion of plots in the reburns at or above my replacement density threshold of 175 seedlings/ha, suggesting some level of influence of reburns on conifer regeneration. Of course, should we have used a more conservative threshold of 494 seedlings/ha, a greater proportion of reburn plots would have not met the cutoff, and we acknowledge the optimistic view this chosen threshold presents. Comparative analyses of past (~1900) and current stand density index (SDI) show historic SDI to be between 23 and 28% of the current maximum (North et al. 2022), and my replacement density threshold reflects an operational opportunity to emulate the resilience that these lower density forests had. Across all control and reburn fires, shade tolerant species were more abundant than pine species, reflective of over a century of fire suppression which allowed the canopy to close and shade tolerant species to thrive and provide the seed source for the next generation (Safford and Stevens 2017, Brodie et al. 2023). In plots that reached replacement density and both pine and shade tolerant species co-occurred, shade tolerant species still dominated in 86% of plots. The 'biological inertia' (Young et al. 2019) of fir abundance is a likely source for this greater white fir regeneration because it was more likely for a nearby seed source to be a white fir than a pine species, even though shade tolerant species like white fir have thinner bark than yellow pines and are often killed in fire (Welch et al. 2016, Zeibig-Kichas et al. 2016).

Pines versus Shade Tolerant Species

The difference in significant predictors of seedling density between pine species models and shade tolerant species models, namely that reburn interval was significant in pine models but not in shade tolerant models, can be attributed to changes in species composition in yellow pine mixed conifer forests and the resulting biological legacy of shade tolerant species dominance (Stephens et al. 2015). As reburn interval increased, seedling density decreased for pine species models but not shade tolerant species models. The negative effect of a greater reburn interval on pine seedling density could be because the initial fire did not reduce shade tolerant density enough to return to historical conditions, and forest succession continued in favor of shade tolerant species and/or species that could outcompete pines. This finding is in alignment with other evidence that single fires are generally not enough to restore forests to their historical conditions due to the degree of departure (Churchill et al. 2021, Greenler et al. 2023, Grupenhoff et al. 2026), and that the restorative effects of low- and moderate-severity fire fade over time (Tortorelli et al. 2024). Additionally, reburn interval could affect pine regeneration and not shade tolerant regeneration due to differences in post-fire outcomes. Fire is likely to kill thin barked shade tolerant species such as white fir, while the thick bark of ponderosa or Jeffrey pine might only cause injury. The time after injury is where the reburn interval may be important, because changes to competition, biophysical characteristics, and insect attack susceptibility may occur, and pines might recover and continue to produce seeds, or ultimately die (Hood et al. 2026). These dynamics align with our observation of variable mature pine survival from the initial fire. Although research on pine species cone production is sparse and mainly looks at pines with low levels of crown injury, there is

evidence suggesting that trees with low to moderate levels of crown scorch can still produce viable seeds, and that variation of cone production depends more on tree size (Rietveld 1976, Ordóñez et al. 2005). Unpublished work from Venuti et al. (2026) shows that at higher levels of crown scorch (>70%), reproductive output of yellow pines and sugar pines is significantly depressed. Conversely, shade tolerant species like white fir have decreased reproduction even at low levels of crown injury (Venuti et al. in review). Given the relatively high proportion of fir and incense cedar compared to historical proportions in the study region (Dolanc et al. 2014, Van Wagtendonk et al. 2018), regeneration can occur from nearby seed sources irrespective of time between fires.

The negative relationship between pine seedling density for all combinations of sampled seedlings ages and percent shrub cover corroborates other findings in the literature that show that high shrub cover may delay or inhibit conifer recruitment (Welch et al. 2016). Although pines are suited to germinate and grow quickly in post-fire environments with high light availability and exposed mineral soil, shade tolerant species like firs often recruit at higher densities (Zald et al. 2008, Crotteau et al. 2013, Lauvaux et al. 2016, Annighöfer et al. 2019, Tubbesing et al. 2021). Increased post-fire fir density can be attributed to shrub competition with pines (Tubbesing et al. 2020), pre-fire tree species composition (Zald et al. 2008), and dispersal limitation (Harvey et al. 2016b). In cases of severe reburns where highly flammable shrubs dominate after the first fire, a positive feedback cycle may lead to non-forested alternative stable states (Coppoletta et al. 2016, Coop et al. 2020), a dynamic that may be borne out by our observations of high shrub and/or black oak percentage in the Freds fire reburn area, which burned at high severity for

both fires. Interestingly, when looking at already established seedlings, there is some evidence to suggest that shrub neighborhood dynamics do not favor white fir for an initial cohort of established seedlings (Tubbesing et al. 2021). This is likely because pine seedlings fare better than firs early on in severely burned sites, as the shade-tolerance of firs does not apply until later in their life history (Zald et al. 2008). More research is needed to track seedling and shrub interactions beyond the first several years post-fire to better understand longer term dynamics between shrubs and conifers under novel fire regimes.

For the shade tolerant species models, climate and topographic variables were more significant predictors of seedling density than reburn interval, except for the 0 year shade tolerant models. Currently, forest structure and species composition throughout mixed conifer forests of the central Sierra Nevada are highly departed from their historical range of variation in that open forests with large distances between yellow pines have been replaced by dense forests of shade tolerant species such as white fir and incense cedar (Stephens et al. 2015, Safford and Stevens et al. 2017). Given that post-fire biological legacies favor shade tolerant species since recent fires have not returned forests to their historical pine dominance (Paudel et al. 2022), it is not surprising that suitable conditions more strongly determine regeneration. Shade tolerant seedling density decreased with increased heat load index and decreased precipitation, which supports other findings in the literature that shaded and mesic conditions are favorable for white and red fir (Barbour et al. 1990, Nelson et al. 2021). Other studies have also documented increased sensitivity of firs (as opposed to pines) to postfire climate (Stewart et al. 2021), and although this study only looked at 30 year normals, incorporation of postfire climate into future studies

might reveal similar dynamics. Further research into the compounding effect of multiple fires in short succession and a warmer climate is warranted, as drier and hotter conditions are expected to negatively impact conifer regeneration and contribute to forest loss (Tepley et al. 2017, Kemp et al. 2019).

In general, the shade tolerant species models performed better than the pine species models, with a higher correlation between observed and fitted values, as well as percent deviance explained. The smaller deviance explained for the pine models is not surprising and similarly, higher error rates in pine models have been documented in Stewart et al. (2021). Pine species regeneration is known to be highly variable and can occur in pulses (League and Veblen 2006, Kolb et al. 2020) and even in the absence of live seed sources (Young et al. 2026). The stochastic nature of pine regeneration may explain the overestimation of pine seedling density at observed values of zero and underestimation at higher observed values. While distance to nearest seed source was not a statistically significant predictor for any of the pine models, it was a very strong predictor for the 0 year shade tolerant species model, which aligns with other studies on influences of conifer regeneration (Donato et al. 2016, Harvey et al. 2016a, Welch et al. 2016, Kemp et al. 2016, Shive et al. 2018, Rodman et al. 2019, Stewart et al. 2021, Gill et al. 2022). For all three shade tolerant species models (as well as the three pine models), seedling density increased with basal area. Although my basal area measurements included dead trees, it is reasonable to consider basal area as a proxy for mature seed bearing trees (since proportionally more of the dead trees had a smaller basal area, as it is easier for fire to kill smaller trees), explaining the positive relationship between basal area and seedling

density. Similarly, a higher percent green canopy volume relating to higher seedling density for the ≥ 1 year and all year shade tolerant models is likely because trees with more green volume are likely to produce more seeds for the next generation. The challenge in modeling pine species regeneration may also be attributable to the fact that although many pine species are initially gravity and/or wind dispersed, many pines are ultimately heavily dependent on animal dispersal of their seeds, including Jeffrey pine and sugar pine, both common in the study site, (although evidence of this has been variable in field observations) (Vander Wall 2008, Lacher 2019). Very few conifer regeneration studies explicitly consider animal (bird and rodent) caching, including this one. In addition, little is known about the impact of fire on animal dispersers and the subsequent effect of postfire regeneration. Only one review paper was identified in the literature as characterizing the impact of changing fire regimes on specialized plant-animal interactions (Charles et al. 2025), and it primarily discussed the impact of fire on avian-dispersed mistletoes and plant-pollinator interactions. In addition to the role of animal-mediated pine seed dispersal, pine seeds are also susceptible to predation (Vander Wall 2008, Charles et al. 2025). Thus, animals can play a bi-directional role on pine seedlings, and it is possible that until these plant-animal interactions are more explicitly measured and quantified, pine regeneration models will continue to have low percent deviance explained.

Reburn interval influences interacting predictors in shade models

While there was no statistically significant relationship between any of the shade tolerant species models and years between fires, there were some instances where the reburn interval significantly interacted with various predictor terms. For example, for the 0

year shade tolerant models, shrub cover interacted with reburn interval. In the case of the control fire (0 years between fires), the predicted 0 year seedling density increases between 30% and 80% shrub cover, suggesting a possible nurse shrub effect. A facilitative effect of shrubs on conifer seedlings being present for only seedlings of the year and not older seedlings could be because seedlings occupy a smaller niche than older conspecifics (Dobrowski et al. 2015). Other studies have documented a facilitative - competitive relationship between conifer seedlings and shrubs along environmental/stress gradients (Urza et al. 2019). Interestingly, this trend was not present for the seedlings in the reburn plots. For example, where there are only two years between fires, the slope for seedling density as a function of shrub cover remained flat through most values of shrub cover percent. This different relationship between the two variables in the case of reburns might be because the Caples reburn burned mostly at low severity, such that not all understory vegetation died and there was enough shade and moisture to allow for shade tolerant seedling establishment. In the case of longer years between fires (10 and 17), seedling density rapidly decreased and flattened out at zero as shrub cover increased, suggesting a more competitive relationship between shrubs and seedlings, although the shade cast by the shrubs is also likely playing a role in affecting seedling microclimate. This potential competitive effect corresponds to evidence of competition between conifer seedlings and shrub species in the study region under ambient snowpack conditions (Werner et al. 2019). Additionally, there is evidence of below-ground water competition between seedlings and shrubs post-fire (Sanders 2025), as well as evidence of shrubs depleting water more rapidly and lower down in the soil than conifers (Royce and Barbour

2001). Competition in the longer intervals between fires could have resulted from a low or moderate severity initial fire followed by high severity fire. For example, after the initial fire, high shrub cover and snag fall may have contributed to fuel build up which then led to a more severe subsequent fire (Lydersen et al. 2019). Then, high-severity-fire-following shrubs that established after the second fire would outcompete seedlings. This contrasts with two low or moderate severity fires where there is not high mortality and competition is not as fierce as it would be after severe disturbance.

For the case of year one and all years shade tolerant seedling models, the relationship between basal area and seedling density depended on the reburn interval. In general, seedling density increased monotonically with basal area. For both models, the trends were the same: a higher starting intercept point and shallower slope for the control (Caldor) and 2 years between fires reburn (Caples), and a lower starting intercept point and steeper slope for the longer term reburns: 10 years between fires (Long) and 17 years between fires (Freds) (Figure 3.8). All four lines intersect at a basal area of about 37 m^2/ha, which could be a coincidence, or perhaps because this about the average basal area of a fir-dominated mixed conifer forest that produces high seedling densities (Stephens et al. 2018). A higher starting density of seedlings that increases slowly could be because a large proportion of the control fire burned a high severity and opened the canopy for seedlings to establish, or because of post-fire competition release where surviving trees grew and provided seeds. The relationship between seedling density and basal area being modulated based on years since fire makes intuitive sense because larger trees are more likely to survive fire and provide seed (Giddey et al. 2022). For the longer intervals between

fires, the apparent relationship could reflect the fact that 10 or 17 years provides time for surviving younger trees to grow to maturity and produce seeds. Notably, the predicted maximum seedling densities for the longer interval reburns are lower than the shorter interval reburns, mainly because the range of the observed basal area densities was lower. A lot of the Freds Fire reburn contained many small stems of black oak throughout the burned area, which likely resprouted and thrived after severe fire. The low live conifer basal area could also be explained by high severity fire: 60% of the Freds fire perimeter burned at moderate and high severity, and the subsequent, predominantly high-severity Caldor fire killed many mature seed-bearing trees.

The complex relationships uncovered between seedling densities and predictor variables depend not only on the occurrence of reburns and the time between successive fires, but also the forest conditions that develop after an initial fire. Perhaps unsurprisingly, the severity (RdNBR) of the first fire was a significant predictor in the shade tolerant species models with interaction terms, although it was not a significant predictor in the models without interaction terms. The severity of the first fire 'sets the stage' for the state of the forest at the time of the second fire. The relationship between seedling density and basal area depending on reburn interval further illustrates the importance of post-disturbance biological legacies in determining forest trajectories (Prichard et al. 2017). We conducted an additional post-hoc investigation of each of the original six models, where we modified each model to include interaction terms between the RdNBR value of the first fire and RdNBR value of the second fire. This analysis did not reveal any statistically significant interactions between the severity of the first and second fires, which was surprising given

the body of work providing evidence for post-second-fire outcomes that depend on the severity of the first fire (Coppoletta et al. 2016, Harvey et al. 2016a, Stevens-Rumann et al. 2016, Tortorelli et al. 2024). The lack of distinguishable relationships is likely due to the small sample size when considering the different combinations of burn severities (especially when classified categorically as moderate-low, high-low). For example, nearly half of the plots in the Caples reburn could be classified as moderate severity in the first fire and low in the second, while most of the plots in the Long reburn were low severity in both the first and second fires. Although we did sample across the full range of burn severities in the field, the small sample size and relatively small reburn areas made producing a balanced sample difficult. Future research that collates larger reburn datasets at a regional scale could help address this challenge.

LIMITATIONS

This study provided evidence that fire history, particularly the time between short interval fires, differentially impacts pine and shade tolerant conifer regeneration in the Central Sierra Nevada. Although prior to Euro-American settlement the mean fire return interval in yellow pine mixed conifer forests was about 10 years, these forests are now highly departed from their historical averages (van de Water and Safford 2011). As such, we consider reburns <30 years 'short interval reburns', especially because the fires are of higher severity than their historical fire regimes. These results are a promising first step in characterizing the importance of past fire history on conifer regeneration. However, this study suffers from a sample size limitation common in ecological investigations,

particularly for opportunistic data collection in small reburned areas. We only sampled reburned areas in three reburn fires (and a no-reburn control), limiting the number of values for the variable 'years between fires' and potentially confounding other aspects of reburn fire identity with years between fires. Further research that collates data from additional reburns would increase sample density across the range of the 'years between fires' variable and reduce the potential for fire-level confounding. More data from distinct fire years could also help to uncover trends in post-second-fire seedling densities at longer intervals between fires, as post-fire climate is known to affect recruitment (Stewart et al. 2021). A larger sample size could also help to further disentangle relationships between seedling density and precipitation and climate, as a hotter, drier future is projected to increase fire frequency and fire weather intensity globally (Restaino and Safford 2018, Jones et al. 2022). Although precipitation and climate were not statistically significant predictors in the pine species models in this study, they might be in a larger study. A larger sample size would allow for more combinations of burn severities in the first and second fires and increase the statistical power in characterizing relationships between the two. Lastly, prediction of pine seedling density is known to be difficult and the fact that little is known about mechanisms of animal-mediated seed dispersal in general, combined with variable seed predation, contributes to this challenge. Another complicating factor is the lack of knowledge about how animal-mediated seed dispersal is affected by changing fire regimes (Gill et al. 2022). The knowledge gap in the role of seed caching by animals and how this impacts pine regeneration post-fire can be filled by interdisciplinary collaborations between forest ecologists and animal and/or movement ecologists.

CONCLUSION

As anthropogenic climate change leads to increased fire frequency and area burned, reburns will increase in likelihood. Given over a century of fire suppression, most of our recent understanding of postfire conifer regeneration and forest successional trajectories is based on investigations into single-entry fires. The results from this study suggest that past fire history (namely, reburns and the years between successive fires) and shrub cover are particularly important to pine species regeneration, while favorable climatic and topographic conditions in addition to seed sources are more important to shade tolerant species regeneration. However, in shade tolerant species models, the relationship between seedling density and variables such as shrub cover and basal area depend on the years between reburns, suggesting that although there might not be a direct relationship, past fire history and biological legacies still influence forest succession. Lastly, although correlations between observed and fitted values were low for all models, binarizing the data at replacement density and calculating AUC showed a more ecologically meaningful and stronger fit for predictability, as it is important to managers to know which areas may not be replaced by forests. Although the sample size and spatial extent of this study are too small to make regional predictions or extrapolations, there are useful management applications to expansion of this work. Increasing the number of plots in reburns can help to improve existing post-fire regeneration planning and web-based decision support systems such as the Postfire Spatial Conifer Regeneration Prediction Tool (POSCRPT) (Shive et al. 2018, Stewart et al. 2021) or RegenMapper (Holden et al. 2025), which currently do not incorporate reburns and/or fire history. Given the reforestation gap

(the difference between postfire reforestation need and reforestation capacity) in the western U.S., (Dobrowski et al. 2024, Safford and Stewart 2026), improvements to reforestation planning tools that can help identify locations where there is reforestation need and the potential for successful recruitment is important to maintain forest ecosystems and avoid unwanted type conversion. North American forests are prone to fire-driven deforestation, and 25% of average annual reforestation need in the western US comes from California alone (Safford and Stewart 2026). Changing patterns of fire regimes in the western US merit efforts to increase our understanding of trends and mechanisms of post-fire conifer regeneration to facilitate adaptive forest management.

REFERENCES

Abatzoglou, J.T., Williams, A.P., 2016. Impact of anthropogenic climate change on wildfire across western US forests. Proceedings of the National Academy of Sciences 113, 11770–11775. https://doi.org/10.1073/pnas.1607171113

Annighöfer, P., Seidel, D., Ammer, C., Stephens, S.L., York, R.A., 2019. Silvicultural implications from analyzing light induced height growth development of eight North American juvenile tree species in mixed-conifer forests. Forestry (Lond) 92, 616–626. https://doi.org/10.1093/forestry/cpz038

Barbour, M.G., Pavlik, B.M., Antos, J.A., 1990. Seedling Growth and Survival of Red and White Fir in a Sierra Nevada Ecotone. American Journal of Botany 77, 927–938. https://doi.org/10.1002/j.1537-2197.1990.tb15187.x

Bell, D.M., Bradford, J.B., Lauenroth, W.K., 2014. Early indicators of change: divergent climate envelopes between tree life stages imply range shifts in the western United States. Global Ecology and Biogeography 23, 168–180. https://doi.org/10.1111/geb.12109

Bohlman, G., H.D. Safford, and C. Skinner. 2021. Natural range of variation (NRV) for yellow pine and mixed conifer forests in northwestern California and southwestern Oregon. General Technical Report PSW-GTR-273, USDA Forest Service, Pacific Southwest Research Station, Albany, CA.

Brodie, E.G., Knapp, E.E., Latimer, A.M., Safford, H.D., Vossmer, M., Bisbing, S.M., 2023. The century-long shadow of fire exclusion: Historical data reveal early and lasting effects of fire regime change on contemporary forest composition. Forest Ecology and Management 539, 121011. https://doi.org/10.1016/j.foreco.2023.121011

Buma, B., Hayes, K., Weiss, S., Lucash, M., 2022. Short-interval fires increasing in the Alaskan boreal forest as fire self-regulation decays across forest types. Sci Rep 12, 4901. https://doi.org/10.1038/s41598-022-08912-8

Busby, S. Moffett K.B., Holz A., 2020. High-severity and short-interval wildfires limit forest recovery in the Central Cascade Range. Ecosphere 11,: e03247. https://doi.org/10.1002/ecs2.3247

Charles, F.E., Reside, A.E., Smith, A.L., 2025. The influence of changing fire regimes on specialized plant–animal interactions. Philos Trans R Soc Lond B Biol Sci 380, 20230448. https://doi.org/10.1098/rstb.2023.0448

Churchill, D.J., Jeronimo, S.M.A., Hessburg, P.F., Cansler, C.A., Povak, N.A., Kane, V.R., Lutz, J.A., Larson, A.J., 2022. Post-fire landscape evaluations in Eastern Washington, USA: Assessing the work of contemporary wildfires. Forest Ecology and Management 504, 119796. https://doi.org/10.1016/j.foreco.2021.119796

Collins, B.M., Lydersen, J.M., Everett, R.G., Stephens, S.L., 2018. How does forest recovery following moderate-severity fire influence effects of subsequent wildfire in mixed-conifer forests? Fire Ecology 14, 3. https://doi.org/10.1186/s42408-018-0004-x

Coop, J.D., Parks, S.A., McClernan, S.R., Holsinger, L.M., 2016. Influences of prior wildfires on vegetation response to subsequent fire in a reburned Southwestern landscape. Ecological Applications 26, 346–354. https://doi.org/10.1890/15-0775

Coop, J.D., Parks, S.A., Stevens-Rumann, C.S., Crausbay, S.D., Higuera, P.E., Hurteau, M.D., Tepley, A., Whitman, E., Assal, T., Collins, B.M., Davis, K.T., Dobrowski, S., Falk, D.A., Fornwalt, P.J., Fulé, P.Z., Harvey, B.J., Kane, V.R., Littlefield, C.E., Margolis, E.Q., North, M., Parisien, M.-A., Prichard, S., Rodman, K.C., 2020. Wildfire-Driven Forest Conversion in Western North American Landscapes. BioScience 70, 659–673. https://doi.org/10.1093/biosci/biaa061

Coppoletta, M., Merriam, K.E., Collins, B.M., 2016. Post-fire vegetation and fuel development influences fire severity patterns in reburns. Ecological Applications 26, 686–699. https://doi.org/10.1890/15-0225

Crotteau, J.S., Morgan Varner, J., Ritchie, M.W., 2013. Post-fire regeneration across a fire severity gradient in the southern Cascades. Forest Ecology and Management 287, 103–112. https://doi.org/10.1016/j.foreco.2012.09.022

Davis, K.T., Robles, M.D., Kemp, K.B., Higuera, P.E., Chapman, T., Metlen, K.L., Peeler, J.L., Rodman, K.C., Woolley, T., Addington, R.N., Buma, B.J., Cansler, C.A., Case, M.J., Collins, B.M., Coop, J.D., Dobrowski, S.Z., Gill, N.S., Haffey, C., Harris, L.B., Harvey, B.J., Haugo, R.D., Hurteau, M.D., Kulakowski, D., Littlefield, C.E., McCauley, L.A., Povak, N., Shive, K.L., Smith, E., Stevens, J.T., Stevens-Rumann, C.S., Taylor, A.H., Tepley, A.J., Young, D.J.N., Andrus, R.A., Battaglia, M.A., Berkey, J.K., Busby, S.U., Carlson, A.R., Chambers, M.E., Dodson, E.K., Donato, D.C., Downing, W.M., Fornwalt, P.J., Halofsky, J.S., Hoffman, A., Holz, A., Iniguez, J.M., Krawchuk, M.A., Kreider, M.R., Larson, A.J., Meigs, G.W., Roccaforte, J.P., Rother, M.T., Safford, H., Schaedel, M., Sibold, J.S., Singleton, M.P., Turner, M.G., Urza, A.K., Clark-Wolf, K.D., Yocom, L., Fontaine, J.B., Campbell, J.L., 2023. Reduced fire severity offers near-term buffer to climate-driven declines in conifer resilience across the western United States. Proceedings of the National Academy of Sciences 120, e2208120120. https://doi.org/10.1073/pnas.2208120120

Dobrowski, S.Z., Swanson, A.K., Abatzoglou, J.T., Holden, Z.A., Safford, H.D., Schwartz, M.K., Gavin, D.G., 2015. Forest structure and species traits mediate projected recruitment declines in western US tree species. Global Ecology and Biogeography 24, 917–927. https://doi.org/10.1111/geb.12302

Dobrowski, S.Z., Aghai, M.M., Chichilnisky du Lac, A., Downer, R., Fargione, J., Haase, D.L., Hoecker, T., Kildisheva, O.A., Murdoch, A., Newman, S., North, M., Saksa, P., Sjoholm, M., Baribault, T., Buonanduci, M.S., Chambers, M.E., Gonzales-Kramer, L., Harvey, B.J., Hurteau, M.D., Loevner, J., Safford, H.D., Sloan, J., 2024. 'Mind the Gap'—reforestation needs vs. reforestation capacity in the western United States. Frontiers in Forests and Global Change 7. https://doi.org/10.3389/ffgc.2024.1402124

Dolanc, C.R., Safford, H.D., Dobrowski, S.Z., Thorne, J.H., 2014. Twentieth century shifts in abundance and composition of vegetation types of the Sierra Nevada, CA, US. Applied Vegetation Science 17, 442-455. https://doi.org/10.1111/avsc.12079

Donato, D.C., Fontaine, J.B., Robinson, W.D., Kauffman, J.B., Law, B.E., 2009. Vegetation response to a short interval between high-severity wildfires in a mixed-evergreen forest. Journal of Ecology 97, 142–154. https://doi.org/10.1111/j.1365-2745.2008.01456.x

Dyer, J.M., 2009. Assessing topographic patterns in moisture use and stress using a water balance approach. Landscape Ecology 24, 391–403. https://doi.org/10.1007/s10980-008-9316-6

Enright, N.J., Fontaine, J.B., Bowman, D.M., Bradstock, R.A., Williams, R.J., 2015. Interval squeeze: altered fire regimes and demographic responses interact to threaten woody species persistence as climate changes. Frontiers in Ecology and the Environment 13, 265–272. https://doi.org/10.1890/140231

Foster, S.D., Bravington, M.V., 2013. A Poisson–Gamma model for analysis of ecological non-negative continuous data. Environmental and Ecological Statistics 20, 533–552. https://doi.org/10.1007/s10651-012-0233-0

Giddey, B.L., Baard, J.A., Kraaij, T., 2022. Fire severity and tree size affect post-fire survival of Afrotemperate forest trees. Fire Ecology 18, 5. https://doi.org/10.1186/s42408-022-00128-5

Gill, N.S., Turner, M.G., Brown, C.D., Glassman, S.I., Haire, S.L., Hansen, W.D., Pansing, E.R., St Clair, S.B., Tomback, D.F., 2022. Limitations to Propagule Dispersal Will Constrain Postfire Recovery of Plants and Fungi in Western Coniferous Forests. BioScience 72, 347–364. https://doi.org/10.1093/biosci/biab139

Gray, A.N., Zald, H.S.J., Kern, R.A., North, M., 2005. Stand Conditions Associated with Tree Regeneration in Sierran Mixed-Conifer Forests. Forest Science 51, 198–210. https://doi.org/10.1093/forestscience/51.3.198

Greenler, S.M., Dunn, C.J., Johnston, J.D., Reilly, M.J., Merschel, A.G., Hagmann, R.K., Bailey, J.D., 2023. Too hot, too cold, or just right: Can wildfire restore dry forests of the interior Pacific Northwest? PLOS ONE 18, e0281927. https://doi.org/10.1371/journal.pone.0281927

Grupenhoff, A.R., Putz, T., Williams, J., Estes, B., Domènech, R., Restaino, J., Safford, H.D., 2026. Short-term effects of single-entry prescribed fire in California's yellow-pine and mixed conifer forests. Forest Ecology and Management 613, 123771. https://doi.org/10.1016/j.foreco.2026.123771

Harvey, B.J., Donato, D.C., Turner, M.G., 2016a. Burn me twice, shame on who? Interactions between successive forest fires across a temperate mountain region. Ecology 97, 2272–2282. https://doi.org/10.1002/ecy.1439

Harvey, B.J., Donato, D.C., Turner, M.G., 2016b. High and dry: post-fire tree seedling establishment in subalpine forests decreases with post-fire drought and large stand-replacing burn patches. Global Ecology and Biogeography 25, 655–669. https://doi.org/10.1111/geb.12443

Holden, Z.A., Jungck, E., Davis, K.T., Warren, D.A., Swanson, A., Dobrowski, S.Z., Maneta, M., Rodman, K.C., Faller, L., Archer, V., 2025. A post-fire reforestation assessment and prioritization tool for the Western United States. Fire Ecology 21, 83. https://doi.org/10.1186/s42408-025-00405-z

Hood, S.M., Bär, A., Battipaglia, G., Mayr, S., Shearman, T., Varner, J.M. and Gandhi, K.J., 2026. Fire Ecology and Ecophysiology of Pinus Species. In *Physiology and Ecology of Pines Worldwide* (pp. 49-85). Cham: Springer Nature Switzerland.

Jones, M.W., Abatzoglou, J.T., Veraverbeke, S., Andela, N., Lasslop, G., Forkel, M., Smith, A.J.P., Burton, C., Betts, R.A., van der Werf, G.R., Sitch, S., Canadell, J.G., Santín, C., Kolden, C., Doerr, S.H., Le Quéré, C., 2022. Global and Regional Trends and Drivers of Fire Under Climate Change. Reviews of Geophysics 60, e2020RG000726. https://doi.org/10.1029/2020RG000726

Kemp, K.B., Higuera, P.E., Morgan, P., 2016. Fire legacies impact conifer regeneration across environmental gradients in the U.S. northern Rockies. Landscape Ecology 31, 619–636. https://doi.org/10.1007/s10980-015-0268-3

Kemp, K.B., Higuera, P.E., Morgan, P., Abatzoglou, J.T., 2019. Climate will increasingly determine post-fire tree regeneration success in low-elevation forests, Northern Rockies, USA. Ecosphere 10, e02568. https://doi.org/10.1002/ecs2.2568

Kolb, T.E., Flathers, K., Bradford, J.B., Andrews, C., Asherin, L.A., Moser, W.K., 2020. Stand density, drought, and herbivory constrain ponderosa pine regeneration pulse. Canadian Journal of Forest Research 50, 862–871. https://doi.org/10.1139/cjfr-2019-0248

Kolden, C.A., Smith, A.M., Abatzoglou, J.T., 2015. Limitations and utilisation of Monitoring Trends in Burn Severity products for assessing wildfire severity in the USA. International Journal of Wildland Fire 24, 1023–1028. https://doi.org/10.1071/WF15082

Kroiss, S.J., HilleRisLambers, J., 2015. Recruitment limitation of long-lived conifers: implications for climate change responses. Ecology 96, 1286–1297. https://doi.org/10.1890/14-0595.1

Lacher, T.E., Jr., Davidson, A.D., Fleming, T.H., Gómez-Ruiz, E.P., McCracken, G.F., Owen-Smith, N., Peres, C.A., Vander Wall, S.B., 2019. The functional roles of mammals in ecosystems. J Mammal 100, 942–964. https://doi.org/10.1093/jmammal/gyy183

Larson, A.J., Belote, R.T., Cansler, C.A., Parks, S.A., Dietz, M.S., 2013. Latent resilience in ponderosa pine forest: effects of resumed frequent fire. Ecological Applications 23, 1243–1249. https://doi.org/10.1890/13-0066.1

Lauvaux, C.A., Skinner, C.N., Taylor, A.H., 2016. High severity fire and mixed conifer forest-chaparral dynamics in the southern Cascade Range, USA. Forest Ecology and Management 363, 74–85. https://doi.org/10.1016/j.foreco.2015.12.016

League, K., Veblen, T., 2006. Climatic variability and episodic *Pinus ponderosa* establishment along the forest-grassland ecotones of Colorado. Forest Ecology and Management 228, 98–107. https://doi.org/10.1016/j.foreco.2006.02.030

Littlefield, C.E., 2019. Topography and post-fire climatic conditions shape spatio-temporal patterns of conifer establishment and growth. Fire Ecology 15, 34. https://doi.org/10.1186/s42408-019-0047-7

Lydersen, J.M., Collins, B.M., Coppoletta, M., Jaffe, M.R., Northrop, H., Stephens, S.L., 2019. Fuel dynamics and reburn severity following high-severity fire in a Sierra Nevada, USA, mixed-conifer forest. Fire Ecology 5, 43. https://doi.org/10.1186/s42408-019-0060-x

Mallek, C., Safford, H., Viers, J., Miller, J., 2013. Modern departures in fire severity and area vary by forest type, Sierra Nevada and southern Cascades, California, USA. Ecosphere 4, art153. https://doi.org/10.1890/ES13-00217.1

McCune, B., Keon, D., 2002. Equations for potential annual direct incident radiation and heat load. Journal of Vegetation Science 13, 603–606. https://doi.org/10.1111/j.1654-1103.2002.tb02087.x

Miller, J.D., Thode, A.E., 2007. Quantifying burn severity in a heterogeneous landscape with a relative version of the delta Normalized Burn Ratio (dNBR). Remote Sensing of Environment 109, 66–80. https://doi.org/10.1016/j.rse.2006.12.006

Miller, J.E.D., Root, H.T., Safford, H.D., 2018. Altered fire regimes cause long-term lichen diversity losses. Global Change Biology 24, 4909–4918. https://doi.org/10.1111/gcb.14393

Nelson, K.N., O'Dean, E., Knapp, E.E., Parker, A.J., Bisbing, S.M., 2021. Persistent yet vulnerable: resurvey of an Abies ecotone reveals few differences but vulnerability to climate change. Ecology 102, e03525. https://doi.org/10.1002/ecy.3525

North, M., Hurteau, M., Fiegener, R., Barbour, M., 2005. Influence of Fire and El Niño on Tree Recruitment Varies by Species in Sierran Mixed Conifer. Forest Science 51, 187–197. https://doi.org/10.1093/forestscience/51.3.187

North, M.P., Tompkins, R.E., Bernal, A.A., Collins, B.M., Stephens, S.L., York, R.A., 2022. Operational resilience in western US frequent-fire forests. Forest Ecology and Management 507, 120004. https://doi.org/10.1016/j.foreco.2021.120004

Ordóñez, J.L., Retana, J., Espelta, J.M., 2005. Effects of tree size, crown damage, and tree location on post-fire survival and cone production of *Pinus nigra* trees. Forest Ecology and Management 206, 109–117. https://doi.org/10.1016/j.foreco.2004.10.067

Parks, S.A., Miller, C., Nelson, C.R., Holden, Z.A., 2014. Previous Fires Moderate Burn Severity of Subsequent Wildland Fires in Two Large Western US Wilderness Areas. Ecosystems 17, 29–42. https://doi.org/10.1007/s10021-013-9704-x

Parks, S.A., Parisien, M.-A., Miller, C., Holsinger, L.M., Baggett, L.S., 2018a. Fine-scale spatial climate variation and drought mediate the likelihood of reburning. Ecological Applications 28, 573–586. https://doi.org/10.1002/eap.1671

Parks, S.A., Holsinger, L.M., Voss, M.A., Loehman, R.A., Robinson, N.P., 2018b. Mean Composite Fire Severity Metrics Computed with Google Earth Engine Offer Improved Accuracy and Expanded Mapping Potential. Remote Sensing 10, 879. https://doi.org/10.3390/rs10060879

Paudel, A., Coppoletta, M., Merriam, K., Markwith, S.H., 2022. Persistent composition legacy and rapid structural change following successive fires in Sierra Nevada mixed conifer forests. Forest Ecology and Management 509, 120079. https://doi.org/10.1016/j.foreco.2022.120079

Paudel, A., Markwith, S.H., 2023. From the severity patch to the landscape: Wildfire and spatial heterogeneity in northern Sierra Nevada conifer forests. Journal of Vegetation Science 34, e13207. https://doi.org/10.1111/jvs.13207

Prichard, S.J., Stevens-Rumann, C.S., Hessburg, P.F., 2017. Tamm Review: Shifting global fire regimes: Lessons from reburns and research needs. Forest Ecology and Management 396, 217–233. https://doi.org/10.1016/j.foreco.2017.03.035

PRISM Climate Group. 2026. http://prism.oregonstate.edu. Oregon State University, Corvallis, Oregon, USA

R Core Team. 2025. R: A language and environment for statistical computing. R Foundation for Statistical Computing, Vienna, Austria. https://www.R-project.org/.

Restaino, C.R. and Safford, H.D., 2018. Fire and climate change. *Fire in California's ecosystems. Second edition. University of California Press, Berkeley, California, USA*, pp.493-505.

Rietveld, W.J., 1976. Cone maturation in ponderosa pine foliage scorched by wildfire. Department of Agriculture, Forest Service, Rocky Mountain Forest and Range Experiment Station.

Rodman, K.C., Veblen, T.T., Battaglia, M.A., Chambers, M.E., Fornwalt, P.J., Holden, Z.A., Kolb, T.E., Ouzts, J.R., Rother, M.T., 2020. A changing climate is snuffing out post-fire recovery in montane forests. Global Ecology and Biogeography 29, 2039–2051. https://doi.org/10.1111/geb.13174

Rother, M.T., Veblen, T.T., 2016. Limited conifer regeneration following wildfires in dry ponderosa pine forests of the Colorado Front Range. Ecosphere 7, e01594. https://doi.org/10.1002/ecs2.1594

Royce, E.B., Barbour, M.G., 2001. Mediterranean climate effects. I. Conifer water use across a Sierra Nevada ecotone. American Journal of Botany 88, 911–918. https://doi.org/10.2307/2657044

Safford, H.D., Stevens, J.T., 2017. Natural range of variation for yellow pine and mixed-conifer forests in the Sierra Nevada, southern Cascades, and Modoc and Inyo National Forests, California, USA. General Technical Report. PSW-GTW-273. Albany, Ca: USDA Forest Service, Pacific Southwest Research Station 146 p.,273.

Safford, H.D., Stewart, J.A.E., 2026. Deforestation and reforestation in a world hotspot of fire-driven forest loss: trends in California conifer forests 1991–2023. Front. For. Glob. Change 9. https://doi.org/10.3389/ffgc.2026.1764379

Sanders, H. 2025. *Effects of Shrubs on Conifer Seedling Performance in High Severity Burned Areas*. Master's Thesis. University of California, Davis.

Shive, K.L., Preisler, H.K., Welch, K.R., Safford, H.D., Butz, R.J., O'Hara, K.L., Stephens, S.L., 2018. From the stand scale to the landscape scale: predicting the spatial patterns of forest regeneration after disturbance. Ecological Applications 28, 1626–1639. https://doi.org/10.1002/eap.1756

Steel, Z.L., Foster, D., Coppoletta, M., Lydersen, J.M., Stephens, S.L., Paudel, A., Markwith, S.H., Merriam, K., Collins, B.M., 2021. Ecological resilience and vegetation transition in the face of two successive large wildfires. Journal of Ecology 109, 3340–3355. https://doi.org/10.1111/1365-2745.13764

Stephens, S.L., Lydersen, J.M., Collins, B.M., Fry, D.L., Meyer, M.D., 2015. Historical and current landscape-scale ponderosa pine and mixed conifer forest structure in the Southern Sierra Nevada. Ecosphere 6, art79. https://doi.org/10.1890/ES14-00379.1

Stephens, S.L., Stevens, J.T., Collins, B.M., York, R.A., Lydersen, J.M., 2018. Historical and modern landscape forest structure in fir (Abies)-dominated mixed conifer forests in the northern Sierra Nevada, USA. Fire Ecology 14, 7. https://doi.org/10.1186/s42408-018-0008-6

Stevens-Rumann, C., Morgan, P., 2016. Repeated wildfires alter forest recovery of mixed-conifer ecosystems. Ecological Applications 26, 1842–1853. https://doi.org/10.1890/15-1521.1

Stevens-Rumann, C.S., Prichard, S.J., Strand, E.K., Morgan, P., 2016. Prior wildfires influence burn severity of subsequent large fires. Canadian Journal of Forest Research. 46, 1375–1385. https://doi.org/10.1139/cjfr-2016-0185

Stewart, J.A.E., van Mantgem, P.J., Young, D.J.N., Shive, K.L., Preisler, H.K., Das, A.J., Stephenson, N.L., Keeley, J.E., Safford, H.D., Wright, M.C., Welch, K.R., Thorne, J.H., 2021. Effects of postfire climate and seed availability on postfire conifer regeneration. Ecological Applications 31, e02280. https://doi.org/10.1002/eap.2280

Tepley, A.J., Thompson, J.R., Epstein, H.E., Anderson-Teixeira, K.J., 2017. Vulnerability to forest loss through altered postfire recovery dynamics in a warming climate in the Klamath Mountains. Global Change Biology 23, 4117–4132. https://doi.org/10.1111/gcb.13704

Tortorelli, C.M., Krawchuk, M.A., Kerns, B.K., 2020. Expanding the invasion footprint: Ventenata dubia and relationships to wildfire, environment, and plant communities in the Blue Mountains of the Inland Northwest, USA. Applied Vegetation Science 23, 562–574. https://doi.org/10.1111/avsc.12511

Tortorelli, C.M., Latimer, A.M., Young, D.J.N., 2024. Moderating effects of past wildfire on reburn severity depend on climate and initial severity in Western US forests. Ecological Applications 34, e3023. https://doi.org/10.1002/eap.3023

Tubbesing, C.L., York, R.A., Stephens, S.L., Battles, J.J., 2020. Rethinking fire-adapted species in an altered fire regime. Ecosphere 11, e03091. https://doi.org/10.1002/ecs2.3091

Tubbesing, C.L., Young, D.J.N., York, R.A., Stephens, S.L., Battles, J.J., 2022. Incorporating Shrub Neighborhood Dynamics to Predict Forest Succession Trajectories in an Altered Fire Regime. Ecosystems 25, 136–154. https://doi.org/10.1007/s10021-021-00645-5

Turner, M.G., Braziunas, K.H., Hansen, W.D., Harvey, B.J., 2019. Short-interval severe fire erodes the resilience of subalpine lodgepole pine forests. Proceedings of the National Academy of Sciences 116, 11319–11328. https://doi.org/10.1073/pnas.1902841116

Tweedie, M.C., 1984. An index which distinguishes between some important exponential families, in: Statistics: Applications and New Directions: Proceedings of the Indian Statistical Institute Golden Jubilee International Conference. pp. 579–604.

Urza, A.K., Weisberg, P.J., Chambers, J.C., Sullivan, B.W., 2019. Shrub facilitation of tree establishment varies with ontogenetic stage across environmental gradients. New Phytologist 223, 1795–1808. https://doi.org/10.1111/nph.15957

USDA Forest Service. 2015. FSVeg Common Stand Exam User Guide. Washington, DC: United States Department of Agriculture Forest Service. Available at: https://www.fs.usda.gov/nrm/fsveg/ (Accessed 18 May 2022).

Van Wagtendonk, J.W., Fites-Kaufman, J.A., Safford, H.D., North, M.P. B.M. Collins, 2018. Sierra Nevada Bioregion. In *Fire in California's Ecosystems* (pp 249-278). University of California Press, Oakland, California, USA.

Van de Water, K.M., Safford, H.D., 2011. A Summary of Fire Frequency Estimates for California Vegetation before Euro-American Settlement. Fire Ecology 7, 26–58. https://doi.org/10.4996/fireecology.0703026

Vander Wall, S.B., 2008. On the Relative Contributions of Wind Vs. Animals to Seed Dispersal of Four Sierra Nevada Pines. Ecology 89, 1837–1849. https://doi.org/10.1890/07-0409.1

Welch, K.R., Safford, H.D., Young, T.P., 2016. Predicting conifer establishment post wildfire in mixed conifer forests of the North American Mediterranean-climate zone. Ecosphere 7, e01609. https://doi.org/10.1002/ecs2.1609

Werner, C.M., Young, D.J.N., Safford, H.D., Young, T.P., 2019. Decreased snowpack and warmer temperatures reduce the negative effects of interspecific competitors on regenerating conifers. Oecologia 191, 731–743. https://doi.org/10.1007/s00442-019-04536-4

Westerling, A.L., 2016. Increasing western US forest wildfire activity: sensitivity to changes in the timing of spring. Philosophical Transactions of the Royal Society B: Biological Sciences 371, 20150178. https://doi.org/10.1098/rstb.2015.0178

Williams, J.N., Safford, H.D., Enstice, N., Steel, Z.L., Paulson, A.K., 2023. High-severity burned area and proportion exceed historic conditions in Sierra Nevada, California, and adjacent ranges. Ecosphere 14, e4397. https://doi.org/10.1002/ecs2.4397

Young, D.J.N., Werner, C.M., Welch, K.R., Young, T.P., Safford, H.D., Latimer, A.M., 2019. Post-fire forest regeneration shows limited climate tracking and potential for drought-induced type conversion. Ecology 100, e02571. https://doi.org/10.1002/ecy.2571

Young, D.J.N., Meyer, M., Estes, B., Gross, S., Wuenschel, A., Restaino, C., Safford, H.D., 2020. Forest recovery following extreme drought in California, USA: natural patterns and effects of pre-drought management. Ecological Applications 30, e02002.https://doi.org/10.1002/eap.2002

Young, D.J.N., Venuti, N.E., Greene, D.F., Latimer, A.M., 2025. Canopy seed survival through extreme fire in non-serotinous conifers: An unexpected source of forest resilience. Ecological Applications 35, e70142. https://doi.org/10.1002/eap.70142

Zald, H.S.J., Gray, A.N., North, M., Kern, R.A., 2008. Initial tree regeneration responses to fire and thinning treatments in a Sierra Nevada mixed-conifer forest, USA. Forest Ecology and Management 256, 168–179. https://doi.org/10.1016/j.foreco.2008.04.022

Zeibig-Kichas, N.E., Ardis, C.W., Berrill, J.-P., King, J.P., 2016. Bark Thickness Equations for Mixed-Conifer Forest Type in Klamath and Sierra Nevada Mountains of California. International Journal of Forestry Research 2016, 1864039. https://doi.org/10.1155/2016/1864039